SAPIENZA
Università di Roma
Facoltà di Farmacia e Medicina

DOTTORATO DI RICERCA
IN SCIENZE MORFOGENETICHE E CITOLOGICHE

XXVI Ciclo
(A.A. 2010/2011)

Defining skeletal muscle resident progenitors and targeting their interactions to improve regeneration in satellite cell-depleted muscle

Dottorando
Luigi Formicola

Tutor
Dr. David Sassoon
Dr. Giovanna Marazzi

Co-tutor
Prof. Antonio Musarò

Coordinatore
Prof. Sergio Adamo

INDEX

* Text, figures, tables and figure legends of "Introduction" (chapter 2), "Results" (chapters 1 and 2), "Discussion" and "Materials and Methods" are partially or completely reproduced in:
- Pannérec A.[†], **Formicola L.**[†], Besson V., Marazzi G. and Sassoon D.A. "Defining skeletal muscle resident progenitors and their cell fate potentials". 2013, *Development* 140, 2879-2891. [†] Equal contribution.
- **Formicola L.**[§], Pannérec A.[§], Besson V., Gayraud-Morel B., Tajbakhsh S., Lachey J., Seehra J.S., Marazzi G. and Sassoon D.A. "Inhibition of the AcvR2B pathway targets the stem cell niche and restores regenerative capacity in satellite cell-depleted skeletal muscle" (*article in preparation*) [§]Equal contribution.

ABBREVIATIONS

AcvR2B: activin-receptor type-2 B
ALP: alkaline phosphatase
ALS: amyotrophic lateral sclerosis
CD31: cluster of differentiation 31
CD34: cluster of differentiation 34
CD45: cluster of differentiation 45
CTX: cardiotoxin
DAPI: 4',6-diamidino-2-phenylindole
DMD: Duchenne muscular dystrophy
DT: diphteria toxin
DTR: diphteria toxin receptor
ECM: extracellular matrix
EOMs: extraocular muscles
FABP4/aP2: fatty acid binding protein 4/adipocyte protein 2
FACS: fluorescence-activated cell sorting
FAPs: fibro/adipogenic progenitors
FGF: fibroblast growth factor
FST: follistatin
FSTL: follistatin-like
GH: growth hormone
HGF: hepatocypte growth factor
IAPs: interstitial adipogenic progenitors
IGF-1: insulin-like growth factor-1
IGF-1R: insulin-like growth factor-1 receptor
MABs: mesoangioblasts
Mash1: mammalian achaete scute homolog-1
mGFP: membranous green fluorescent protein
MHC/MF20: myosin heavy chain
MPCs: muscle progenitor cells
MRFs: muscle regulatory factors
MST: myostatin
mTOR: mammalian target of rapamycin
Myf5: myogenic factor 5

MyoD: myogenic differentiation 1
NG2: neuronal-glial antigen 2 chondroitin sulfate proteoglycan
Pax3: paired-box gene 3
Pax7: paired-box gene 7
PDGF: platelet-derived growth factor
PDGFRα: platelet-derived growth factor receptor alpha
PDGFRβ: platelet-derived growth factor receptor beta
PICs: PW1-positive interstitial cells
PI3K: phosphatidylinositol-3 kinase
Prdm16: PR domain containing 16
PW1/Peg3: paternally expressed gene 3
SAT: satellite cells
Sca1: stem cell antigen-1
SM22α: smooth muscle protein 22 kDa alpha
Sma: smooth muscle actin
Sox2: Sex Determining Region Y-Box 2
SP: side population
TA: *tibialis anterior*
TGFβ: transforming growth factor beta
Tie2: tyrosine kinase with immunoglobulin and EGF homology domains 2
TNFα: tumor necrosis factor alpha
Ucp1: uncoupling protein 1
VEGF: vascular endothelial growth factor

ABSTRACT

Satellite cells are the major resident stem cell population in postnatal skeletal muscle and they are necessary to achieve a proper regeneration response. However in recent years other resident progenitor populations have been described. PW1/Peg3 is expressed in stem cells and progenitor populations in several murine postnatal tissues. In skeletal muscle PW1/Peg3 is expressed in satellite cells and a subset of interstitial cells (PICs, PW1+ Interstitial Cells). Microarray analysis revealed that PICs express a broad range of genes common to mesenchymal stem cells while satellite cells express genes consistent with a committed myogenic progenitor. We found that juvenile and adult PICs are more plastic than satellite cells, as they are able to differentiate *in vitro* into smooth and skeletal muscle as well as fat, while satellite cells only exhibit a committed skeletal muscle fate. Moreover, we found that PICs can be separated into 2 sub-populations on the basis of platelet derived growth factor receptor alpha (PDGFRα) expression: $PW1^{+}PDGFR\alpha^{+}$ with adipogenic capacity and $PW1^{+}PDGFR\alpha^{-}$ with myogenic capacity.

Transforming growth factor beta (TGFβ) and insulin-like growth factor-1 (IGF-1) signalling pathways are involved in important processes regulating postnatal muscle growth and homeostasis and have recently become pharmaceutical and clinical targets in several chronic diseases in which muscle regeneration is impaired. We found that PICs can rescue myostatin inhibitory effects on satellite cells proliferation *in vitro* through release of antagonist factors, including follistatin and IGF-1, demonstrating cellular crosstalk within the muscle stem cell niche. Moreover, administering an inhibitor of the TGFβ pathway *in vivo* acts on the stem cell niche interactions by altering the ratio between PICs and satellite cells and it is able to rescue regenerative capacity in satellite cell-deprived muscles by creating a favourable microenvironment where rare residual satellite cells can be mobilized and participate to muscle fiber regeneration.

RIASSUNTO

Le cellule satelliti costituiscono la principale popolazione di progenitori cellulari presenti nel muscolo scheletrico postnatale e contribuiscono alla rigenerazione muscolare (Relaix et al., 2012; Yin et al., 2013). Tuttavia, negli ultimi decenni sono stati descritti altri tipi di progenitori cellulari con capacità miogenica *in vitro* e in seguito a iniezione sistemica o intramuscolare, che contribuiscono alla rigenerazione muscolare *in vivo* (Cappellari and Cossu, 2013; Mitchell et al., 2010; Pannerec et al., 2012; Yin et al., 2013). Il possibile ruolo di questi progenitori nella crescita muscolare postnatale è al momento in corso di studio (Pannerec et al., 2012). Nel nostro laboratorio è stata in precedenza descritta nel muscolo postnatale una sottopopolazione di cellule interstiziali esprimenti PW1/Peg3, definite PICs ($PW1^+$ Interstitial Cells) e dotate di un'alta capacità miogenica *in vitro* e in seguito a trapianto in muscoli danneggiati (Mitchell et al., 2010). Inoltre, le PICs trapiantate in un muscolo danneggiato non soltanto partecipano alla rigenerazione delle fibre muscolari, ma possono anche generare satelliti ed altre PICs, esibendo quindi capacità di autorinnovamento (Mitchell et al., 2010). *In vitro* le PICs sono bipotenti, in quanto in grado di differenziare non solo in cellule muscolari scheletriche, ma anche in cellule muscolari lisce (Mitchell et al., 2010). Queste osservazioni suggeriscono che le PICs siano progenitori cellulari dotati di una maggiore plasticità rispetto alle cellule satelliti. Una tale ipotesi è inoltre sostenuta da un recente studio svolto nel nostro laboratorio sul modello murino reporter $PW1^{IRESnLacZ}$, da cui è emerso che PW1/Peg3 è espresso nel topo adulto nelle differenti popolazioni di cellule staminali presenti in tutti i tessuti esaminati (muscolo scheletrico, intestino, sistema nervoso centrale, midollo osseo, gonadi, pelle) (Besson et al., 2011). E' dunque plausibile che le cellule esprimenti PW1 nel muscolo scheletrico, tra cui satelliti e PICs, siano progenitori cellulari dotati di diverse capacità differenziative. **Il primo scopo di questo lavoro è di descrivere le capacità di differenziamento**

delle differenti popolazioni di progenitori cellulari del muscolo scheletrico nel periodo di crescita postnatale. A questo fine, abbiamo messo a punto una tecnica di isolamento tramite citometria a flusso (FACS, Fluorescence-Activated Cell Sorting) delle cellule satelliti e delle PICs dai muscoli scheletrici degli arti inferiori, attraverso una selezione negativa per i marcatori ematopoietici di membrana CD45 e Ter119, seguita da una selezione positiva per i marcatori di cellule staminali CD34 e Sca1, come precedentemente descritto (Sacco et al., 2008; Joe et al., 2010; Mitchell et al., 2010). Nei topi giovani (1 settimana di vita postnatale), abbiamo distinto sulla base dei livelli di espressione di Sca1 due popolazioni di PICs ($Sca1_{MED}$ e $Sca1_{HIGH}$): la popolazione $Sca1_{MED}$ è arricchita in PICs, mentre la $Sca1_{HIGH}$ è una popolazione mista in cui sono presenti cellule PW1-positive e PW1-negative (Mitchell et al., 2010). Per tale ragione, in precedenza abbiamo limitato la descrizione delle PICs alla popolazione $Sca1_{MED}$ (Mitchell et al., 2010). La disponibilità del modello murino transgenico "reporter" $PW1^{IRESnLacZ}$ (Besson et al., 2011) ci ha permesso di isolare tramite FACS le cellule esprimenti PW1 nella popolazione $Sca1_{HIGH}$ e di analizzare sistematicamente le capacità di differenziamento *in vitro* delle PICs (sia $Sca1_{MED}$ che $Sca1_{HIGH}$), a partire da 1 settimana di vita postnatale fino all'adulto (7 settimane). Abbiamo osservato che le PICs sono in grado di differenziare in cellule muscolari lisce, cellule muscolari scheletriche e adipociti, contrariamente alle cellule PW1-negative, le quali possono differenziare soltanto in cellule muscolari lisce. Recentemente, sono state descritte nel muscolo scheletrico adulto cellule interstiziali esprimenti Sca1 e PDGFRα e dotate di capacità adipogenica (Joe et al., 2010; Uezumi et al., 2010; Uezumi et al., 2011), qui denominate IAPs (Interstitial Adipogenic Progenitors). *In vivo* le IAPs non partecipano direttamente alla rigenerazione delle fibre muscolari danneggiate, tuttavia sono rapidamente indotte a proliferare in seguito a danno (Joe et al., 2010; Uezumi et al., 2010; Uezumi et al., 2011). *In vitro* le IAPs mostrano un effetto promiogenico nei confronti delle cellule

satelliti, mentre la presenza di cellule muscolari differenziate in coltura è in grado di inibire il differenziamento adipogenico delle IAPs (Joe et al., 2010; Uezumi et al., 2010). Ciò lascia supporre l'esistenza di un'interazione reciproca tra le IAPs e le cellule satelliti durante la rigenerazione muscolare e un ruolo importante delle IAPs nel regolare l'attivazione e il differenziamento delle cellule satelliti. Per determinare se le PICs e le IAPs fossero popolazioni correlate o distinte, abbiamo purificato le cellule in base alla loro espressione di PDGFRα e di PW1 ed analizzato le capacità di differenziamento *in vitro* delle popolazioni ottenute. In questo modo abbiamo dimostrato che le IAPs costituiscono una sottopopolazione delle PICs ad esclusiva capacità adipogenica e che le PICs comprendono anche un'altra sottopopolazione di cellule non esprimenti PDGFRα e dotate di capacità miogenica, ma non adipogenica. Dalle nostre analisi è inoltre emerso che la popolazione di PICs esprimenti livelli intermedi di Sca1 ($Sca1_{MED}$) decresce progressivamente dopo la nascita fino a scomparire tra le 3 e le 5 settimane di vita postnatale. Vari studi suggeriscono che il principale meccanismo di crescita postnatale fino alle 3 settimane consista nella fusione di progenitori cellulari alle fibre muscolari, mentre dopo questa fase la crescita muscolare avvenga generalmente per un'ipertrofia delle fibre (White et al., 2010). Questo cambiamento nel programma cellulare miogenico postnatale è anche sostenuto da un cambiamento di espressione genica (Lepper et al., 2009). In base ai risultati da noi ottenuti, possiamo supporre che questa popolazione transitoria di PICs ($Sca1_{MED}$) sia coinvolta nella prima fase della miogenesi postnatale, sia direttamente attraverso la fusione alle fibre muscolari, sia indirettamente come elemento di supporto funzionale per altri progenitori cellulari, in primo luogo le cellule satelliti, attraverso la secrezione di molecole di segnalazione.

Una più dettagliata comprensione della nicchia delle cellule staminali del muscolo scheletrico e delle sue componenti è importante in quanto può fornire una base teorica e sperimentale per progettare trattamenti terapeutici per le malattie muscolari.

Nelle malattie degenerative come le distrofie muscolari congenite, nell'atrofia muscolare presente in patologie croniche (cancro, diabete, insufficienza renale o cardiaca) o nell'invecchiamento, si assiste ad una perdita della massa e della forza contrattile dei muscoli scheletrici, fenomeni generalmente associati ad una cattiva prognosi e alla morte (Mann et al., 2011; Tabebordbar et al., 2013). Queste miopatie sono inoltre associate ad un aumento dell'attività catabolica muscolare e/o ad una degenerazione delle fibre muscolari, eventi che si verificano contemporaneamente ad una deposizione di tessuto fibrotico e adiposo, nonché ad una riduzione del numero delle cellule satelliti o ad un'alterazione della loro competenza (Mann et al., 2011; Bonaldo and Sandri, 2013; Hikida, 2011; Jang et al., 2011). In queste condizioni patologiche l'attivazione della via di trasduzione del segnale che fa capo al recettore dell'activina di tipo 2B (AcvR2B, Activin Receptor type 2B) è perturbata (Serrano et al., 2011; Tabebordbar et al., 2013). L'inibizione di questa via di comunicazione attraverso la somministrazione di molecole solubili o in modelli murini transgenici è in grado di ridurre la perdita di massa e forza muscolari in condizioni patologiche, diminuire la fibrosi e probabilmente attivare le cellule satelliti promuovendone la fusione alle fibre muscolari (George Carlson et al., 2011; Pistilli et al., 2011; Morrison et al., 2009; Zhou et al., 2010a; Chiu et al., 2013; McCroskery et al., 2003; McCroskery et al., 2005). Gli studi effettuati sulle IAPs hanno mostrato che tali progenitori possono differenziare in adipociti *in vivo* soltanto in modelli in cui la rigenerazione muscolare è compromessa (Joe et al., 2010; Uezumi et al., 2011). Inoltre un'attivazione cronica della via di trasduzione dell'AcvR2B è uno dei principali stimoli responsabili del differenziamento adipogenico delle IAPs *in vivo* e della produzione e deposizione di matrice extracellulare fibrotica nel modello murino *mdx* per la distrofia muscolare di Duchenne (Uezumi et al., 2011). Negli ultimi anni sono stati generati diversi modelli murini in cui il compartimento delle cellule satelliti può essere selettivamente ridotto, che offrono un eccellente paradigma per lo

studio delle patologie muscolari caratterizzate da una drastica diminuzione del numero di cellule satelliti (Lepper et al., 2011; Sambasivan et al., 2011b). Grazie a tali modelli è stato dimostrato che le cellule satelliti sono necessarie per garantire una corretta rigenerazione muscolare e che altri progenitori cellulari con capacità miogenica nota, come ad esempio le PICs, non possono compensare l'assenza delle cellule satelliti (Lepper et al., 2011; Sambasivan et al., 2011b). Queste osservazioni hanno condotto a formulare l'ipotesi di un "livello soglia" o *quorum*, ossia di un numero minimo di cellule satelliti necessarie per assicurare una corretta rigenerazione muscolare, numero al di sotto del quale il processo rigenerativo è compromesso e si assiste ad una deposizione di tessuto fibrotico e adiposo (Sambasivan et al., 2011b). **Il secondo scopo di questo lavoro è dunque chiarire il ruolo delle PICs nel muscolo adulto e le possibili interazioni con le cellule satelliti**, durante fenomeni quali l'ipertrofia muscolare e la rigenerazione. Un'analisi del trascrittoma delle PICs e delle cellule satelliti isolate da topi giovani ha rivelato che gli effettori della via di trasduzione del segnale dell'AcvR2B sono diversamente espressi tra le PICs e le cellule satelliti, suggerendo l'esistenza di una comunicazione tra questi due tipi cellulari. Abbiamo dimostrato che *in vitro* le PICs esercitano un effetto promiogenico sulle cellule satelliti attraverso la secrezione di IGF-1 e follistatina, molecole che agiscono antagonizzando la via del segnale dell'AcvR2B nelle cellule satelliti. Per meglio definire tale interazione *in vivo*, abbiamo utilizzato una forma solubile dell'AcvR2B (RAP-031, Acceleron Pharma, USA) che compete con l'AcvR2B endogeno per il legame alle relative molecole attivatrici. Abbiamo osservato che la somministrazione per via intraperitoneale di RAP-031 in topi adulti causa una notevole alterazione della nicchia delle cellule staminali attraverso un aumento del numero delle cellule satelliti e, in misura maggiore, delle PICs. La somministrazione di RAP-031 non recupera in modo significativo le poche cellule satelliti presenti in un modello murino di deplezione delle cellule satelliti ($Pax7^{DTR/+}$)

(Sambasivan et al., 2011b), nonostante il significativo e notevole aumento delle PICs. Avendo dimostrato in precedenza in questo lavoro che le PICs adulte includono una sottopopolazione di cellule a capacità miogenica, abbiamo investigato la possibilità che tale popolazione cellulare potesse essere mobilitata *in situ* nel modello murino $Pax7^{DTR/+}$ attraverso l'inibizione della via di trasduzione dell'AcvR2B. I risultati ottenuti hanno mostrato che, in muscoli privati delle cellule satelliti, il trattamento con RAP-031 è in grado di migliorare l'omeostasi tissutale in seguito a danno, attraverso una riduzione della deposizione di tessuto fibrotico e adiposo ed un significativo recupero della capacità rigenerativa. Tramite uno studio di "lineage tracing", abbiamo inoltre dimostrato che l'aumento delle fibre rigeneranti in tali condizioni è dovuto a fusione delle cellule satelliti sopravvissute all'ablazione e non coinvolge altri progenitori cellulari, ad esempio le PICs, confermando risultati ottenuti da studi precedenti (Lepper et al., 2011; Sambasivan et al., 2011b). Proponiamo, quindi, che il marcato aumento delle PICs causato dall'inibizione della via di trasduzione del segnale dell'AcvR2B sia in grado di creare un microambiente promiogenico, attraverso un aumentato rilascio di fattori quali IGF-1 e follistatina, capace di stimolare le cellule satelliti residue promuovendo la rigenerazione. I nostri studi di "lineage tracing" indicano che la maggioranza delle fibre rigenerate nel modello murino $Pax7^{DTR/+}$ in seguito a inibizione della via di trasduzione dell'AcvR2B deriva dalle cellule satelliti residue, tuttavia non possiamo escludere che le PICs o altri progenitori muscolari partecipino alla rigenerazione muscolare quando il compartimento delle cellule satellite è intatto. Questa questione richiederà ulteriori studi e la creazione di nuovi modelli murini con marcatori specifici della genealogia delle PICs miogeniche. Questi risultati indicano che future strategie terapeutiche per il miglioramento del potenziale rigenerativo del muscolo scheletrico in patologie croniche dovranno includere terapie mirate alla nicchia delle cellule staminali.

Alcuni muscoli, tuttavia, come i muscoli extraoculari (EOMs, ExtraOcular Muscles), sono resistenti a diverse distrofie muscolari (Porter et al., 1995; Porter, 2002). Ciò suggerisce l'esistenza di meccanismi endogeni muscolo-specifici presenti nella nicchia delle cellule staminali capaci di regolare in maniera più efficiente i processi rigenerativi. **Il terzo scopo di questo lavoro è di analizzare la nicchia delle cellule staminali dei muscoli extraoculari in topi wild-type e nel modello murino *mdx***. Abbiamo osservato che gli EOMs possiedono per tutto l'arco della vita postnatale un numero di PICs più elevato rispetto alle cellule satelliti, contrariamente ai muscoli scheletrici degli arti in cui le PICs e le cellule satelliti sono presenti ad un rapporto costante 1:1 durante la crescita postnatale e l'età adulta. Abbiamo osservato che questo rapporto è alterato nei muscoli degli arti provenienti da topi anziani (18 mesi), con una forte diminuzione del numero delle PICs. Il rapporto tra questi due tipi cellulari è conservato negli EOMs, nonostante il declino nel numero di PICs e cellule satelliti con l'età negli EOMs come nei muscoli degli arti. L'analisi della nicchia delle cellule staminali degli EOMs di topi *mdx* non ha mostrato particolari differenze rispetto ad animali wild-type, a conferma dell'osservazione che gli EOMs di topi *mdx* non presentano segni patologici tipici della distrofia muscolare di Duchenne. E' tuttavia interessante notare che il processo rigenerativo tipicamente osservato nei muscoli degli arti dei topi *mdx* induce un aumento del numero delle PICs e delle cellule satelliti a livelli paragonabili a quelli osservati negli EOMs di animali wild-type. Ciò lascia supporre che meccanismi normalmente presenti durante la rigenerazione muscolare capaci di promuovere eventi come la sopravvivenza cellulare, l'attivazione e il differenziamento dei progenitori cellulari, siano intrinseci alla nicchia delle cellule staminali degli EOMs. Ulteriori analisi di questo particolare tipo di muscoli scheletrici potranno svelare elementi utili per progettare trattamenti terapeutici per vari tipi di miopatie congenite, così come per l'atrofia muscolare.

INTRODUCTION

1. The postnatal skeletal muscle stem cell niche

Skeletal muscle is composed of post-mitotic multinucleated myofibers that constitute the minimal functional unit responsible for voluntary muscular contraction (Yin et al., 2013). In 1961, Alexander Mauro described a subset of cells in postnatal skeletal muscle that he called "satellite cells" because of their localization underneath the basal lamina but outside the myofiber plasma membrane (Mauro, 1961). Since this discovery, a significant effort by many laboratories has confirmed that satellite cells are the major muscle progenitor cell in postnatal skeletal muscle underlying both muscle regeneration and postnatal growth (Relaix and Zammit, 2012; Yablonka-Reuveni, 2011). In the past decade, other resident cell progenitor populations have been discovered, indicating that the muscle stem cell niche is more complex than previously thought and that multiple cell types are important regulators of muscle growth and regeneration (Pannerec et al., 2012). As such, these cells provide novel therapeutic targets for genetic diseases or chronic disorders in which the muscle stem cell niche is compromised (Pannerec et al., 2012).

1.1. Satellite cells

1.1.1. Origin and role of satellite cells during muscle growth

Adult satellite cells express the *Pax7* gene, both in a quiescent and activated state (Sambasivan and Tajbakhsh, 2007). Satellite cells express other specific markers, such as M-cadherin (Irintchev et al., 1994) and α7-integrin (Burkin and Kaufman, 1999; Yin et al., 2013), and can be detected by using the SM/C-2.6 antibody (Fukada et al., 2004). Trunk and limb muscles, as well as their satellite cell compartment, derive from *Pax3*$^{+}$ muscle progenitor cells (MPCs) migrating from the hypaxial domain of the

somites during embryonic development (Gros et al., 2005; Relaix et al., 2005; Schienda et al., 2006). These MPCs express *Pax7* and undergo myogenic differentiation coupled with progenitor cell expansion (Kanisicak et al., 2009). The myogenic program includes a specific sequence of gene expression involving initial activation of *Myf5* and *MyoD*, which in turn activate the expression of terminal differentiation genes including myogenin leading to cell cycle exit (Bismuth and Relaix, 2010; Sassoon et al., 1989; Shih et al., 2008). *Myogenin* promotes expression of genes coding for structural and contractile proteins of the myofibers, such as the myosin heavy chain (MHC) (Wright et al., 1989). Myoblasts which have exited the cell cycle then fuse with each other to generate multinucleated myofibers (Bismuth and Relaix, 2010). Some undifferentiated proliferating MPCs become enveloped by the basal lamina surrounding the emerging fibres and constitute the future pool of satellite cells in postnatal life (Bismuth and Relaix, 2010; Yin et al., 2013). A switch in the myogenesis program occurs at birth and a part of the proliferating satellite cells starts entering quiescence, while the remaining satellite cells complete fusion to the existing myofibers to support postnatal muscle growth until 3 weeks of postnatal life in mice (Bismuth and Relaix, 2010). At birth, *Pax7*$^{-/-}$ mice have normal muscles and are morphologically indistinguishable from their wild-type littermates, indicating that *Pax7* expression is not required during embryonic development (Relaix et al., 2006; Seale et al., 2000). However, *Pax7* expression is necessary after birth to promote satellite cell survival (Relaix et al., 2006). *Pax7*$^{-/-}$ mice fail to grow properly and are incapable of muscle regeneration and typically die around 14 days after birth (Seale et al., 2000). Recent studies using inducible *Pax7* knock-out mouse models confirm a strict requirement for *Pax7* after birth until 3 weeks of postnatal life indicating the different genetic requirements for satellite cells during embryogenesis, postnatal growth and adult stages (Lepper et al., 2009; Lepper et al., 2011; Sambasivan et al., 2011b).

Unlike trunk and limb MPCs, head muscles are derived from the most anterior portion of the mesoderm, called cranial mesoderm, which does not undergo segmentation into somites during embryonic development (Sambasivan et al., 2011a). The early genetic programs underlying head muscle formation are different in limb and trunk muscles, however (Harel et al., 2009; Shih et al., 2008). All head muscles except for the extraocular muscles (EOMs) derive from the paraxial portion of the cranial mesoderm and require *Tbx1* as initiator of the MPC commitment program (Kelly et al., 2004; Sambasivan et al., 2009). The subset of EOMs originates from the prechordal cranial mesoderm (PCM), which is located anterior to the notochord and develops separately from the rest of the cranial mesoderm to later dislocate caudally and fuse with it (Evans and Noden, 2006; Noden and Francis-West, 2006; Noden and Schneider, 2006; Sambasivan et al., 2011a). MPCs from the EOMs strictly require *Pitx2* for their survival and for subsequent expression of EOM fiber specific genes (Kitamura et al., 1999; Zacharias et al., 2011; Zhou et al., 2011). In contrast, the genetic program driving commitment of head MPCs, including those originating the EOMs involve genes common to trunk and limb MPCs (i.e. *Myf5*, *MyoD* and *myogenin*) (Sambasivan et al., 2009; Sambasivan et al., 2011a).

1.1.2. Role of satellite cells during regeneration

Satellite cells enter the G0 cell cycle phase after completing postnatal muscle growth (Bismuth and Relaix, 2010; Buckingham and Montarras, 2008). This quiescent state is characterized by the expression of *Pax7* in the absence of downstream markers such as *MyoD* or *myogenin* (Relaix and Zammit, 2012; Yin et al., 2013). Several soluble cytokines and molecules released by the surrounding cells (myofibers, microvasculature, interstitial cells, neuromuscular junctions and circulating or resident immune cells) as well as systemic factors maintain this quiescent state in satellite cells (Ten Broek et al., 2010). Moreover, the physical interactions

with the sarcolemma and the basal lamina also regulate satellite cell quiescence (Ten Broek et al., 2010; Yin et al., 2013). Freshly isolated satellite cells will spontaneously re-enter the cell cycle and activate the myogenic differentiation program (Musaro and Barberi, 2010), however contact with the myofiber is not sufficient to drive quiescence suggesting that other factors coming from the environment are needed (Beauchamp et al., 2000; Keire et al., 2013). Satellite cells are able to re-enter the cell cycle in response to an acute injury or prolonged exercise and will execute that myogenic program through the expression of *Myf5* and *MyoD* to generate a myoblast pool which then becomes committed to fuse to damaged fibres and generate new fibres (Yin et al., 2013; Zammit et al., 2006a; Zammit et al., 2006b). Some activated $MyoD^+$ satellite cells then turn off *MyoD* expression and return to a quiescent state, conferring to satellite cells the status of real stem cells, as they are also able to self-renew and refill their pool (Yin et al., 2013; Zammit, 2008; Zammit et al., 2006a).

1.2. Non-satellite cell progenitor populations

In addition to satellite cells, other progenitor populations in postnatal skeletal muscle have been described, including pericytes, side population cells, $\beta4\text{-integrin}^+$ interstitial cells, interstitial adipogenic progenitors and PICs (Pannerec et al., 2012; Yin et al., 2013).

1.2.1. Pericytes

Pericytes are vessel-associated cells and are considered to be the adult counterpart of the embryonic mesoangioblasts (MABs) (Dellavalle et al., 2011; Dellavalle et al., 2007; Tonlorenzi et al., 2007). Although MABs can be isolated from embryonic dorsal aorta and express endothelial markers, such as CD31, pericytes are found around small vessels of postnatal skeletal muscles and heart and do not express endothelial markers but they can be identified

through other specific markers such as alkaline phosphatase (ALP), neuronal-glial antigen 2 chondroitin sulfate proteoglycan (NG2), cluster of differentiation-146 (CD146) and platelet-derived growth factor receptor beta (PDGFRβ) (De Angelis et al., 1999; Dellavalle et al., 2007; Tonlorenzi et al., 2007). Nonetheless, similar to the situation with MABs, pericytes can be isolated from different species (mouse, dog, human), proliferate in culture and undergo differentiation into several mesodermal lineages including osteoblasts, chondroblasts, adipocytes, smooth muscle cells and myoblasts following appropriate stimulation *in vitro* (Barbuti et al., 2010; De Angelis et al., 1999; Dellavalle et al., 2007; Doherty et al., 1998; Farrington-Rock et al., 2004; Tonlorenzi et al., 2007). In addition, pericytes injected into the systemic blood circulation of dystrophic mice are able to invade skeletal muscles and replace degenerated fibres as well as colonize the satellite cell niche (Dellavalle et al., 2011; Sampaolesi et al., 2006). Pericytes also play a role during normal unperturbed perinatal muscle growth by contributing to the growth of a minor amount of myofibers and by replenishing the satellite cell pool (Dellavalle et al., 2011). However, this contribution is minimal in adulthood and does not increase after injury, demonstrating that local resident pericytes do not directly participate in myofiber repair in the adult (Dellavalle et al., 2011). Pericytes constitute an heterogeneous population with regard to cell fate: two subpopulations of NG2+ pericytes have been recently described, one with myogenic capacity ($PDGFR\alpha^{-}$ $Nestin^{-}$) and one with adipogenic capacity ($PDGFR\alpha^{+}Nestin^{+}$) (Birbrair et al., 2013). Moreover, pericytes isolated from adult human brain can be reprogrammed *in vitro* to differentiate into neurons after retroviral-transduction with the neuronal differentiation regulators Sex Determining Region Y-Box 2 (Sox2) and mammalian achaete scute homolog-1 (Mash1) demonstrating a high plasticity in these cells (Karow et al., 2012).

1.2.2. β4-integrin$^+$ cells

It has been shown recently that β4-integrin is expressed in a population of cells located in the interstitium (Liadaki et al., 2012). A subset of the β4-integrin$^+$ cells coexpress the endothelial marker CD31, however no β4-integrin$^+$ cell expresses NG2 or Pax7, indicating that these cells are distinct from pericytes and satellite cells (Liadaki et al., 2012). The β4-integrin$^+$ cells are highly myogenic, as they are able to differentiate into myotubes *in vitro* and repair damaged myofibers following engraftment *in vivo*, whereas the β4-integrin$^-$ cells do not share this behaviour (Liadaki et al., 2012). This study raises the possibility of an overlap of these described β4-integrin$^+$ cells with a subpopulation of endothelial cells with myogenic capacity that has been described in human (Okada et al., 2008; Zheng et al., 2007) and possibly in mouse (Tamaki et al., 2002). Human myogenic endothelial cells also exhibit chondrogenic and osteogenic capacity (Zheng et al., 2013), however these cell fates were not tested for the β4-integrin$^+$ cells (Liadaki et al., 2012).

1.2.3. Side population cells

Side population (SP) cells have been isolated from several tissues, notably hematopoietic stem cells (HSCs), based upon their capacity to exclude Hoesch33342 dye via the ATP-binding cassette sub-family G-member 2 transporter (Abcg2). SP cells exhibit a pronounced capacity to repopulate the stem cell niche (Bunting, 2002; Zhou et al., 2001). In skeletal muscle, SP cells can be found in the interstitium and express Sca1 and CD45, but no known markers for satellite cells but nonetheless can differentiate into myotubes *in vitro* or in myoblasts co-cultures (Asakura et al., 2002; Doyle et al., 2011; Meeson et al., 2004). Muscle SP cells can also efficiently participate in myofiber repair and satellite cell pool replenishment following engraftment (Doyle et al., 2011; Meeson et al., 2004). However, even though Abcg2$^+$ cells markedly

increase after injury, they do not directly contribute to myofiber repair *in situ* and *Abcg2*$^{-/-}$ mice display an impaired regenerative response primarily due to disruption of proper macrophage recruitment (Doyle et al., 2011). Interestingly, a small subset of satellite cells are Abcg2^{+}Sca1^{+} cells, in contrast to the Abcg2^{-}Sca1^{-} majority of satellite cells, and efficiently engraft in injured muscles (Tanaka et al., 2009).

1.2.4. Interstitial adipogenic progenitors

In 2010, two independent reports described the isolation of a skeletal muscle resident cell population with adipogenic potential. In one study, these cells were described as CD45^{-}CD31^{-} CD34^{+}Sca1^{+} cells, also called fibroadipogenic progenitors (FAPs) (Joe et al., 2010) whereas the second group described the isolation of CD45^{-}CD31^{-}SM/C-2.6^{-}Sca1^{+}PDGFRα^{+} cells, which are able to differentiate into fibroblasts, adipocytes and osteoblasts in culture (Uezumi et al., 2010). FAPs also express PDGFRα (Joe et al., 2010). Further analyses showed the existence of a common Sca1^{+}PDGFRα^{+} progenitor cell type responsible for adipose tissue and fibrosis deposition, thus confirming that these two populations constituted the same cell type (Uezumi et al., 2011). These progenitor cells, here referred to as interstitial adipogenic progenitors (IAPs), do not express Pax7, α7-integrin or other satellite cells markers and do not share a common developmental origin with satellite cells (Joe et al., 2010; Uezumi et al., 2010)). IAPs are not able to directly participate to myofiber repair nor to undergo adipocyte differentiation *in vivo* although they are activated following injury (Joe et al., 2010; Uezumi et al., 2010). In experimental models promoting compromised muscle regeneration and fibrosis, these progenitors differentiate in adipocytes and lead to fat and fibrotic tissue deposition following engraftment (Joe et al., 2010; Uezumi et al., 2010). Importantly, FAPs were described to promote differentiation of satellite cells *in*

vitro, suggesting important interactions between these two populations within the muscle stem cell niche (Joe et al., 2010).

1.2.5. PICs

Our laboratory described that *PW1/Peg3* gene identifies both the satellite cells and a subset of interstitial cells which do not express satellite cell markers, nor CD31 nor smooth muscle actin (Sma) in juvenile muscle (Mitchell et al., 2010). These $PW1^{+}$ Interstitial Cells termed PICs, were isolated from limb muscles after a negative selection for erythrocyte and haematopoietic stem cell markers Ter119 and CD45 and a positive selection for CD34 and Sca1 (Mitchell et al., 2010). The $Sca1^{+}$ cells can be subdivided into two subpopulations based on the level of Sca1 expression: $Sca1_{MEDIUM}$ and $Sca1_{HIGH}$ (Mitchell et al., 2010). PICs are present at high purity in the $Sca1_{MEDIUM}$ population (>80%), whereas they only accounted for about 50% of $Sca1_{MEDIUM}$ population (Mitchell et al., 2010). Due to the absence of specific markers for FACS isolation of PICs, all the *in vitro* and *in vivo* analyses were performed initially using the $Sca1_{MEDIUM}$ PICs (Mitchell et al., 2010). In culture, PICs display a bipotent cell fate capacity as they can spontaneously generate smooth muscle cells and myotubes (Mitchell et al., 2010). We demonstrated that PICs were not derived from $Pax3^{+}$ progenitors during development, indicating that they do not share the same origin with satellite cells (Mitchell et al., 2010). Moreover, after engraftment *in vivo* into injured muscles, they are able to repair the damaged myofibers as well as replenish both the satellite cell and their own niche (Mitchell et al., 2010). PIC number declined after birth, however in homeostatic muscles PICs remain in a 1:1 ratio with satellite cells (Mitchell et al., 2010). Nonetheless, PICs increased following muscle injury and interestingly in $Pax7^{-/-}$ mice, where they are present at even increased numbers (Mitchell et al., 2010), suggesting that the deregulation of a cell component may have dramatic consequences on the entire stem cell niche.

The role of PW1/Peg3 in progenitor cells in skeletal muscle has not been fully elucidated. Previous studies from our group showed that *PW1* is expressed *in vivo* during early embryonic mesoderm and then downregulated as tissues differentiate (Relaix et al., 1996). A similar downregulation of *PW1* is seen in primary myoblasts as well as myogenic cell line C2C12 *in vitro* (Coletti et al., 2002; Nicolas et al., 2005; Relaix et al., 1996; Schwarzkopf et al., 2006).

Our group recently generated a $Pw1^{IRESnLacZ}$ transgenic reporter mouse model where a nuclear operon lactose gene (nLacZ) was inserted into the exon 9 of the *PW1* gene locus using bacterial artificial chromosome (BAC) recombination technology (Besson et al., 2011). Through this model, PW1 was found to be expressed in stem/progenitor populations of all tissues examined in the adult, including skeletal muscle, intestine, testis, central nervous system, bone marrow and skin (Besson et al., 2011). In particular, the PW1 expression is tightly associated with stem cell competence and self-renewal capacity (Besson et al., 2011). Previous studies reported that PW1 participates in the tumor necrosis factor-alpha (TNFα) inflammatory pathway as well as the p53-mediated cell stress response leading to growth arrest and regulation of the myogenic differentiation (Coletti et al., 2002; Nicolas et al., 2005; Relaix et al., 2000; Relaix et al., 1998; Schwarzkopf et al., 2006). Taken together, these data suggest a role for PW1 in mediating cell stress responses in adult stem cells as well as cell fate outcomes.

2. Interactions within the muscle stem cell niche

Satellite cells have long been considered to be the only muscle progenitor underlying postnatal muscle growth and regeneration (Relaix and Zammit, 2012; Wang and Rudnicki, 2012; Yin et al., 2013). The discovery of multiple resident as well as non-resident progenitor populations with or without myogenic capacity raised fundamental issues concerning the direct or indirect contribution that these "alternative" populations to muscle growth and regeneration as well as the importance of satellite cells in orchestrating these processes (Pannerec et al., 2012). These findings also raised the question as to whether it would be possible to improve muscle regeneration by stimulating or engrafting non-satellite cell progenitors in pathological settings where the satellite cell pool is reduced or has lost regenerative capacity as found in congenital muscular dystrophies, muscle atrophy or other muscle degenerative disorders (Johns et al., 2013; Mann et al., 2011; Sakuma and Yamaguchi, 2013; Serrano et al., 2011). The emerging idea from these studies is that the skeletal muscle stem cell niche is a complex environment in which cell-cell interactions are finely regulated to assure normal growth and regeneration and that the deregulation of any component compromises tissue homeostasis and repair.

2.1. Regulation of muscle regeneration

Adult skeletal muscle is a stable tissue with negligible cellular turn-over, but able to efficiently regenerate in response to tissue damage (Yin et al., 2013). Muscle regeneration is a complex phenomenon involving satellite cells as well as other local cell populations and a precise sequence of molecular and cellular events (Tabebordbar et al., 2013) (**Fig. 1**).

After damage, necrotic myofibers release chemotactic factors for circulating neutrophils, which are recruited 1-6 hours after injury (Tabebordbar et al., 2013; Ten Broek et al., 2010; Yin et al.,

2013). Proinflammatory macrophages, called M1, then invade the damaged site, reaching a peak at 24 hours after damage, and secrete TNFα, interleukin-1 (IL-1) and other inflammatory cytokines able to promote phagocytosis of cellular debris (Tabebordbar et al., 2013; Ten Broek et al., 2010; Yin et al., 2013). 2-4 days after injury, anti-inflammatory macrophages, called M2, massively colonize the damaged tissue, where they reside until the end of regeneration, and secrete anti-inflammatory cytokines such as IL-10 as well as promyogenic factors, such as IGF-1 and hepatocyte growth factor (HGF), which promote satellite cell activation and proliferation (Tabebordbar et al., 2013; Ten Broek et al., 2010; Yin et al., 2013). Satellite cells in turn secrete attractive and stimulating factors for immune cells (Chazaud et al., 2003). Active immune cells also secrete a variety of matrix metalloproteinases, which contribute to the release of growth factors bounded to the molecules of the extracellular matrix and also properly direct the remodelling of muscle tissue structure (Carmeli et al., 2004; Yin et al., 2013). Several members of the fibroblast growth factor (FGF) family are also involved in muscle regeneration, although their exact role has still to be fully elucidated (Ten Broek et al., 2010; Yin et al., 2013). Inflammatory cells are fundamental, especially in the early phases after damage, as regeneration fails if recruitment of these cells is prevented (Lescaudron et al., 1999).

IAPs and other populations of interstitial cells are additional key regulators of the regenerative process (Joe et al., 2010; Murphy et al., 2011; Uezumi et al., 2010). After injury, quiescent IAPs initiate a rapid and massive proliferation and accumulate in the damaged site (Joe et al., 2010; Uezumi et al., 2010; Uezumi et al., 2011). In co-culture experiments, IAPs favor satellite cell differentiation and their differentiation into adipocytes is inhibited in presence of myofibers, suggesting an important role during *in vivo* regeneration (Joe et al., 2010; Rodeheffer, 2010; Uezumi et al., 2010). Moreover, genetic depletion of $Tcf4^{+}$ fibroblasts results in a precocious differentiation of satellite cells after injury,

depletion of the satellite cell pool and impaired myofiber formation (Murphy et al., 2011), indicating that other interstitial cell subpopulations regulate muscle regeneration. The vasculature is another important player during muscle regeneration: vascular endothelial growth factor (VEGF) and platelet-derived growth factor (PDGF) secreted by endothelial cells stimulate local angiogenesis, thus providing oxygen and nutrients (Yin et al., 2013). Differentiating satellite cells and active immune cells are able to release these factors and satellite cells in turn secrete factors stimulating endothelial cells (Ten Broek et al., 2010).

At the end of the regeneration process, signals coming from activated satellite cells, myofibers and immune cells, as TGFβ1 and myostatin (MST), inhibit further activation of the myogenic program so that the repaired muscle can re-enter an homeostatic resting condition (Ten Broek et al., 2010).

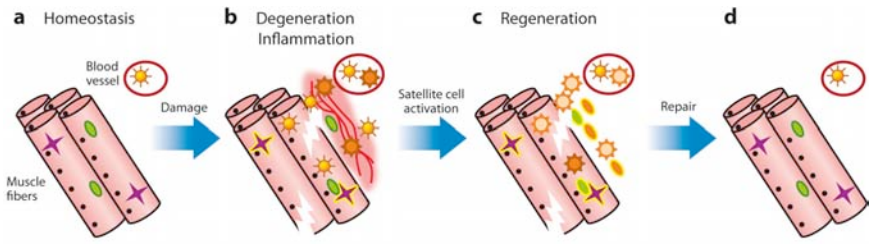

Figure 1. **The muscle regeneration process**. In normal homeostatic muscle (a), satellite cells (green) as well as IAPs (purple) are in a quiescent state. After an acute injury (thunder), circulating macrophages are attracted to the damaged site and start an inflammation response that culminates with the activation of satellite cells (b). Activated satellite cells repair the damaged myofibers, and this process is sustained by IAPs as well as anti-inflammatory macrophages (c). Once muscle fibres are completely repaired, both satellite cells and IAPs return to a quiescent state. Adapted from Tabebordbar et al., 2013.

2.2. Deregulation of muscle regeneration

Several murine models have been generated in which satellite cells are specifically ablated providing compelling evidence that satellite cells are strictly required for proper muscle regeneration (Lepper et al., 2011; Murphy et al., 2011; Relaix and Zammit, 2012; Sambasivan et al., 2011b). The satellite cell population is not completely eliminated in these satellite cell depletion models such that 5-10% of the population is spared (Sambasivan et al., 2011b) suggesting that a minimal number or quorum of satellite cells is required for proper regeneration (Sambasivan et al., 2011b). While proper regeneration does not occur when satellite cells are reduced in number, there is a significant accumulation of ectopic fat and fibrotic tissue (Lepper et al., 2011; Sambasivan et al., 2011b). Although these models demonstrate a key role for satellite cells, it has also been shown that muscle regeneration is severely compromised in the absence of interstitial cells consistent with the hypothesis that non-satellite cell progenitors play an important role for proper satellite cell function (Murphy et al., 2011). These results have particular bearing on a number of clinical settings including physiological age-related sarcopenia, cachexia (muscle atrophy) and muscular dystrophies in which patients show severely compromised regenerative capacity coupled with fat and fibrotic accumulation and a markedly reduced number of satellite cells (Sakuma and Yamaguchi, 2013; Serrano et al., 2011). It is therefore important to understand why the remaining satellite cells cannot compensate and expand further to properly execute the regenerative program. It has been shown that a small number of satellite cells (< 20) can generate thousands of muscle fibres and repopulate the satellite cell compartment when engrafted into healthy muscle tissue (Sacco et al., 2008). These data lead to the model that prolonged muscle disease alters the stem cell environment that further compromise the competence and potential of few remaining satellite cells.

Consistent with this notion, members of the TGFβ pathway have been shown to promote fibrosis in muscle tissue (Bernasconi et al., 1999; Serrano et al., 2011). These include TGFβ1, TGFβ2, TGFβ3 as well as PDGF, which are upregulated in muscles displaying a high level of fibrosis, as the diaphragm in mdx mice, a murine model for Duchenne muscular dystrophy (DMD) (Bernasconi et al., 1995; Partridge, 2013; Zhao et al., 2003; Zhou et al., 2006). In addition, transgenic mice displaying a constitutively active PDGFRα exhibit systemic fibrosis, including in the skeletal muscles (Olson and Soriano, 2009). These molecules are able to target IAPs by inducing proliferation and expression of ECM-related genes associated to fibrosis (Uezumi et al., 2011), indicating that IAPs are an important source of fibrosis when muscle regeneration signals are altered. Interestingly, IAPs are able to differentiate into adipocytes *in vivo* only in models where regeneration is defective, such as glycerol-injected muscles, indicating that an altered microenvironment can have profound effects on these cells (Joe et al., 2010; Uezumi et al., 2010). Furthermore, several reports showed that satellite cells exhibit a fibrogenic fate switch as well as lower regenerative capacity and increased apoptosis in aged mice but can be restored to normal adult function when exposed to circulating factors of young mice (Brack et al., 2007; Conboy et al., 2005; Day et al., 2010; Smythe et al., 2008). These data confirm the importance of the environment in regulating satellite cell biology and also that an altered niche, as the niche in aged or chronically ill individuals, account for satellite cell altered capacities.

2.3. TGFβ and IGF-1 pathways

TGFβ and IGF-1 pathways are key regulators of muscle homeostasis and the balance of these signals is altered in sarcopenia, muscle atrophy and chronic diseases (Glass, 2010).

One of the most studied TGFβ signaling pathway in skeletal muscle is triggered by the binding of specific extracellular ligands

to the activin transmembrane receptor (AcvR) type-2B (AcvR2B), which in turn binds to type-1 co-receptors Alk-4 or Alk-5 leading to the phosphorylation of intracellular Smad proteins and their subsequent translocation to the nucleus where they control gene expression and cell cycle arrest (Joulia et al., 2003; Rebbapragada et al., 2003; Zhu et al., 2004). Ligands for the AcvR2B include MST, growth/differentiation factor 11 (GDF-11/BMP-11) and activin A, while antagonists of this pathway are follistatin (FST), follistatin-like 3 (FSTL-3), GASP-1/GASP-2 and the myostatin propeptide (Amthor et al., 2004; Hill et al., 2002; Lee et al., 2010; Lee and McPherron, 2001; McPherron et al., 2009; Thies et al., 2001). These molecules act through different combinations of type-2 and type-1 receptors and show promiscuity for receptor binding, with a preference for the co-receptor type-1 depending on the cell type (Kemaladewi et al., 2012; Rebbapragada et al., 2003). For instance, MST can bind at high affinity to AcvR2B and at lower affinity to AcvR2A and has a preference for Alk-4 in myoblasts and for Alk-5 in nonmyogenic cells (Kemaladewi et al., 2012). MST is a major ligand for AcvR2B and a potent negative regulator of muscle growth, which blocks myogenic progression (Joulia et al., 2003; Lee and McPherron, 2001; McPherron et al., 1997; Rios et al., 2002; Thomas et al., 2000). *Mst*-null ($Mst^{-/-}$) mice display a massive increase in muscle mass concomitant with a decrease in fat accumulation coupled with improved muscle regeneration and reduced fibrosis following injury (McCroskery et al., 2005; McPherron et al., 1997; McPherron and Lee, 2002). Natural occurring mutations in *Mst* have been described in cattle (Grobet et al., 1997; Kambadur et al., 1997; Oldham et al., 2001), dog (Mosher et al., 2007; Shelton and Engvall, 2007), sheep (Clop et al., 2006) and human (Schuelke et al., 2004), all displaying an increase in muscle mass similar to $Mst^{-/-}$ mice.

Igf-1 is a multi-exon gene which undergoes alternative splicing to generate different isoforms that act either locally (non-diffusible) or diffusibly as a function of tissue type and age (Oberbauer, 2013). Transcripts containing exon 1 are referred to as

"class 1", while those containing exon 2 are referred to as "class 2" (Oberbauer, 2013; Philippou et al., 2007). IGF-1 isoforms also differ on the basis of their carboxy-terminus: in mouse, subclass named Ea includes exon 6 but not exon 5, while subclass Eb includes exon 5 and only a portion of exon 6 (Oberbauer, 2013; Philippou et al., 2007; Shavlakadze et al., 2005), although this splicing pattern is different for human IGF-1 (Adamo et al., 1993). The biological significance of these isoforms is still unclear, however class 1 transcripts have been proposed to act in an autocrine/paracrine way, while class 2 transcripts to be the circulating isoform (Gilmour, 1994; Oberbauer, 2013; Sussenbach et al., 1992). The *Igf-1* promoter contains response elements to growth hormone (GH) as well as steroid hormones (androgens and estrogens) (Gentile et al., 2010; Hewitt et al., 2010; O'Sullivan et al., 2002a; O'Sullivan et al., 2002b; Ohtsuki et al., 2007) and also contains a binding site for MyoD (McLellan et al., 2006), indicating an important role for IGF-1 during myogenic progression. The binding of IGF-1 to its transmembrane receptor (IGF-1R) is a potent activator of phosphatidylinositol-3 kinase (PI3K)/Akt intracellular response (Oberbauer, 2013; Rommel et al., 2001). Activation of Akt results in the downstream activation of the mammalian target of rapamycin (mTOR) which stimulates protein synthesis and inhibits atrophy-related pathways and protein degradation (Bodine et al., 2001; Bonaldo and Sandri, 2013; Latres et al., 2005; Rommel et al., 2001). Both IGF-1 and TGFβ pathways regulate the PI3K/Akt/mTOR pathway (Glass, 2010): MST and other molecules activating the TGFβ pathway have inhibitory effects on PI3K/Akt/mTOR, which can be dominantly overcome by IGF-1 (Trendelenburg et al., 2009). Taken together, these data indicate that a balance between the TGFβ and IGF-1 pathways determines muscle homeostasis and that alterations of this balance can account for muscle atrophy and impaired regeneration. For this reason these pathways have been proposed as therapeutic targets in the case of several chronic diseases and muscle degenerative disorders. Suppression of MST or administration of soluble forms

of the AcvR2B triggers an increase in muscle mass and ameliorates prognosis of congenital myopathies, such as DMD, amyotrophic lateral sclerosis (ALS), as well as antagonize muscle wasting during sarcopenia and cancer-induced cachexia (Akpan et al., 2009; Lawlor et al., 2011; Morrison et al., 2009; Pistilli et al., 2011; Siriett et al., 2006; Wagner et al., 2002; Zhou et al., 2010a). Moreover, mice genetically over-expressing a muscle local isoform of IGF-1 exhibit myofiber hypertrophy, are protected against muscle atrophy as well as display a higher regeneration capability during aging (Musaro et al., 2001; Schulze et al., 2005). In addition to this, overexpression of IGF-1 in muscles affected by ALS is able to reduce catabolism and promote motoneuron survival (Dobrowolny et al., 2008; Dobrowolny et al., 2005; Musaro et al., 2007; Scicchitano et al., 2009).

3. A specialized case of skeletal muscles: the extraocular muscles

The extraocular muscles (EOMs) are six muscles surrounding the ocular globe responsible for eye movements in vertebrates (Bohnsack et al., 2011). These muscles do not share the same embryological origin with the other skeletal muscles of the body and display characteristics of both skeletal and cardiac muscle (Porter, 2002). Regarding innervation, adult mammalian skeletal muscles exhibit a specific pattern, with one motoneuron contacting several muscle fibres (the 'motor unit'), however EOMs also contain 15-20% of multiply innervated myofibers (Porter et al., 1995; Spencer and Porter, 1988). Moreover, contrary to the other skeletal muscles of the body, EOMs show a great heterogeneity in MHC isoforms expression at the single fiber level as well as depending on the location within the muscle (external/orbital vs. internal/global layers) (Porter, 2002; Zhou et al., 2010b): some EOM fibres retain embryonic isoforms while expressing at least one adult isoform (Brueckner et al., 1996; Jacoby et al., 1990) and some multiply innervated fibres also express α-cardiac myosin (Rushbrook et al., 1994). Finally, adult EOMs express EOM-unique MHC isoform 13 (MHC13) (Brueckner et al., 1996; Porter, 2002; Wieczorek et al., 1985). All these features probably reflect an evolutionary adaptation to a rapid control of eye movements as well as a common embryological origin with cardiac muscle (Porter, 2002). EOMs have drawn attention of the scientific community as they are selectively spared in several myopathies which progressively affect the other skeletal muscles of the body, as DMD and ALS, while they are selectively targeted by myopathies which do not affect the other skeletal muscles of the organism or only at later stages, such as the oculopharyngeal muscular dystrophy and myasthenia gravis (Abu-Baker and Rouleau, 2007; Davies et al., 2006; Khurana et al., 1995; Porter et al., 1995; Soltys et al., 2008). Some reports described the presence of activated satellite cells in uninjured normal EOMs from

different species (McLoon et al., 2004; McLoon and Wirtschafter, 2002a; McLoon and Wirtschafter, 2003; McLoon and Wirtschafter, 2002b) as well as an increase in the total number of satellite cells (McLoon et al., 2007), leading to the hypothesis that a continuous myonuclei addition to the fibres would lead to a constant remodelling of EOMs throughout life and could account for their sparing in several degenerative diseases. However none of these reports presents an exhaustive overlook of neither the satellite cell nor the entire niche status in EOMs.

Other studies suggested that intrinsic differences in EOMs could account for their resistance to degenerative diseases. Structural intrinsic properties of the EOM fibres could in fact possibly prevent their degeneration during myopathies: EOM fibres from *mdx* mice retain the dystrophin-protein complex and are more resistant to oxidative stress (Porter et al., 2003) as well as to the damages caused by the excess of intracellular calcium observed in DMD, because of an increased capacity to regulate calcium homeostasis (Pertille et al., 2010; Zeiger et al., 2010). Also differences between EOM and limb muscle gene expression profiles have been found (Khanna et al., 2004; Khanna et al., 2003; Pacheco-Pinedo et al., 2009; Porter et al., 2006; Porter et al., 2001; Porter et al., 2003), for example EOMs show increased levels of chaperones, as well as IL-10 receptor β (IL10Rβ) and several molecules involved in the TGFβ pathway, as follistatin-like 1 (Fstl-1) and TGFβ-induced protein (TGFβi) (Porter et al., 2003). Consistent with these data, SP cells isolated from EOMs exhibit increased expression of TGFβi and Fstl-1, as well as FST and bone morphogenetic proteins (BMPs) involved in the TGFβ pathway (Pacheco-Pinedo et al., 2009). In addition, differences between the orbital and global layers of EOMs have been also described: FST and IGF-binding protein-3 (IGFBP3) are more expressed in the orbital layer whereas MST is more expressed in the global layer (Khanna et al., 2004). In EOMs, TGFβ and IGF-1 pathways are able to trigger the same signals as in limb muscles, thus regulating muscle mass and force (Anderson et al., 2008; Chen and von

Bartheld, 2004). However, EOMs show interesting features, for instance Schwann cells of the EOM-related nerves constitute a major source of local IGF-1 for EOMs, which is anterogradely transported along the throclear nerve (Feng and Von Bartheld, 2010), possibly explaining the sparing of EOMs in ALS. A peculiar regulation of the TGFβ and IGF-1 pathways resulting in favour of positive signals in normal as well as diseased EOMs may account for their innate resistance to muscle degenerative disorders and regulate EOM satellite cell specific properties. EOM satellite cells can efficiently differentiate into myofibers when engrafted into limb muscles, but the EOM satellite cell-derived fibres do not express MHC13 in this location, indicating that signals coming from the EOM niche are important to regulate EOM satellite cell specific phenotype (Sambasivan et al., 2009). Progenitor populations within the niche may be involved: interestingly, microarray analysis revealed that *PW1/Peg3* is strongly upregulated in normal EOMs compared to limb muscles (Porter et al., 2003), suggesting a possible increase of *PW1* gene expression or an increase of the total number of *PW1*-expressing cells in EOMs muscles. A recent study also described the isolation of a novel subpopulation of cells from EOMs exhibiting myogenic capacity *in vitro*: these cells were isolated within the SP and were positive for CD34 but negative for Sca1, satellite cell markers (i.e. Pax7 or M-cadherin), endothelial markers and leukocyte marker CD45 (Kallestad et al., 2011). These $CD34^+$ cells were increased in adult wild-type EOMs compared to limb muscles, retained in aged EOMs as well as elevated in EOMs from *mdx* mice but absent in limb muscles from the same DMD mouse model (Kallestad et al., 2011). However, more detailed studies on the EOM stem cell niche are still missing.

AIMS

Satellite cells are the major resident progenitor population in postnatal skeletal muscle and they are strictly necessary for muscle regeneration (Relaix and Zammit, 2012), although other progenitors are also involved in regulating regeneration and probably postnatal growth (Pannerec et al., 2012). We previously described a subpopulation of interstitial cells expressing PW1 (PICs), exhibiting strong myogenic capacity *in vitro* as well as after engraftment in damaged muscles in juvenile mouse muscle (Mitchell et al., 2010). In particular, engrafted PICs can participate in myofiber repair as well as repopulate the satellite cell and PIC niches (Mitchell et al., 2010). PICs can generate smooth muscle cells in addition to skeletal muscle cells *in vitro* (Mitchell et al., 2010). Taken together, these data suggested that PICs and satellite cells are distinct and that PICs are more plastic than satellite cells. A recent report from our laboratory demonstrated that PW1 is a pan-stem cell marker in the adult (Besson et al., 2011), supporting the hypothesis that PW1-expressing cells in skeletal muscle are progenitor cells with different capacities. **The first aim of this work was to describe postnatal muscle progenitor cell fates**. We set up FACS conditions to isolate satellite cells and PICs from postnatal limb muscles using CD34 and Sca1 markers, as previously reported (Mitchell et al., 2010). In juvenile mice, PICs can be found in two populations expressing Sca1 at different levels ($Sca1_{MED}$ and $Sca1_{HIGH}$): PICs are highly enriched in the $Sca1_{MED}$ population, whereas the $Sca1_{HIGH}$ population was mixed with PW1 non-expressing cells (Mitchell et al., 2010). Our initial description of PICs was restricted to the $Sca1_{MED}$ fraction in juvenile mice (Mitchell et al., 2010). In order to characterize the PW1-expressing cells from the $Sca1_{HIGH}$ fraction in wild-type mice, we used the $Pw1^{IRESnLacZ}$ reporter mouse model generated in our laboratory (Besson et al., 2011). In parallel, we performed microarray analyses comparing juvenile $Sca1_{MED}$ PICs and satellite cells, which indicated that these two cell types have distinct

transcriptomes. We then systematically tested PICs (both $Sca1_{MED}$ and $Sca1_{HIGH}$) differentiation capacity into several lineages *in vitro* from juvenile to adult stage, investigating other possible lineages not explored in previous studies. Since recent studies have described the presence of interstitial $Sca1^{+}$ cells expressing PDGFRα with adipogenic capacity (IAPs) (Joe et al., 2010; Uezumi et al., 2010), we tested whether PICs and IAPs consisted of overlapping or distinct populations based upon both PDGFRα and adipogenic potential *in vitro*.

An understanding of the muscle stem cell niche and its cellular components provides an important knowledge base for designing therapeutic approaches for a variety of muscle diseases. In the case of muscle degenerative diseases as well as muscle atrophy induced by cancer, diabetes, heart and renal failure or ageing, skeletal muscles undergo a loss of mass and force, associated with poor prognosis and death. These myopathies are also associated with degeneration of the myofibers and a reduction in satellite cell number and/or regenerative capacity, concomitant with fibrosis and fat deposition (Mann et al., 2011). Furthermore, the abnormal increase of catabolic activity observed in atrophic muscles leads to a profound alteration of satellite cell behavior. All these conditions display activation of the AcvR2B pathway (Serrano et al., 2011; Tabebordbar et al., 2013) and inhibition of this pathway reduces the loss of muscle mass and strength (George Carlson et al., 2011; Pistilli et al., 2011; Zhou et al., 2010a). The hypertrophic effect induced by AcvR2B inhibition has been proposed to be coupled with an activation of the satellite cell compartment (McCroskery et al., 2003; McCroskery et al., 2005). Several murine models have been generated in which the satellite cell compartment can be selectively depleted leading to the proposal that a minimal number of satellite cells is necessary for proper regeneration and that other progenitors cells with myogenic capacities, such as PICs, cannot compensate under these conditions (Lepper et al., 2011; Sambasivan et al., 2011b). **The second aim of this work was to elucidate the role of PICs in adult muscle and**

their relationships with satellite cells, in context of hypertrophy and regeneration. Microarray analyses revealed that effectors of the AcvR2B pathway are differentially regulated between PICs and satellite cells suggesting a crosstalk between these two cell types. To explore niche interactions *in vivo*, we used a soluble form of the AcvR2B, (RAP-031, Acceleron Pharma, USA) which competes with the endogenous AcvR2B through competitive interactions. Previous studies using this molecule in wild-type mice, as well as murine models for DMD, ALS and other muscular diseases, revealed that RAP-031 treatment leads to an increase in muscle mass and force (Akpan et al., 2009; George Carlson et al., 2011; Koncarevic et al., 2010; Morrison et al., 2009; Pistilli et al., 2011; Pistilli et al., 2010). We then analysed the effects of the blockade of AcvR2B pathway after RAP-031 injection on muscle niche progenitors (PICs and satellite cells) in wild-type adult mice. Moreover, as previous work demonstrated that PICs show a pronounced myogenic capacity *in vitro* and after engraftment *in vivo* (Mitchell et al., 2010), we assessed whether PICs are mobilized *in situ* under conditions in which the satellite cell population is depleted (Sambasivan et al., 2011b) coupled with AcvR2B pathway inhibition.

While most studies have focused extensively on limb muscles, there are unique muscle groups that are spared in many degenerative diseases or affected only at very advanced stages of these diseases including the extra-ocular muscles (EOMs) (Porter et al., 1995). Understanding the intrinsic properties of EOMs may provide insights into endogenous protective mechanisms in skeletal muscle. It has been proposed that an altered stem cell niche underlies the resistance of EOMs in these pathologies, however, to date, no reports have provided a detailed characterization of EOM progenitor cells. **Therefore the third aim of this work was to analyze the EOM stem cell niche in wild type and DMD model (mdx) mice** in order to determine if variations in the number or activation state of PICs and satellite cells were present which could eventually explain EOM unique phenotype.

RESULTS

1. Defining the muscle stem cell niche

1.1. Juvenile PICs and satellite cells have distinct gene expression profiles

We performed transcriptome analyses (Affymetrix) using RNA from wildtype PICs and satellite cells freshly isolated from 1 week old murine limb muscles corresponding to a stage of active postnatal muscle growth. At this stage, satellite cells have not entered a completely quiescent state (Pallafacchina et al., 2010) nonetheless, PICs and satellite cells are clearly distinguishable based upon their location (sublaminal versus interstitial) and by the expression of Pax7 (satellite cells) and PW1/Peg3 (satellite cells and PICs) (Mitchell et al., 2010). We observed distinct transcriptome signatures with 1345 and 1233 genes expressed specifically in PICs and satellite cells respectively **(Fig. 2A** and **http://www.ncbi.nlm.nih.gov/geo/query/acc.cgi?acc=GSE40523)**.
Gene Ontology database analyses revealed that satellite cell-specific genes are related primarily to the skeletal muscle lineage (i.e. c-met, desmin). As expected, we observed the expression of genes known to be expressed in satellite cells and/or proliferating myoblasts (i.e. Pax7, MRFs, CXCR4, integrin-α7, FGFR4) (Fukada et al., 2007; Pallafacchina et al., 2010) (**Fig. 2B**). In contrast, PICs express genes that are associated with multiple cell fates including FoxC2 and ephrins (mesenchymal stem cells), VEGF and angiogenin (angiogenesis), and numerous genes governing cell interaction and cell migration (**Fig. 2C,D**). We confirmed the expression of PW1/Peg3 in both cell types **(http://www.ncbi.nlm.nih.gov/geo/query/acc.cgi?acc=GSE40523).**
We observed that specific growth factors and their cognate receptors were reciprocally expressed by PICs and satellite cells suggesting paracrine interactions between these two cell types (**Tables 1, 2**). We observed that PDGFRα was highly expressed in

juvenile PICs as compared to satellite cells (**Table 1**) suggesting that resident adipogenic populations (Joe et al., 2010; Uezumi et al., 2010) overlap with PICs. These analyses were performed using juvenile muscle in which the PICs and satellite cells are presumably not fully quiescent. We therefore verified the proliferative status of these populations by staining 1 week old hindlimb muscle for the cell cycle marker, Ki67. We observed that only ~15% of PICs and ~25% of satellite cells are cycling whereas the majority of these cell populations are quiescent (**Fig. 2E**). The distinct gene expression profiles observed here for juvenile satellite cells and PICs, combined with our previous analyses demonstrating that PICs do not arise from a Pax3 lineage (Mitchell et al., 2010), support the hypothesis that PICs and satellite cells are distinct progenitor populations and that PICs represent a less committed progenitor compared to satellite cells. Furthermore, despite residual postnatal proliferative activity of satellite cells used for these analyses, we noted that the satellite cells have already assumed a gene expression profile closely resembling that found in adult satellite cells (Pallafacchina et al., 2010) (and see **Fig. 5E**).

1.2. Juvenile PICs display multipotent potentials *in vitro*

We reported previously that PICs can be enriched from juvenile muscle (1-2 weeks of age) by sorting for the cell surface markers CD34 and Sca1 (Mitchell et al., 2010). At this stage, PICs are present in the $CD34^{+}Sca1^{+}$ population, which can be subdivided into two populations based on Sca1 expression levels ($Sca1_{MED}$ and $Sca1_{HIGH}$). In our previous study, we limited our analyses to the $Sca1_{MED}$ population due to the enriched number of PW1/Peg3 cells in this fraction (>90%) (Mitchell et al., 2010). We were unable to isolate the $PW1/Peg3^{+}$ cells in the $Sca1_{HIGH}$ population due to a lack of appropriate markers. We have shown previously that the $PW1^{nlacZ}$ reporter mouse allows for the purification of PW1/Peg3 expressing cells using a fluorescent

substrate (C_{12}FDG) for β−galactosidase activity from a wide array of tissues and that reporter expression corresponds to endogenous PW1/Peg3 expression with >98% fidelity in these tissues including skeletal muscle (Besson et al., 2011). We therefore used the $PW1^{nlacZ}$ reporter mouse to purify PW1/Peg3 expressing cells from juvenile muscle and observed reporter gene expression in satellite cells and in the $Sca1_{MED}$ and $Sca1_{HIGH}$ populations as expected (**Fig. 3A** and see (Besson et al., 2011; Mitchell et al., 2010). $Sca1_{MED}$ cells isolated from 1-week old muscle were >90% pure for PW1/Peg3 expression while the $Sca1_{HIGH}$ fraction contains only 60% of PW1/$Peg3^{+}$ cells (**Fig. 3A** and (Mitchell et al., 2010), confirming that reporter expression in skeletal muscle reflected faithfully endogenous PW1/Peg3 expression. We therefore used the $PW1^{nlacZ}$ reporter mouse to sort the $PW1^{+}Sca1_{HIGH}$ population to >90% purity ($Sca1_{HIGH}$ PICs) (**Fig. 3B)**. We compared and verified expression of a subset of genes from our microarray analysis in satellite cells, $Sca1_{MED}$ PICs, $Sca1_{HIGH}$ PICs, and $Sca1_{HIGH}PW1^{-}$ cells, from 1-week old hindlimb muscle (**Fig. 3C**). Neither population expressed the hematopoietic marker CD68, demonstrating the reliability of the FACS sorting (**Fig. 3C**). As expected, only the satellite cell fraction expressed Pax7, Myf5, and FGFR4 (Pallafacchina et al., 2010) consistent with our previous observations (Mitchell et al., 2010) and further demonstrating that the PIC fractions were not contaminated by satellite cells. We note that only PICs express P2Y14 and QPRT, two of the most represented genes specific to PICs in our micro-array analysis (**Table 1**). Interestingly, while all populations expressed the embryonic marker vimentin, only the $Sca1_{HIGH}$ PICs fraction expressed the mesenchymal marker Tie2, which has been shown recently to mark adipogenic progenitors suggesting a link between these populations (Uezumi et al., 2010). This correlation was further confirmed by the fact that PDGFRα is highly expressed in both PICs fractions (**Fig. 3C** and **Table 1)**. We showed previously that $Sca1_{MED}$ PICs from juvenile mouse muscle are capable of differentiating into smooth and skeletal muscle *in vitro* (Mitchell et

al., 2010). In order to test all $PW1^{+}$ populations (satellite cells, $Sca1_{MED}$ and $Sca1_{HIGH}$ PICs), we purified these fractions using 1-week old $PW1^{nLacZ}$ reporter mice and tested their myogenic and adipogenic potentials (**Fig. 3D,E**). As expected, we observed that satellite cells are highly myogenic (fusion index >80%) and do not display detectable adipogenic capacity, whereas $Sca1_{MED}$ PICs gave rise to skeletal muscle (fusion index=40%) and smooth muscle cells. In addition, the $Sca1_{MED}$ PICs gave rise to adipocytes (adipogenic potential=40%) when cultured in adipogenic media (**Fig. 3D,E**). In contrast, $Sca1_{HIGH}$ PICs displayed lower skeletal myogenic (fusion index=20%) and adipogenic potentials (30%) as compared to $Sca1_{MED}$ PICs (**Fig. 3D,E**). We noted that all PIC fractions displayed smooth muscle cell fates (**Fig. 3D**). In contrast to PICs, we found that $Sca1_{HIGH}$ $PW1^{-}$ cells adopt a smooth muscle phenotype but do not display myogenic nor adipogenic potential (**Fig. 3D,E)**.

1.3. The $Sca1_{MED}$ PICs population is restricted to early postnatal stages

Having confirmed the reliability of the $PW1^{nlacZ}$ reporter mouse and our FACS protocol in juvenile skeletal muscle, we set out to systematically isolate and test the lineage potential of $PW1/Peg3^{+}$ cells from both Sca1 expressing fractions throughout postnatal development and early adulthood. These analyses revealed a progressive decline of the $Sca1_{MED}$ fraction during the first 3 weeks of life such that it was no longer detectable 5 weeks after birth (**Fig. 4A**). During this period, we observed that the $Sca1_{HIGH}$ cell fraction increased from ~30% to ~70% of the $CD45^{-}$ $Ter119^{-}$ muscle cells (**Fig. 4B**). While the $Sca1_{HIGH}$ cells increased in number, the proportion of $PW1/Peg3^{+}$ cells declined from ~60% to ~40% (**Fig. 4C**). We isolated $PW1^{+}$ cells in the $Sca1_{HIGH}$ fraction from 7 weeks old $PW1^{nlacZ}$ reporter mouse muscle using $C_{12}FDG$ as described for the juvenile muscle (**Fig. 3B, 5A**). We verified reporter and PW1/Peg3 expression in freshly sorted

cytospun cells as previously described (Besson et al., 2011) **(Fig. 3B)**. We verified Pax7 expression to confirm the purity of the satellite and non-satellite cell fractions (**Fig. 5B**). These data revealed that the $Sca1_{MED}$ population of PICs is restricted to the first 3 weeks of postnatal life raising the question as to what stem cell potential, if any, is present in the $Sca1_{HIGH}$ population.

1.4. Adult PICs show multiple cell fates *in vitro*

We next tested the myogenic (skeletal and smooth) and adipogenic potentials of all PW1/$Peg3^{+}$ populations (satellite cells, $Sca1_{HIGH}$ PICs) in adult muscle (7 weeks) (**Fig. 5C**). As expected, adult satellite cells were highly myogenic (fusion index=80%) and did not form smooth muscle or fat. Adult PICs generated skeletal muscle (fusion index=25%), smooth muscle, and fat (adipogenic potential=60%) (**Fig. 5C,D**). In contrast, the $Sca1_{HIGH}$ PW1- cells did not show any myogenic nor adipogenic potential but adopted a smooth muscle-like phenotype. Semi-quantitative PCR analysis showed no expression of Pax7 and myogenic markers in the adult $Sca1_{HIGH}$ PICs, confirming the reliability of our purification protocol. We note that adult $Sca1_{HIGH}$ and juvenile $Sca1_{HIGH}$ PICs show a similar gene profile (**Fig. 5E**). Notably, both juvenile and adult $Sca1_{HIGH}$ PICs express Tie2 and PDGFRα, consistent with an adipogenic potential (Uezumi et al., 2010; Uezumi et al., 2011) (**Fig. 3C** and **5E**). We next examined whether cell fate potentials of PICs changed during the juvenile to adult transition. We found that the PW1/$Peg3^{-}$ cells do not display myogenic nor adipogenic capacity at all stages examined (**Figs. 6-8**). Up to 3 weeks of postnatal development, when the $Sca1_{MED}$ PIC population is still detectable, we find this fraction retains the capacity to form fat and skeletal muscle (**Figs. 6, 7**). While the $Sca1_{HIGH}$ PIC population also shows a similar cell fate potential, we noted that this fraction was more adipogenic (**Figs. 6, 7**). At 5 weeks, when we no longer detect the $Sca1_{MED}$ PICs, we observed a much higher skeletal myogenic capacity (~20%) in the $Sca1_{HIGH}$ PIC population (**Fig. 8**)

similar to what we observed at 7 weeks of age. Taken together, these results demonstrate that PW1/Peg3 identifies multiple progenitor populations in adult and juvenile skeletal muscle.

1.5. Adult PICs are composed of two subpopulations

Adult skeletal muscle contains resident progenitor cells that can adopt an adipogenic fate under pathological conditions (Joe et al., 2010; Uezumi et al., 2010). These adipogenic progenitors had been isolated previously based upon Sca1 expression (Joe et al., 2010) or coexpression of Sca1 and PDGFRα (Uezumi et al., 2010). The potential overlap of these interstitial adipogenic progenitors (referred to here as IAPs) had not been elucidated, however the population of $Sca1^{+}PDGFR\alpha^{+}$ cells is presumably contained within the $Sca1^{+}$ population. We observed that both juvenile and adult PICs expressed high levels of PDGFRα and display significant adipogenic potential (**Figs. 3, 5**). We therefore determined whether PICs and IAPs represent distinct or overlapping populations in the adult. Histological analyses of 7-weeks old mouse tibialis anterior revealed that PW1/Peg3 was co-expressed with PDGFRα in interstitial cells, however not all $PW1/Peg3^{+}$ cells express PDGFRα (**Fig. 9A**). As reported by Uezumi and colleagues (Uezumi et al., 2010), and confirmed in our studies here **(Figs. 3C** and **5E)**, PDGFRα expression is restricted to the $Sca1^{+}$ cells in muscle. We therefore isolated PDGFRα positive and negative cells from the total $Sca1_{HIGH}$ fraction to assess PW1/Peg3 expression (**Fig. 9B**). Immunostaining for PW/Peg3 and PDGFRα on freshly isolated cells revealed that all $PDGFR\alpha^{+}$ cells in the $Sca1_{HIGH}$ fraction expressed PW1/Peg3 whereas the PDGFRα negative cells from the $Sca1_{HIGH}$ fraction contained a small proportion of cells expressing PW1/Peg3 (12% ±0,9) (**Fig. 9E**). We next tested the $Sca1_{HIGH}PDGFR\alpha^{+}$ and $Sca1_{HIGH}PDGFR\alpha^{-}$ populations for myogenic and adipogenic potential and observed that adipogenic potential was restricted to the $Sca1_{HIGH}PDGFR\alpha^{+}$ population (**Fig.**

9C,D) consistent with previously reported results (Uezumi et al., 2010). The $Sca1_{HIGH}PDGFR\alpha^-$ population did not display any myogenic nor adipogenic potential. We next separated the $Sca1_{HIGH}$ population on the basis of PW1/Peg3 reporter gene expression and PDGFRα to obtain $PDGFR\alpha^+$ and $PDGFR\alpha^-$ PICs (**Fig. 10A**). As expected, the $PDGFR\alpha^+$ PICs did not form any myogenic colonies but were strongly adipogenic (adipogenic potential=60%) (**Fig. 10B,C**). These differentiated adipocytes expressed genes related to adipogenesis (FABP4/aP2) as well as genes specific to brown adipose tissue specific markers (Ucp1, Prdm16) and white/'beige' fat (Hoxc9) (**Fig. 10F**). In contrast, the $PDGFR\alpha^-$ PICs were highly myogenic (fusion index=50%) but did not display adipogenic capacity (**Fig. 10B,C**). Fraction purity was confirmed by immunofluorescence for Pax7 and PW1/Peg3 on freshly sorted cytospun cells (**Fig. 10D**) as well as by semi-quantitative PCR on freshly sorted cells (**Fig. 10E**). All PIC populations were negative for Pax7 and myogenic genes. Only the $PDGFR\alpha^+$ PICs express the adipogenic markers Tie2 and PDGFRα, as expected. Taken together, these results demonstrate that adult PICs can be separated by PDGFRα expression into two distinct populations with different cell fate potentials.

We have shown that adult PICs and juvenile $Sca1_{MED}$ and $Sca1_{HIGH}$ PICs express PDGFRα, while only adult and juvenile $Sca1_{HIGH}$ PICs express Tie2 **(Fig 3C** and **5E)**. We therefore separated juvenile (1 week) $Sca1_{MED}$ and $Sca1_{HIGH}$ PICs based on PDGFRα expression and tested their myogenic and adipogenic potentials. As expected, only the $PDGFR\alpha^-$ fractions ($Sca1_{MED}$ and $Sca1_{HIGH}$) displayed myogenic capacity (**Fig. 11**). Surprisingly, the juvenile $Sca1_{MED}PDGFR\alpha^+$ cells were weakly adipogenic (~5%) (**Fig.11**) as compared to the total $Sca1_{MED}$ fraction (~35% adipogenic potential, **Fig. 3D,E**), suggesting that cell-cell interactions regulate cell fate outcomes. Juvenile $Sca1_{HIGH}PDGFR\alpha^+$ PICs, like adult $Sca1_{HIGH}PDGFR\alpha^+$ PICs, were strongly adipogenic (~40% adipogenic potential) (**Fig.11**).

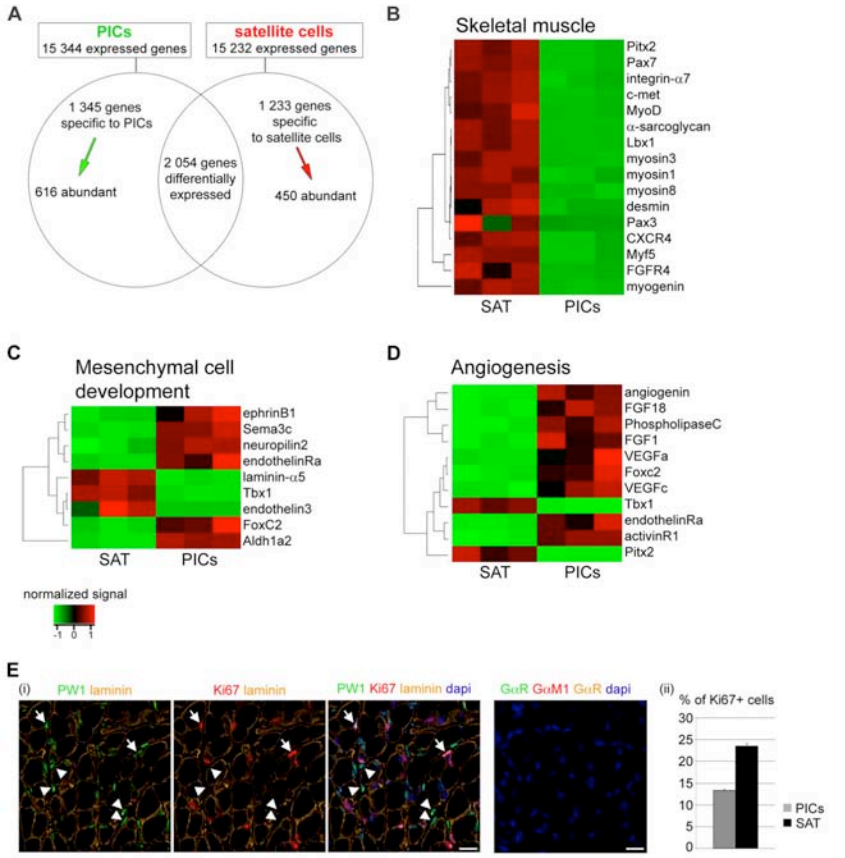

Figure 2. PICs and satellite cells are distinct progenitors. (**A**) Venn diagram presenting the gene distribution of PICs and satellite cells. Data were obtained from Affymetrix micro-array analysis of 1-week old C57bl6 mice with n=3 for each population. Fold Change threshold=1, p-value=0,01. Gene Ontology clustering analysis for Skeletal Muscle (B), Mesenchymal Cell Development (C) and Angiogenesis (D) gene categories. The gene tree is shown on the left and gene coloring was based on normalized signals as shown in the color bar. (**E**) (i) Cross-section of 1-week old hindlimb muscle from C57Bl6 mice stained for PW1 (green) and the proliferation marker Ki67 (red). Laminin staining (orange) shows the basal lamina. Nuclei were counterstained by DAPI (blue). Arrows indicate proliferative PICs, arrowheads indicate quiescent PICs. Scale bar, 20µm. (ii) Quantification of proliferative (Ki67+) PICs (gray) and satellite cells (black) for 1 week old mice from cross sections stained as shown in (i). Values represent the mean number of positive satellite cells or PICs ± s.e.m. per 100

cells respectively. At least 500 cells for each cell types from 3 independent experiments were counted.

Gene symbol	Gene name	Average intensity		Fold Change	p-value
		PICs	SAT		
Qprt	quinolinate phosphoribosyltransferase	793	14	-62.7	0.0027
P2ry14	purinergic receptor P2Y, G-protein coupled, 14	1477	32	-46.5	0.0005
Itgb3	integrin beta 3	518	14	-41.4	0.0019
Apod	apolipoprotein D	1403	39	-39.1	0.0077
Gpr133	G protein-coupled receptor 133	438	13	-35.6	0.0025
Aldh1a2	aldehyde dehydrogenase family 1, subfamily A2	1444	49	-35.4	0.0048
Myoc	myocilin	1549	50	-35.2	0.0035
Adam33	a disintegrin and metallopeptidase domain 33	398	13	-34.8	0.0043
Fst	follistatin	381	11	-32.8	0.0073
Foxd1	forkhead box D1	724	21	-32.4	0.0025
Ptch2	patched homolog 2	840	35	-31.8	0.0094
Il1rl2	interleukin 1 receptor-like 2	499	19	-29.3	0.0027
Pdgfra	platelet derived growth factor receptor, alpha polypeptide	897	124	-28.3	0.0016
Ebf2	early B-cell factor 2	224	8	-28.1	0.0005
Gjb2	gap junction membrane channel protein beta 2	950	35	-27.3	0.0013
Vtn	vitronectin	1201	49	-26.2	0.0023
Il15	interleukin 15	204	8	-25.6	0.0005
Cd55	CD55 antigen	438	18	-25.2	0.0015
Mmp16	matrix metallopeptidase 16	892	44	-23.3	0.0066
Arhgap20	Rho GTPase activating protein 20	473	24	-22.8	0.0041
Dnm1	dynamin 1	1517	91	-19.8	0.0084
Avpr1a	arginine vasopressin receptor 1A	331	20	-19.4	0.0088
Adra2a	adrenergic receptor, alpha 2a	369	21	-18.8	0.0040
Bmp7	bone morphogenetic protein 7	123	6	-18.2	0.0025
Wnt5a	wingless-related MMTV integration site 5A	1293	75	-18.1	0.0018
Ednra	endothelin receptor type A	261	15	-17.7	0.0026
Ephb2	ephrin receptor B2	300	19	-16.7	0.0030
Pi15	Peptidase inhibitor 15	171	12	-16.6	0.0083
Fgf1	fibroblast growth factor 1	462	31	-16.6	0.0060
Twist1	twist gene homolog 1 (Drosophila)	523	33	-16.5	0.0018
Negr1	neuronal growth regulator 1	136	8	-16.4	0.0012
Lepr	leptin receptor	173	11	-16.2	0.0013
Twist2	twist homolog 2 (Drosophila)	114	7	-16.1	0.0013
Efnb1	ephrin B1	315	46	-6.7	0.0013
NG2	chondroitin sulfate proteoglycan 4	965	153	-5.9	0.0107
Pdgfrb	platelet derived growth factor receptor, beta polypeptide	4916	1050	-4.8	0.0089
Tgfbr2	transforming growth factor, beta receptor II	9019	2521	-3.6	0.0023

Table 1. Genes preferentially expressed by PICs. For each gene, the average expression intensity was calculated from Affymetrix analysis. Fold change and p-value are indicated.

Table 2. Genes preferentially expressed by satellite cells. For each gene, the average expression intensity was calculated from Affymetrix analysis. Fold change and p-value are indicated.

Gene symbol	Gene name	Average intensity		Fold Change	p-value
		PICs	SAT		
Gpr50	G-protein-coupled receptor 50	10	1012	117.6	0.0016
Fgfr4	fibroblast growth factor receptor 4	13	1032	86.5	0.0048
Ryr1	ryanodine receptor 1, skeletal muscle	8	640	80.8	0.0019
Chrna1	cholinergic receptor, nicotinic, alpha polypeptide 1 (muscle)	75	4851	74.8	0.0028
Pitx3	paired-like homeodomain transcription factor 3	4	310	68.9	0.0005
Myod1	myogenic differentiation 1	47	2275	57.1	0.0036
Sgca	sarcoglycan, alpha (dystrophin-associated glycoprotein)	6	350	55.6	0.0002
Cdh15	cadherin 15	59	2648	55.3	0.0040
Lbx1	ladybird homeobox homolog 1 (Drosophila)	7	332	48.4	0.0007
Tnnt2	troponin T2, cardiac	23	989	44.5	0.0014
Pitx2	paired-like homeodomain transcription factor 2	8	329	42.6	0.0007
Traf3ip3	TRAF3 interacting protein 3	21	891	41.6	0.0004
Lama5	laminin, alpha 5	13	364	33.8	0.0090
Pde1c	phosphodiesterase 1C	6	166	26.6	0.0005
Arpp21	cyclic AMP-regulated phosphoprotein, 21	13	349	26.1	0.0005
Atp2a1	ATPase, Ca++ transporting, cardiac muscle, fast twitch 1	64	1481	22.4	0.0022
Tnik	TRAF2 and NCK interacting kinase	28	593	22.0	0.0041
Myh3	myosin, heavy polypeptide 3, skeletal muscle, embryonic	18	378	21.3	0.0016
Neb	nebulin	7	155	21.1	0.0002
Dcx	doublecortin	10	194	19.5	0.0046
Ephb1	ephrin receptor B1	8	124	16.0	0.0016
Chrng	cholinergic receptor, nicotinic, gamma polypeptide	8	134	15.8	0.0031
Myh8	myosin, heavy polypeptide 8, skeletal muscle, perinatal	21	289	15.5	0.0077
Ank1	ankyrin 1, erythroid	88	1245	15.4	0.0035
Pdgfa	platelet derived growth factor, alpha polypeptide	125	1532	13.7	0.0095
Ppargc1b	peroxisome proliferative activated receptor, gamma, coactivator 1 beta	12	154	13.3	0.0025
Edn3	endothelin 3	7	109	13.0	0.0089
Tbx1	T-box 1	9	109	11.7	0.0008
Hdac11	histone deacetylase 11	53	520	9.8	0.0009
Des	desmin	52	442	8.6	0.0091
Gdf15	growth differentiation factor 15	45	390	8.6	0.0074
Drp2	Dystrophin related protein 2	73	563	8.3	0.0066
Tpm2	tropomyosin 2, beta	17	134	8.1	0.0019
Acvr2b	activin receptor IIB	21	159	8.2	0.0148

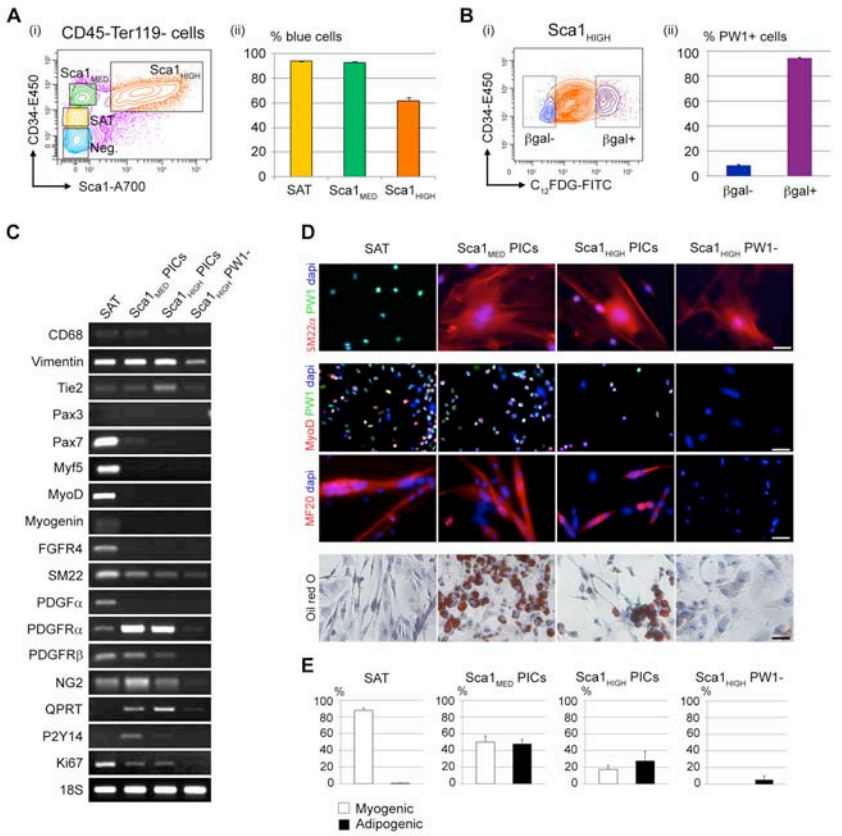

Figure 3. Juvenile PICs display multiple potentials *in vitro*. (**A**) Flow cytometric analyses of single cells from 1-week old $PW1^{nLacZ}$ mice limb muscles stained with antibodies against Sca1 and CD34. CD45 and Ter119HIGH cells were excluded as described previously (Mitchell et al., 2010). The gates used to isolate $CD34^{-}Sca1^{-}$, $CD34^{+}Sca1^{-}$, $CD34^{+}Sca1_{MED}$ and $CD34^{+}Sca1_{HIGH}$ cells are shown (i). The four fractions are indicated directly on the scatter plot (i). Reporter expression for each population was confirmed by β -galactosidase staining on freshly sorted cytospun cells and the percentage of β-galactosidase positive (β-gal+) cells was counted (ii). **(B)** The $CD34^{+}Sca1_{HIGH}$ population was sorted based on β-galactosidase expression (i). PW1 expression was confirmed by immunofluorescence on freshly sorted β -gal^{+} and β-gal^{-} cells and the percentages of PW1 expressing cells were counted. The $CD34^{+}Sca1_{HIGH}$ β-gal^{+} fraction was ~ 94% positive for PW1 (ii). (**C**) Semi-quantitative PCR of selected genes from our microarray analysis in satellite cells (SAT), $Sca1_{MED}$ PICs, $Sca1_{HIGH}$ PICs, and $Sca1_{HIGH}PW1^{-}$ cells freshly sorted as described above. (**D**)

Representative images of FACS isolated populations grown in myogenic or adipogenic conditions and immunostained for the smooth muscle marker, SM22α (top panel), myogenic markers (MyoD, MF20, middle panels) or stained with Oil red O for adipocytic differentiation (bottom panel). Scale bars, 20μm. (**E**) Quantitative analysis of myogenic and adipogenic potential of cells treated as described in (D). Myogenic values show the mean percentage ± s.e.m. of nuclei incorporated into MHC^{+} cells. Adipogenic values show the percentage of Oil red O positive cells. For all graphs, values are presented as percentage of positive cells ± s.e.m. from at least 3 independent experiments.

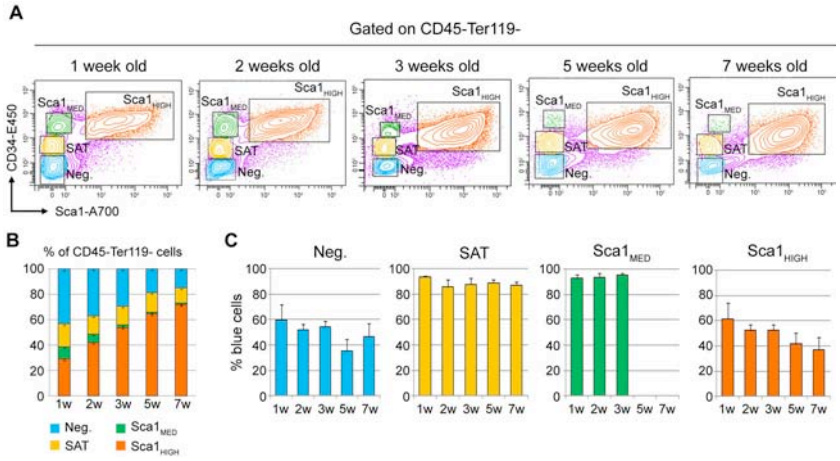

Figure 4. FACS profiles of muscle cells during 1-7 weeks postnatal life. (**A**) FACS profile of muscle cells from 1, 2, 3, 5 and 7-week old $PW1^{nLacZ}$ mice limb muscles. (**B**) Distribution of cell populations described in (A) presented as the mean percentage ± s.e.m. of $CD45^{-}Ter119^{-}$ cells from at least 3 independent experiments. (**C**) Quantification of cells positive for PW1 in each population described in (A) on freshly sorted cytospun cells presented as the mean percentage ± s.e.m. from at least 3 independent experiments.

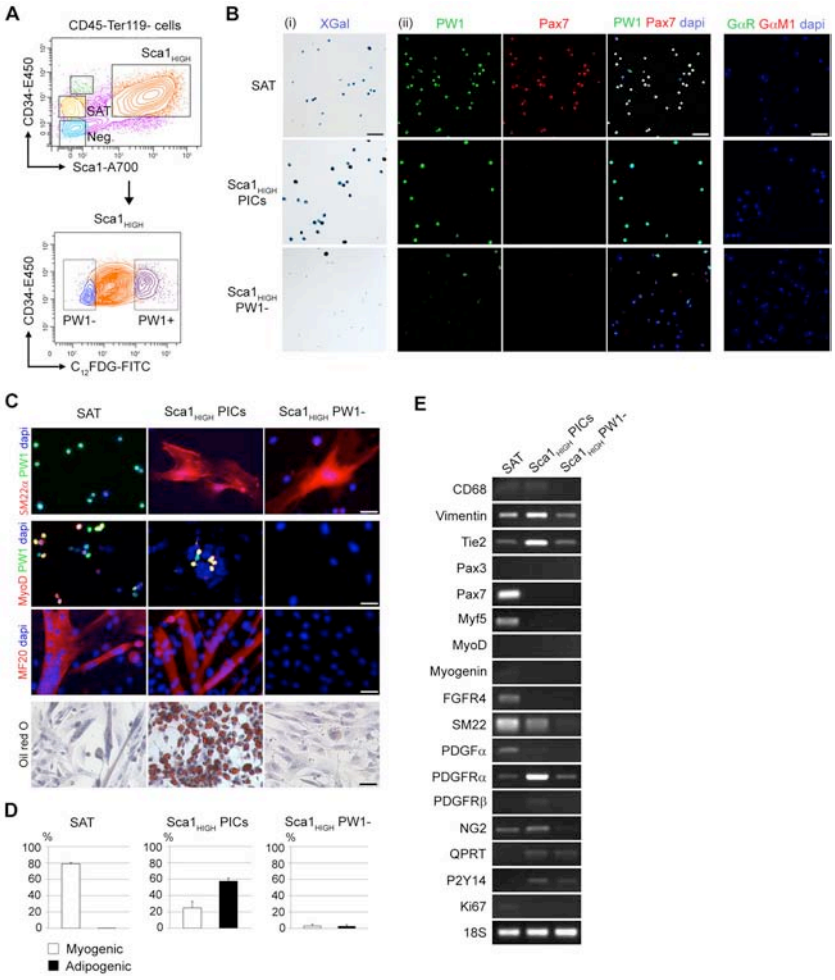

Figure 5. Adult PICs show multiple lineage capacities. (**A**) Flow cytometric analyses of single cells from 7-week old $PW1^{nLacZ}$ mice limb muscles stained for CD45, Ter119, CD34, Sca1 and C_{12}FDG. The gates used to isolate $CD34^{+}Sca1^{-}$ (SAT), $CD34^{+}Sca1_{HIGH}PW1^{+}$ (PW1+) and $CD34+Sca1_{HIGH}PW1^{-}$ (PW1-) populations are shown. (**B**) Histochemical (i) and immunolocalization (ii) of PW1 (green) and Pax7 (red) in freshly sorted cytospun cell fractions, as shown in (a). Nuclei are shown by DAPI staining (blue). Secondary antibodies controls are shown (ii, right panels). Scale bars, 30μm. (**C**) Representative images of FACS isolated populations grown in myogenic or adipogenic conditions and

immunostained for the smooth muscle marker (SM22α, top panel) and myogenic markers (MyoD, MF20, middle panels) or histochemically stained for adipocytic differentiation (Oil red O, bottom panel). Nuclei were counterstained by DAPI or haematoxylin. Scale bars, 20μm. (**D**) Quantitative analysis of myogenic and adipogenic potential of cells treated as described in (C). Myogenic values show the mean percentage ± s.e.m. of nuclei incorporated into MHC^{+} cells. Adipogenic values show the percentage of Oil red O positive cells. (**E**) Semi-quantitative PCR of selected genes from the microarray analysis in freshly sorted cells fractions, as shown in (A).

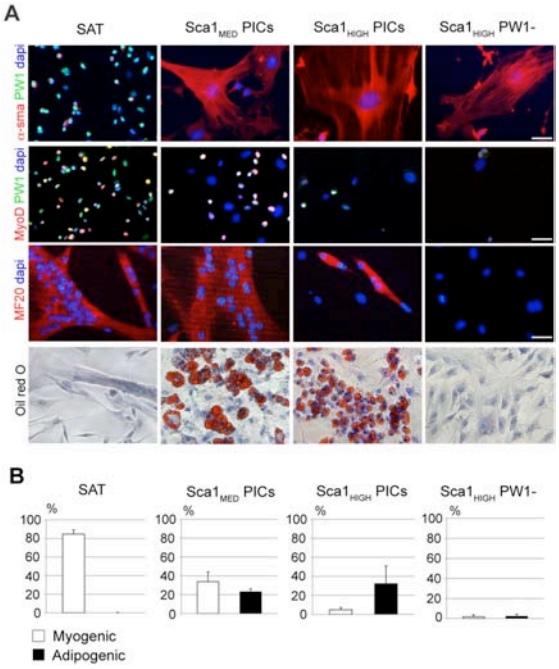

Figure 6. Cell fate potentials of 2-weeks old muscle cells. (**A**) Representative images of FACS isolated populations from 2-week old $PW1^{nLacZ}$ mice immunostained for smooth muscle marker (α-sma, top panel), myogenic markers (MyoD, MF20, middle panels), or histochemically stained for adipocytic differentiation (Oil red O, bottom panel). Nuclei were counterstained by DAPI or haematoxylin. Scale bars, 20μm. (**B**) *In vitro* myogenic and adipogenic potential of cells presented in (A). Myogenic potential was assessed by fusion index after 1 week in GM followed by 2 days in DM, and adipogenic potential was assessed by the percentage of adipocytes after 1 week in GM followed by 5 days in ADM. Values are presented as percentage of positive cells ± s.e.m. from at least n=3 independent experiments.

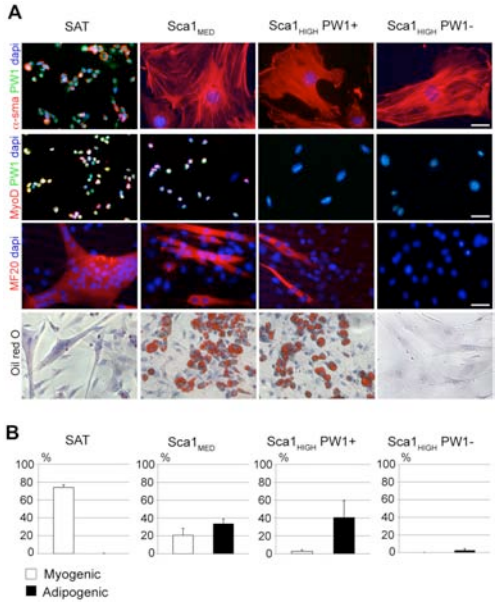

Figure 7. Cell fate potentials of 3-weeks old muscle cells. (**A**) Representative images of FACS isolated populations from 3-week old PW1^{nLacZ} mice immunostained for smooth muscle marker (α-sma, top panel), myogenic markers (MyoD, MF20, middle panels), or histochemically stained for adipocytic differentiation (Oil red O, bottom panel). Nuclei were counterstained by DAPI or haematoxylin. Scale bars, 20μm. (**B**) Quantification of myogenic and adipogenic potentials of cells treated as described in (A). Values are presented as percentage of positive cells ± s.e.m. from at least 3 independent experiments for each condition.

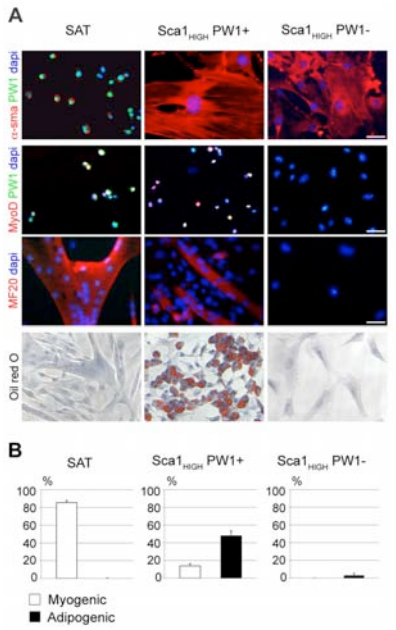

Figure 8. Cell fate potentials of 5-weeks old muscle cells. (**A**) Representative images of FACS isolated populations from 5-week old PW1^{nLacZ} mice immunostained for smooth muscle marker (α-sma, top panel), myogenic markers (MyoD, MF20, middle panels), or histochemically stained for adipocytic differentiation (Oil red O, bottom panel). Nuclei were counterstained by DAPI or haematoxylin. Scale bars, 20μm. (**B**) Quantification of myogenic and adipogenic potentials of cells treated as described in (A). Values are presented as percentage of positive cells ± s.e.m. from at least 3 independent experiments for each condition.

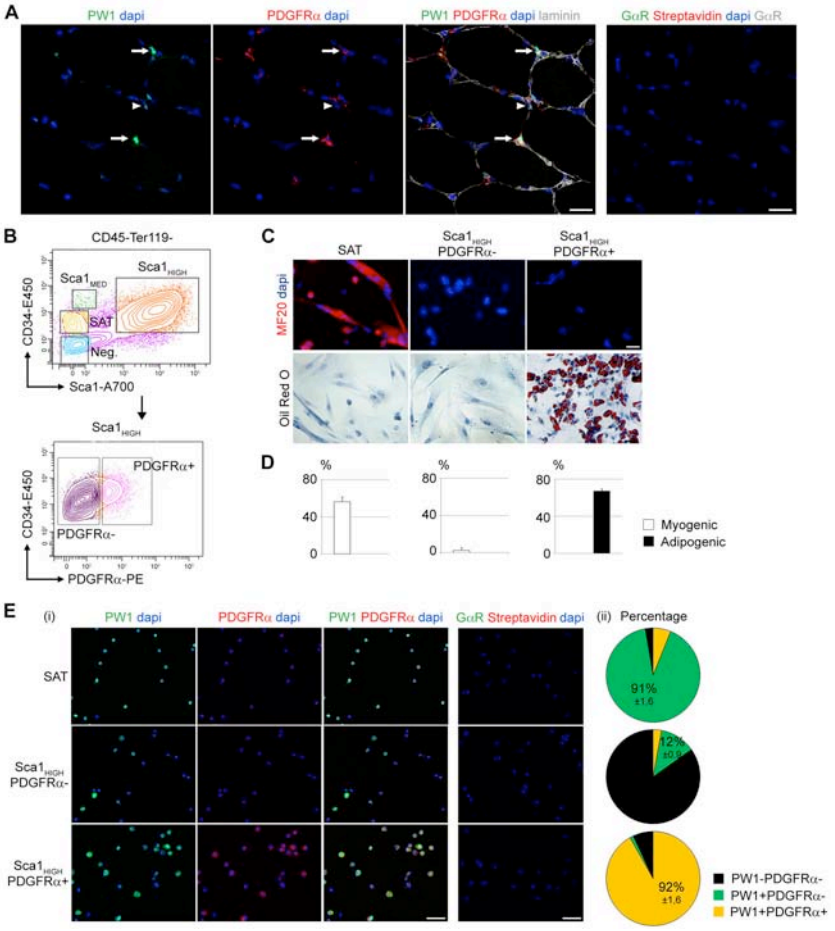

Figure 9. IAPs constitute a sub-population of PICs. (**A**) Cross-section of a 7-week old *Tibialis anterior* muscle immunostained for PW1 (green), PDGFRα (red), laminin (orange). Nuclei were counterstained by DAPI (blue). Species-specific antibodies controls are shown. Arrows: PDGFRα^{+} cells. Arrowheads: PICs which do not express PDGFRα. (**B**) FACS isolation of PDGFRα^{+} and PDGFRα^{-} cells from 7-week old Sca1$_{HIGH}$ cells. (**C**) Representative images of FACS sorted populations cultured under myogenic or adipogenic conditions, immunostained for the myogenic marker (MF20, top panels) or histochemically stained for adipocytic differentiation (Oil red O, bottom panel). (**D**) Quantification of myogenic and adipogenic potentials of cells treated as described in (C). Values represent the mean ± s.e.m., *n* = 3 independent

experiments for each condition. Scale bars, 20μm. (**E**) (i) Immunolocalization of PW1 (green) and PDGFRα (red) in freshly sorted cytospun cell fractions, as shown in (B). Nuclei were counterstained by DAPI (blue). Negative controls are shown. (ii) Quantification of cells positive or negative for PW1 and PDGFRα. Values show the mean percentage ± s.e.m. of positive cells from 3 independent experiments.

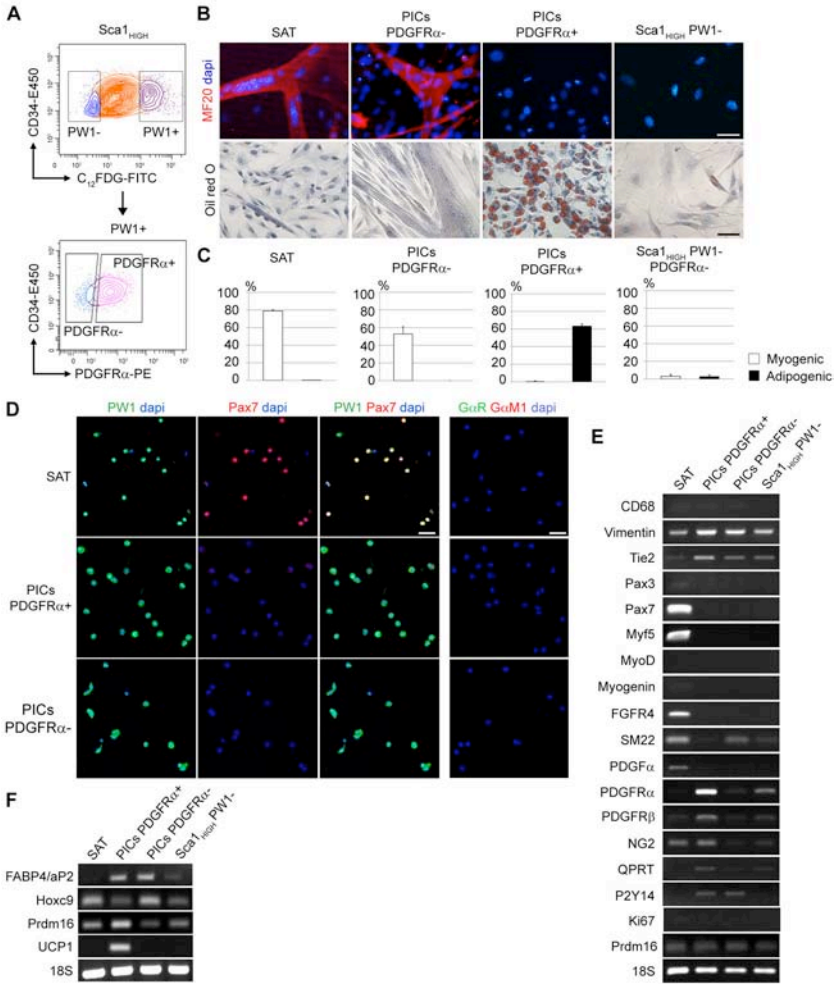

Figure 10. Adult PICS cell fate can be identified by PDGFRα expression. (**A**) FACS isolation of PDGFRα$^+$ and PDGFRα$^-$ cells from 7-week old Sca1$_{HIGH}$ PW1$^+$ fraction. (**B**) Representative images of FACS sorted populations cultured under myogenic (top panel) or adipogenic (bottom panel) conditions, immunostained for the myogenic marker (MF20, top panels) or histochemically stained for adipocytic differentiation (Oil red O, bottom panel). Nuclei were counterstained by DAPI or haematoxylin. Scale bars, 20μm. (**C**) Quantification of myogenic and adipogenic potentials of cells treated as described in (B). Values are presented as percentage of positive cells ± s.e.m. from at least 3

independent experiments for each condition. (**D**) Immunolocalization of PW1 (green) and Pax7 (red) in freshly sorted cytospun cell fractions, as shown in (A). Nuclei are shown by DAPI staining. Secondary antibodies controls are shown. (**E**) Semi-quantitative PCR of selected genes from microarray analysis in freshly sorted cells fractions, as shown in (A). (**F**) Semi-quantitative PCR of adipocyte specific genes in FACS sorted populations cultured under adipogenic conditions.

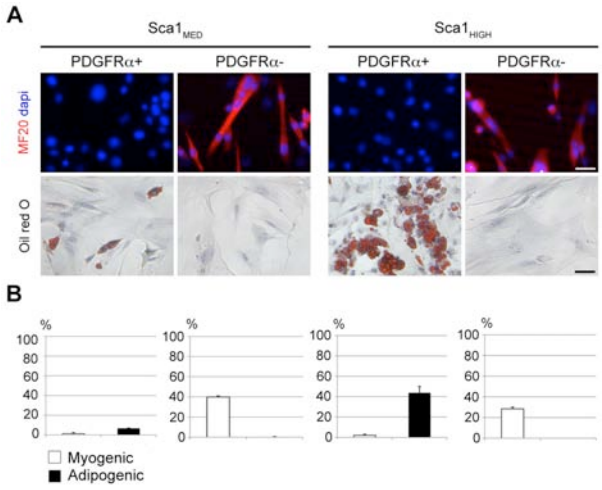

Figure 11. PDGFRα expression is absent in myogenic juvenile PICs. (**A**) Isolated juvenile PICs populations separated on the basis of PDGFRα expression grown in myogenic (top panel) or adipogenic (bottom panel) conditions. Scale bars, 20μm. (**B**) Quantification of myogenic and adipogenic potentials of cells presented in (A). Values are presented as percentage of positive cells ± s.e.m. from at least 3 independent experiments.

2. Targeting the muscle stem cell niche interactions

2.1. PICs promote satellite cell proliferation via TGFβ and IGF-1 pathways

As outlined in the previous chapter, we reported that PICs and satellite cells display distinct transcriptome signatures. Detailed examination of these transcriptomes revealed that follistatin (FST) and insulin-like growth factor 1 (IGF-1) are expressed by PICs but not by satellite cells (**Fig. 12A,B)**. Furthermore, AcvR2A is expressed by PICs, whereas AcvR2B and IGF-1R are expressed by satellite cells (**Fig. 12A,B)**. These data suggest an interaction between PICs and satellite cells in which PICs secrete promyogenic factors and block myostatin activity. To test this hypothesis, we cultured freshly isolated adult satellite cells (SAT) in the presence or absence of PICs plated in the upper chamber of a semipermeable membrane insert system allowing for diffusion of secreted factors (**Fig. 12C**). Consistent with previous studies (Amthor et al., 2009; Langley et al., 2002; McCroskery et al., 2003), we observed that satellite cell proliferation was inhibited by MST in a dose-dependent manner (**Fig. 12D**). This inhibition was reversed when satellite cells were grown in the presence of PICs and even at high doses of MST (200 ng/ml and 2 mg/ml), the presence of PICs rescued satellite cell proliferation to levels comparable to normal growing conditions (**Fig. 12D**). Adding specific blocking antibodies for follistatin (αFST) resulted in a significant reduction of satellite cell proliferation at 200 ng/ml and 2 mg/ml of MST (**Fig. 12D**). We observed a similar inhibition of the PIC-mediated rescue of satellite cell proliferation at 200 ng/ml of MST when using specific blocking antibodies for IGF-1 (αIGF1) (**Fig. 12D**). While a previous study has shown that MST is localized to satellite cells (McCroskery et al., 2003) and since MST is not represented in the Affymetrix chip used for transcriptome analyses, we measured MST levels and confirmed FST and IGF-1 expression in freshly purified adult satellite cells,

PDGFRα^{+} PICs, PDGFRα^{-} PICs as well as Sca1^{+}PW1^{-} cells, sorted as previously described (Mitchell et al., 2010) (**Fig. 12E**). We found that FST and IGF1-IEa were strongly expressed by PDGFRα^{+} PICs whereas MST and AcvR2B were specifically expressed in satellite cells (**Fig. 12E**). These data demonstrate that PICs produce pro-myogenic factors (FST and IGF-1) that antagonize MST activity and provide a mechanistic basis for the promyogenic effect exerted by FAPs (Joe et al., 2010).

2.2. Inhibition of AcvR2B pathway *in vivo* targets the muscle stem cell niche

It has been shown previously that a soluble form of the AcvR2B (RAP-031) containing the ligand-binding site is able to block AcvR2B mediated responses *in vivo* (Akpan et al., 2009; George Carlson et al., 2011; Koncarevic et al., 2010; Pistilli et al., 2011). To determine whether crosstalk between PICs and satellite cells occurs *in vivo*, we injected RAP-031 twice a week for 2 weeks, in 5 weeks old C57Bl6 male mice as described previously (Akpan et al., 2009; George Carlson et al., 2011) (**Fig. 13A**). RAP-031-treated mice displayed a marked increase in body weight as compared to vehicle injected controls, comparable to the increase in body weight seen in age-matched MST mutant mice (*Mst*$^{-/-}$) (CTL=18.38g±2.05; RAP-031=43.61g±3.82l; *Mst*$^{-/-}$=52.84g±2.85. CTL vs RAP-031 p=0.0002; CTL vs *Mst*$^{-/-}$ p<0.0001). Analyses of the *Tibialis Anterior* (TA) muscles showed a marked weight and fiber size increase comparable to *Mst*$^{-/-}$ mice (**Fig. 13B,C**). Interestingly, we noted that increases in weight and fiber size were accompanied by an increase in the interstitial and sublaminal nuclei only following RAP-031 treatment whereas no significant change in the interstitial cells was observed in the *Mst*$^{-/-}$ TA however we noted a significant decrease in the sublaminal nuclei in *Mst*$^{-/-}$ TA (**Fig. 13D,E**). We noted that in all cases, the overall sublaminal/interstitial nuclei ratio remained constant (**Fig. 13F**) suggesting that cell populations are tightly controlled in adult

muscle. To determine whether muscle progenitor cell number was affected by interfering with the AcvR2B-mediated pathway, we measured PICs and satellite cell number by immunostaining for PW1 and Pax7. In *Mst*$^{-/-}$ TA muscles, we noted a significant increase in the number of satellite cells and PICs (2- and 3-fold respectively) compared to wildtype. In contrast, RAP-031 treatment resulted in a larger increase in the number of satellite cells and PICs (2.5- and 4-fold respectively) (**Fig. 13G**). Satellite cells and PICs are normally present at a 1/1 ratio (**Fig. 13H** and (Mitchell et al., 2010). We note that loss of *Mst* or treatment with RAP-031 resulted in a higher proportion of PICs (**Fig. 13H**). Similar results were obtained in *gastrocnemius*, *plantaris* and *soleus* muscles from RAP-031-treated mice (data not shown). These data suggest that inhibition of the AcvR2B pathway induces proliferation of the progenitor populations in skeletal muscle, therefore we stained TA cross-sections for the cell cycle marker, Ki67. As expected, the majority of the satellite cells and PICs were mitotically quiescent in control mice(Pallafacchina et al., 2010) (**Fig. 13I**). RAP-031 treatment resulted in a significant increase in satellite cells and PICs proliferation (**Fig. 13I**). Taken together, we conclude that inhibition of the AcvR2B pathway increases the number of muscle progenitors, however the PIC population undergoes a larger expansion and alters the PIC/satellite cell ratio.

We demonstrated previously that PICs can generate skeletal muscle when cultured or directly engrafted into injured limb muscle (Mitchell et al., 2010). We therefore sought to determine whether PICs contribute to fiber hypertrophy by entering the skeletal muscle lineage and fusing with existing fibers. To distinguish between satellite cell and non-satellite cell myonuclear contribution during hypertrophy, we used an inducible satellite cell-depleted mouse model in which the diphteria toxin (DT) receptor is expressed under the control of *Pax7* promoter so that DT injection induces the depletion of satellite cells as previously described (*Pax7*$^{DTR/+}$ mice)(Sambasivan et al., 2011b). *Pax7*$^{DTR/+}$ mice were injected with DT in the TA and PBS in the contralateral

muscle as a control and allowed to recover for 2 weeks prior to RAP-031 treatment (**Fig. 14A**). In all cases, RAP-031 induced muscle fiber hypertrophy (**Fig. 14B,C**). Consistent with previous results (McCarthy et al., 2011), we observed an increase in myonuclei number concomitant with fiber hypertrophy in control muscle (satellite cell intact), whereas fiber hypertrophy still occurred in the absence of an increase in myonuclei number in the satellite cell-depleted TAs in response to RAP-031 treatment (**Fig. 14D**). These data reveal that RAP-031 does not result in a recruitment of PICs into the myofibers during hypertrophy in the absence of satellite cells. Since we demonstrated that RAP-031 treatment induces an increase in satellite cells and PICs, we sought to determine whether PICs and the few remaining satellite cells following depletion were similarly affected. We therefore stained muscle tissue sections from PBS or DT-injected muscles from both control or RAP-031 treated mice for PW1 (to label both PICs and satellite cells) and M-Cadherin (to label satellite cells) (**Fig. 14E**). As expected, few satellite cells survive DT injection (Sambasivan et al., 2011b) and we did not see any change in satellite cell number following RAP-031 treatment (**Fig. 14E**). As shown previously (Sambasivan et al., 2011b) and observed here, PICs are easily detectable following satellite cell depletion (**Fig. 14F**). Surprisingly, we observe that PICs undergo an even greater increase in cell number in satellite cell depleted muscle in response to RAP-031 (**Fig. 14F**). We conclude that in the absence of satellite cells, RAP-031 treatment induces an increase in the PIC population but PICs are unable to neither replace the satellite cell pool nor contribute directly to myofibers.

2.3. Targeting the AcvR2B pathway rescues proper regeneration in satellite cell-depleted muscles.

Our previous data demonstrating that PICs can enter the myogenic lineage were obtained in culture conditions or following engraftment into injured muscle (Mitchell et al., 2010 and **Figs. 3,**

5). It has been shown previously that muscle regeneration is severely compromised in the *Pax7*$^{DTR/+}$ model even though 3-5% of the satellite cell population is still present (Sambasivan et al., 2011b). Here we demonstrated that PICs promote satellite cell proliferation via FST and IGF-1 secretion (**Fig. 12D**) and undergo a marked increase in number following RAP-031 treatment even in satellite cell-depleted muscle (**Fig. 14F**). To test whether the increase in PICs following RAP-031 treatment leads to a more pro-myogenic microenvironment and either rescue the small number of remaining satellite cells and/or promote the recruitment of resident non-satellite cell myogenic progenitors, we crossed *Pax7*$^{DTR/+}$ mice with *Tg:Pax7CreER*^{T2} mice (Mourikis et al., 2012) and with reporter line *Rosa26*^{mTomatoSTOPmGFP}. The resulting Pax7$^{DTR/+}$:Pax7CreER^{T2}:Rosa26^{mTomatoSTOPmGFP} mice express a tamoxifen-inducible Cre (Metzger and Chambon, 2001) so that *Pax7*-expressing satellite cells and their progeny are marked by GFP (Mourikis et al., 2012). Young adult mice were first injected with tamoxifen to activate mGFP expression in satellite cells followed by a single injection of DT in the right TA and PBS in the contralateral muscle 4 weeks after the last tamoxifen injection. Muscles were allowed to recover for 2 weeks and then treated with RAP-031. Muscles were injured by cardiotoxin one day before the last RAP-031 injection and the level of regeneration was assessed 2 weeks later (**Fig. 15A).** As expected, all RAP-031-treated (n=9) and untreated (n=9) TA muscles injected with PBS showed robust myofiber regeneration while satellite cell depletion severely compromised regeneration coupled with fat deposition and fibrosis (**Fig. 15B**). In 2 of the 5 vehicle injected mouse muscles in which the satellite cells were depleted, we observed rare and highly focal areas of newly regenerated fibers suggesting that the few surviving satellite cells can be mobilized but cannot extend into neighbouring muscle tissue. In contrast, RAP-031 treatment of satellite cell depleted muscles resulted in a marked increase in overall regeneration coupled with a marked reduction of fat and fibrosis in 7 out of 9 samples. We note that while RAP-031 treatment results

in a marked recovery of regeneration in the satellite cell depleted muscle, depletion of satellite cells in vehicle injected mice resulted in a strong decrease of the number of centrally nucleated fibers after injury compared to muscles injected with PBS (8.8-fold), whereas this decrease was less than 1.5-fold in RAP-031 mice injected with DT as compared to muscles from vehicle injected with PBS from vehicle treated mice (**Fig. 15C**).

The $Pax7^{DTR/+}$:Pax7CreER^{T2}:$Rosa26^{mTomatoSTOPmGFP}$ mice provides a genetic tool to determine if newly regenerated fibers derive from remaining satellite cells as these fibers are predicted to express mGFP whereas the presence of $mGFP^{-}mTomato^{+}$ regenerating fibers would indicate a contribution of unlabelled satellite cells or other non-satellite progenitor cells. In satellite cell-depleted muscles from RAP-031 mice, we observed that more than 80% of centrally nucleated fibers were $mGFP^{+}$, comparable to CTL PBS and RAP-031 PBS conditions (**Fig. 16A,B)**. Interestingly, in RAP-031 PBS TA muscles we found a 10% significant decrease of $mGFP^{+}$ centrally nucleated fibers as compared to PBS injected TA (**Fig. 16B**), concomitant with an increase of $mGFP^{-}mTomato^{+}$ centrally nucleated fibers (**Fig. 16B**), suggesting that RAP-031 favors the mobilization of non-satellite cells over satellite cells in the context of myofiber repair. The presence of mTomato labeled fibers may result either from a non-satellite cell population or reflect a small number of satellite cells that did not efficiently recombine to initiate GFP expression. Surprisingly, we observed very few satellite cells in DT TAs from RAP-031 mice and no significant increase in their number as compared to DT TAs of vehicle injected mice (**Fig. 16D)**. These data reveal that inhibition of the AcvR2B pathway activates the few satellite cells spared by DT-mediated depletion and recruit them into new myofibers, however additional factors are needed in order to restore the satellite cell pool.

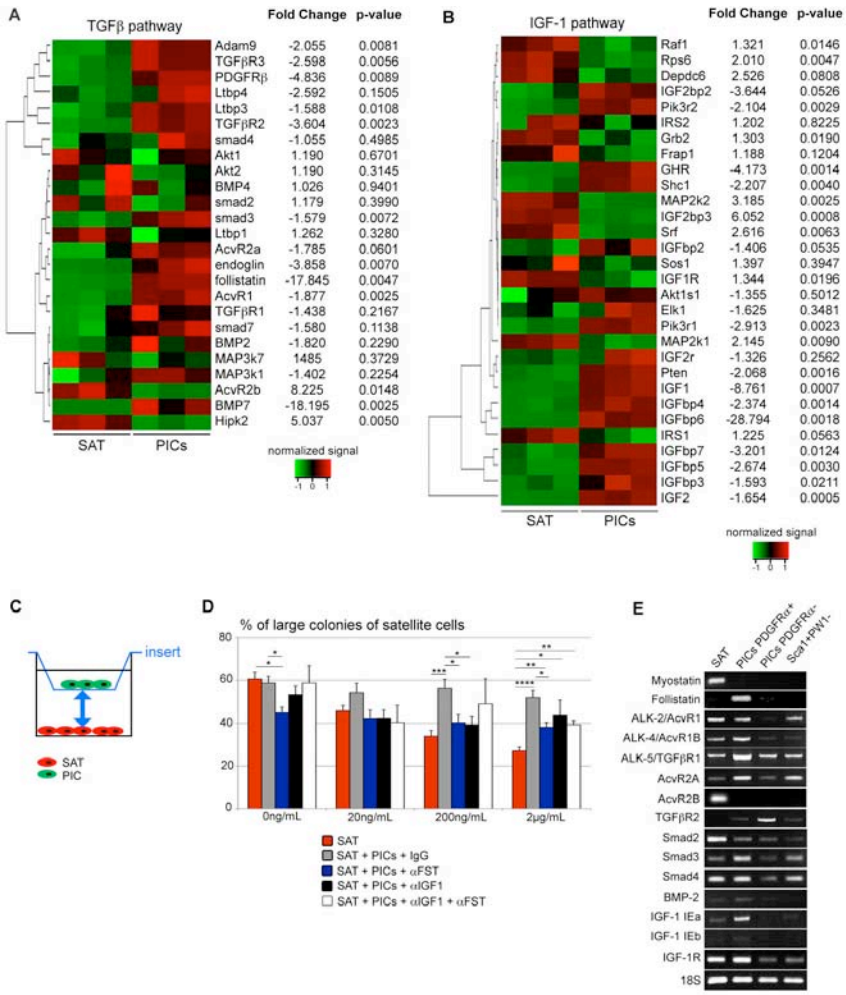

Figure 12. PICs antagonize the inhibitory effects of myostatin via TGFβ and IGF-1 pathways. (**A-B**) Gene Ontology clustering analyses of the TGFβ pathway (A) and IGF-1 pathway (B) genes. Heatmap colors reflect normalized signals as shown in the color bar. The gene tree is shown on the left and fold-change and p-value are indicated for each gene. (**C**) Schematic transwell membrane system used: PICs (green) were plated in the upper well on a semipermeable membrane (insert) and satellite cells (red) were plated in the lower chamber. (**D**) Quantitative analyses of satellite cell proliferation in growth medium containing 0, 20, 200 ng/ml or 2 μg/ml of recombinant myostatin. Satellite cells were cultured alone (red bars) or in the presence of PICs and

isotype-matched IgG (grey bars). Satellite cells and PICs were co-cultured in presence of a blocking antibody to follistatin (αFST, blue bars) or to IGF-1 (αIGF-1, black bars) or blocking antibodies to IGF-1 and FST together (αFST + αIGF1, white bars). Large colonies (>12 cells) were counted and shown as a percentage of the number of total colonies. **(E)** Semi-quantitative PCR of selected genes from the microarray gene list in freshly sorted adult satellite cells (SAT), PDGFRα^{+} PICs, PDGFRα^{-} PICs and Sca1$_{HIGH}$PW1^{-} cells. Statistical significance represents the mean ± s.e.m of at least 3 different experiments. *p<0.05 **p<0.01 ***p<0.001 ****p<0.0001.

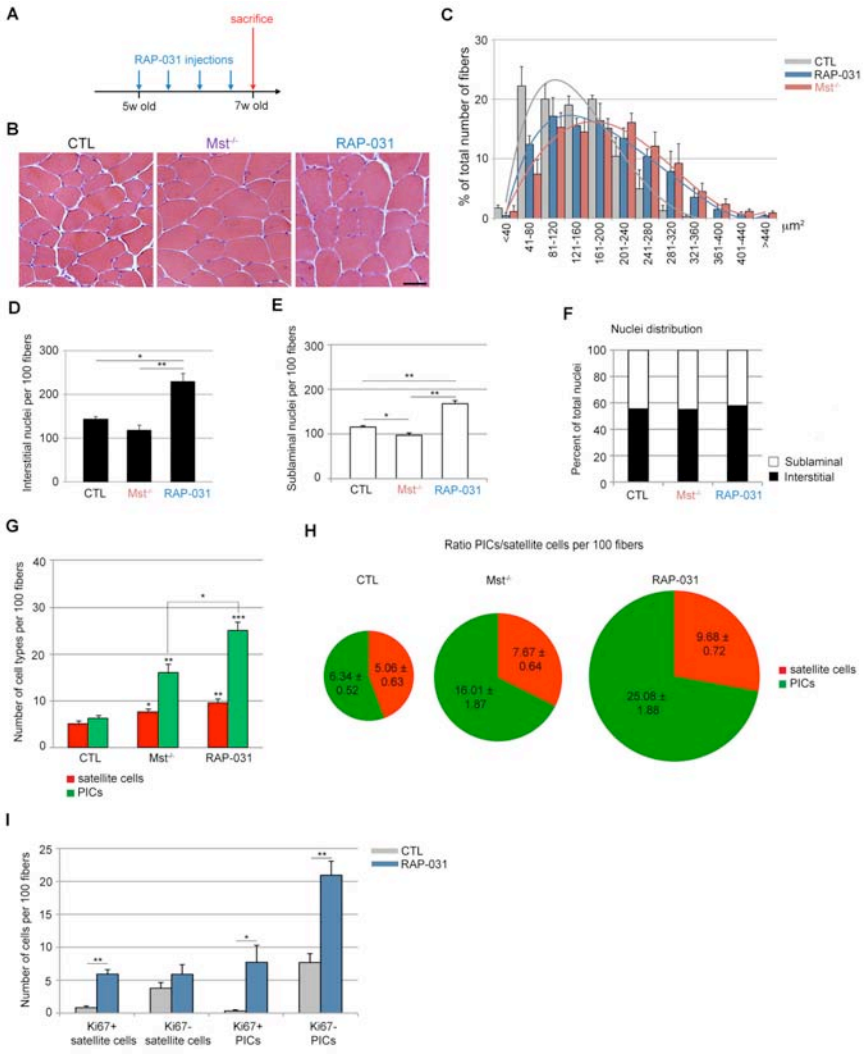

Figure 13. Inhibition of AcvR2B pathway *in vivo* alters muscle tissue and stem cell niche homeostasis. (**A**) Strategy: 5 week-old male wild-type mice were intraperitoneally injected with RAP-031 or vehicle (CTL) every 3 days and sacrificed 2 weeks after the first injection. (**B**) Cross-sections of TA from CTL, *Mst*$^{-/-}$ and RAP-031 mice stained with hematoxylin and eosin. Scale bar, 50µm. (**C**) Fiber size distribution in CTL (gray), *Mst*$^{-/-}$ (red) and RAP-031 (blue) TA. RAP-031 and *Mst*$^{-/-}$ muscles exhibit fiber hypertrophy. (**D- F**) Quantification of

the number of interstitial (D) and sublaminal (E) nuclei per 100 fibers, and nuclei distribution (F) in TAs from CTL, $Mst^{-/-}$ and RAP-031 mice. RAP-031 treatment resulted in an increase in the number of nuclei, but no change in their overall distribution. Values represent the mean number of nuclei ± s.e.m. per 100 fibers. **(G- H)** Quantification of PICs (green) and Satellite cells (red) (G) and their ratio (H) for CTL, $Mst^{-/-}$ and RAP-031 TAs. PICs were determined as interstitial $PW1^{+}Pax7^{-}$ cells, satellite cells as $Pax7^{+}$ cells underneath the basal lamina. Circle area is relative to the total number of PICs and satellite cells per 100 fibers. In *Mst*$^{-/-}$ and RAP-031 the number of PICs and satellite cells was significantly increased and the ratio was altered in favor of PICS. **(I)** Histograms showing the number of $Ki67^{+}$ and $Ki67^{-}$ satellite cells and PICs per 100 fibers in CTL and RAP-031 TAs. PICs were determined as interstitial $PW1^{+}$M-Cadherin^{-} cells, satellite cells as M-Cadherin^{+} cells underneath the basal lamina. For G-I, values represent the mean number of positive cells ± s.e.m. per 100 fibers.

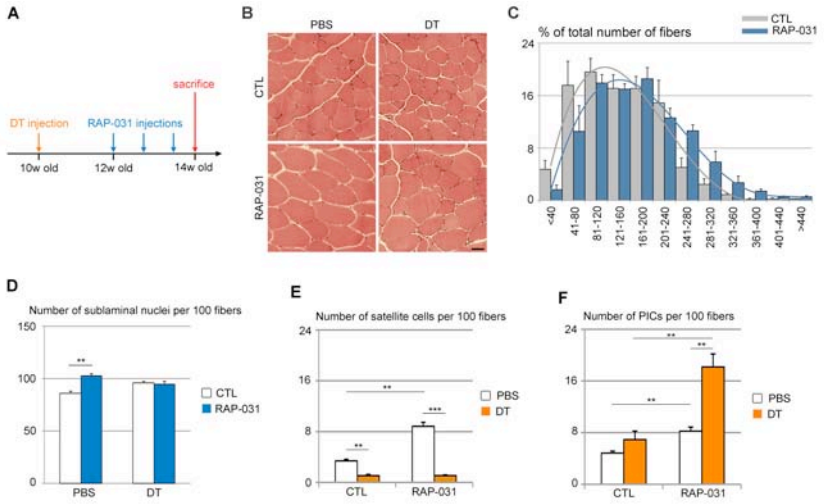

Figure 14. PICs increase in number but do not directly participate in fiber hypertrophy following AcvR2B pathway inhibition in satellite cell-depleted muscles. (**A**) Strategy: the right TA of 10 week-old $Pax7^{DTR/+}$ males was injected with diphteria toxin (DT) to deplete satellite cells while the contralateral muscle was injected with PBS 2 weeks before RAP-031 treatment. Mice were intraperitoneally injected with RAP-031 or vehicle (CTL) every 3 days and sacrificed 8 days after the first injection. (**B**) Cross-sections of TA muscles from CTL (upper panel) or RAP-031 (lower panel) mice injected with PBS (left panel) or DT (right panel) stained with hematoxylin and eosin. Scale bar, 60µm. (**C**) Fiber size distribution in CTL (gray) and RAP-031 (blue) TAs injected with DT. RAP-031 treatment resulted in muscle hypertrophy even in the absence of satellite cells. Values represent the mean number ± s.e.m. per 100 fibers for each size. (**D**) Quantification of the number of sublaminal nuclei per 100 fibers in TA from CTL and RAP-031 mice injected with PBS or DT. RAP-031 treatment did not result in myonuclei addition when satellite cells are depleted. (**E**) Quantification of satellite cells per 100 fibers in TA from CTL and RAP-031 mice injected with PBS or DT. Satellite cells were determined as $M\text{-}Cadherin^{+}$ cells underneath the basal lamina. The number of satellite cells was markedly decreased after DT injection in both CTL and RAP-031 treated mice. (**F**) Number of PICs per 100 fibers in TAs from CTL and RAP-031 mice injected with PBS or DT revealed that PICs number was still increased after RAP-031 treatment in a satellite cell-depleted environment. PICs were determined as interstitial $PW1^{+}M\text{-}cadherin^{-}$ cells. In D-F, values represent the mean number of positive cells ± s.e.m. per 100 fibers. For all graphs, statistical significance was calculated from at least 3 animals of each condition. *p<0.05 **p<0.01 ***p<0.001.

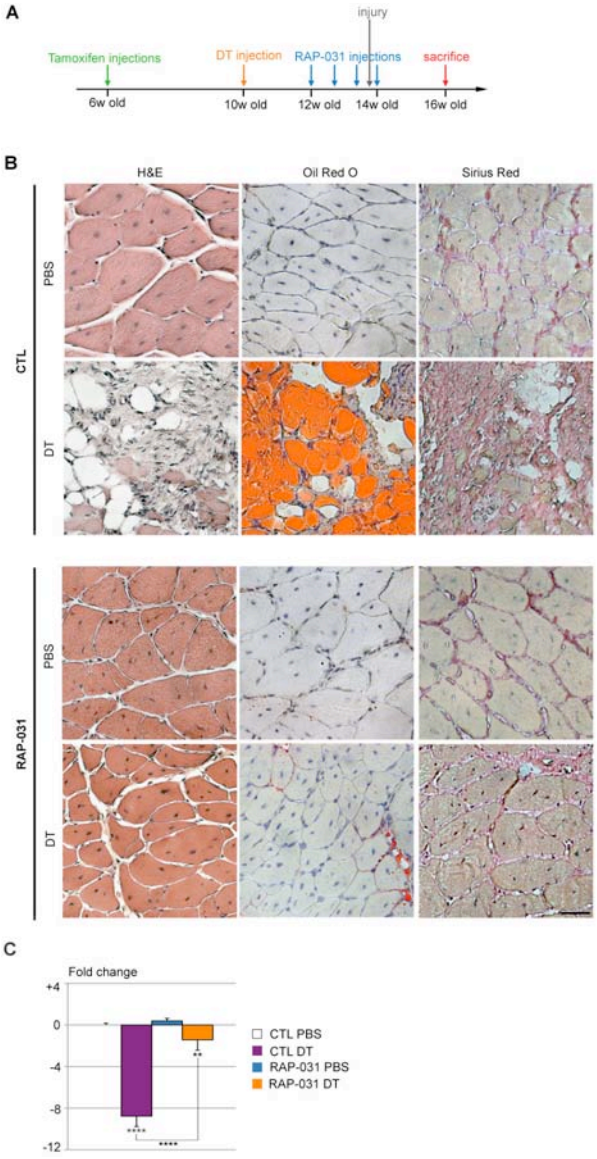

Figure 15. Inhibition of AcvR2B pathway improves fiber regeneration and ameliorates tissue homeostasis of injured SAT-depleted muscles. (**A**) Experimental design: 6 week-old $Pax7^{DTR/+}$: $Pax7CreER^{T2}$: $Rosa26^{mTomatoSTOPmGFP}$ mice were injected with tamoxifen to label satellite cells. 4 weeks later, the right TA was injected with DT to ablate satellite cells. The contralateral muscle was injected with PBS. After 2 weeks, mice were injected with either RAP-031 or vehicle (CTL) twice a week for 2 weeks. The day before the last injection of RAP-031 or vehicle both TAs were injured by cardiotoxin injection. Mice were sacrificed 2 weeks after injury. (**B**) Cross-sections of TA muscle from CTL (upper panels) and RAP-031 (lower panels) mice treated as described in (A) stained with hematoxylin and eosin (left panels), Oil-Red O (middle panels) and Sirius Red (right panels). Regeneration is more efficient in DT RAP-031 mice as compared to DT CTL mice, with a marked reduction in fat and fibrotic tissue deposition Scale bar, 50μm. **(C)** Quantitative analysis of regenerative capacity of TA

muscles from mice treated as described in (A). The number of centrally nucleated fibers per field in TAs from CTL mice injected with PBS was considered as the baseline (zero) and values represent the fold change ± s.e.m. normalized accordingly. Muscle fiber regeneration is significantly rescued in DT RAP-031 mice as compared to DT CTL mice. *p<0.05 **p<0.01 ***p<0.001.

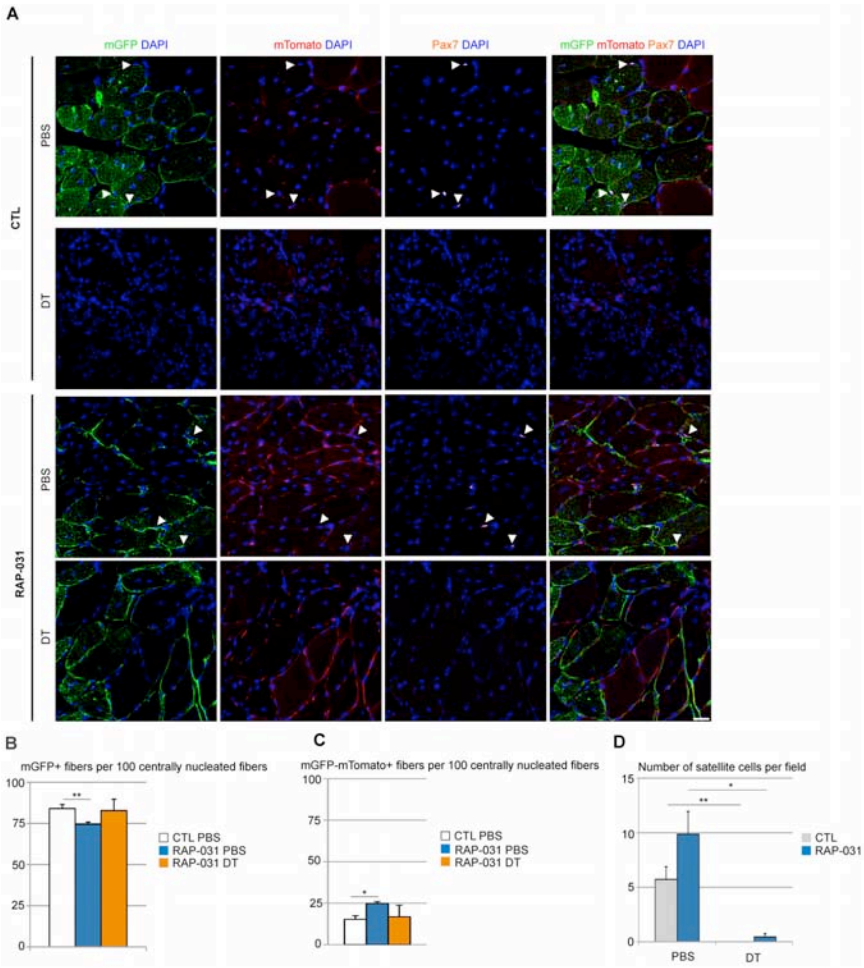

Figure 16. Inhibition of AcvR2B pathway in injured satellite cell-depleted muscles promotes activation of the few spared satellite cells to a threshold level allowing for muscle regeneration. (**A**) Representative images of cross-sections from injured TA muscles of CTL (upper panels) and RAP-031 (lower panels) mice injected with DT or PBS as described in fig. 15A, immunostained

for mGFP (green) to identify satellite cell-derived fibers and Pax7 (orange) to identify satellite cells. mTomato fluorescence is shown in red, dapi staining identifies nuclei. The majority of regenerating fibers are satellite cell-derived (green) regardless of treatment. White arrowheads: satellite cells. Scale bars, 30μm. **(B-C)** Quantification of the number of $mGFP^+$ (B) and $mGFP^-mTomato^+$ (C) fibers per 100 centrally nucleated fibers for CTL and RAP-031 mice treated as described in fig. 15A. Values represent the mean number of positive fibers ± s.e.m. per 100 centrally nucleated fibers. (**D**) Number of satellite cells per field indicated no significant increase in RAP-031 DT mice as compared to CTL DT mice. Satellite cells were determined as $Pax7^+$ cells. Values represent the mean number of positive cells ± s.e.m. per field. *p<0.05 **p<0.01 ***p<0.001.

3. Analysis of the EOM stem cell niche

3.1. EOM stem cell niche is conserved throughout aging

The EOMs is a group of skeletal muscles that are required for movement of the eyes. As outlined in chapter 3 of Introduction, these muscles are particularly resistant to the degenerative pathologies that are seen in limb muscles in dystrophic boys and mice (Porter, 2002; Porter et al., 1995). We therefore analysed the EOM progenitor cell niche and compared our results with those obtained previously for limb muscles during both postnatal and adult stages. In limb muscle, we had reported previously that both PICs and satellite cells undergo a progressive decline after birth (**Fig. 4** and Mitchell et al., 2010), however these two cell types maintain a 1:1 ratio in homeostatic conditions (**Fig. 13H** and Mitchell et al., 2010). We therefore compared 7 week-old wild type EOMs and TA muscles and found a 2-fold higher number of PICs in EOMs as compared to TA, whereas the number of satellite cells was unchanged between the two sets of muscles (**Fig. 17A,B**) leading to a PICs/satellite cells ratio of 2:1 in EOMs as compared to 1:1 found in the TA (**Fig. 17C**). Given the observation that PICs secrete promyogenic factors, we suggest that the increased number of PICs may account for the maintenance of EOMs under myopathic conditions including aging. We next compared 7 week-old and 18 month-old wild type EOMs and TA. While both muscle groups show a decrease in PICs and satellite cell number with age, we noted that the PICs/satellite cells ratio remained unchanged in old EOMs as compared to young EOMs (**Fig. 17C**). Specifically, PICs from limb muscles undergo a marked decline as compared to satellite cells, as old TA exhibits a 0.3:1 ratio between PICs and satellite cells (**Fig. 17C**), suggesting that factors regulating progenitor cells within the niche are different in these muscles. We further noted a rare population of $PW1^{+}$ interstitial cells that co-expressed Pax7 in 7 week-old EOMs, completely or partially surrounded by the basal lamina (**Fig. 17D,E**), raising the

possibility that a subset of PICs that are committed to the myogenic lineage is present in EOMs. In contrast, $PW1^{+}Pax7^{+}$ interstitial cells were absent in age-matched TA (**Fig. 17E**). These data indicate that the EOM stem cell niche composition is different from that seen in limb muscles. However, we failed to detect expression of proliferation markers (as Ki67 or PH3) as well as myogenic activation marker MyoD in PICs or satellite cells from EOMs (data not shown), consistent with observations in TA and other skeletal muscles (**Fig. 13I** and Pallafacchina et al., 2010) in contrast with previous reports (McLoon et al., 2004; McLoon and Wirtschafter, 2002a).

3.2. *Mdx* mice display an unaltered EOM stem cell niche

Mdx skeletal muscles undergo continuous cycles of degeneration and regeneration due to a defect in the dystrophin gene making it a valuable model for the study of Duchenne muscular dystrophy (Burghes et al., 1987; Partridge, 2013; Tabebordbar et al., 2013). While the mice and humans vary in the degree of disease severity, both share the feature that the EOMs are not affected (Porter et al., 1995; Porter et al., 2003). We analyzed the EOM and TA stem cell niche in 7 week-old wild-type and *mdx* mice. EOM cross-sections from *mdx* mice did not display histological signs of ongoing regeneration and looked as their wild-type counterparts, whereas TA cross-sections showed widespread regions with centrally nucleated fibers, as also previously reported (Wallace and McNally, 2009) (**Fig. 18A,B**). We observed only one restricted region containing some centrally nucleated fibers in 1 out of 3 EOMs examined. We also observed an increase in the number of interstitial cells in *mdx* TA as compared to wild type TA, but no change in EOMs (**Fig. 18C**), confirming that *mdx* EOMs were unperturbed. Both satellite cells and PICs were increased in *mdx* TA as compared to its wild-type counterpart (**Fig. 18D,E**), whereas *mdx* EOMs displayed an unchanged content of PICs and satellite cells as compared to wild-type (**Fig. 18D,E**). Moreover, no

increase in sublaminal nuclei content was observed in *mdx* EOMs as compared to their wild-type counterpart (**Fig. 18F**), demonstrating no addition of progenitor cells to myofibers in *mdx* mice (but see McLoon et al., 2007; McLoon and Wirtschafter, 2002a; Porter, 2002). Taken together, these data support the hypothesis that EOM stem cell niche is unperturbed in *mdx* as compared to wild-type. Interestingly, the number of PICs is comparable in *mdx* TA and wild-type EOMs (**Fig. 18E**). During muscle regeneration, FAPs secrete pro-myogenic factors for satellite cells (Joe et al., 2010). We demonstrated that PICs include the FAPs (**Fig. 9**) and they secrete FST and IGF-1 (**Fig. 12).** Taken together, these data also suggest that the high number of PICs present in EOMs can be a major cause of their sparing in degenerative diseases through an increased amount of promyogenic and hypertrophic factors which can protect both the fibers and the satellite cells, preventing the loss of regenerative capacity observed in late stages of muscular dystrophies.

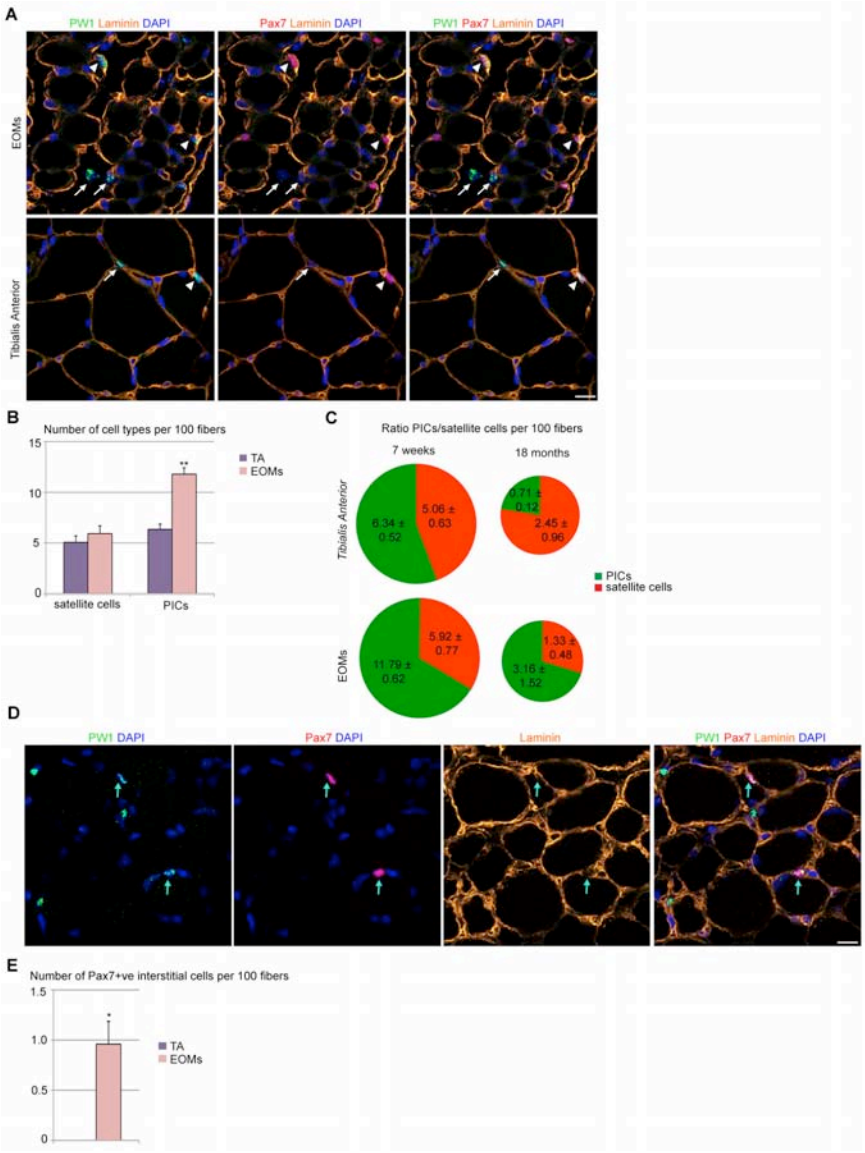

Figure 17. **Wild-type EOM stem cell niche is intrinsically different from limb muscles.** (**A**) Cross-sections of 7-week old EOMs (upper panels) and TA (lower panels) from C57Bl6 mice stained for PW1 (green) and the satellite cell marker Pax7 (red). Laminin staining (orange) shows the basal lamina. Nuclei

were counterstained by DAPI (blue). Arrows indicate PICs, arrowheads indicate satellite cells. **(B)** Number of PICs and satellite cells per 100 fibers in 7-week old EOMs and TA cross-sections as stained in (A) revealed a bigger amount of PICs but not satellite cells in EOMs compared to TA. (**C**) Ratio between PICs and Satellite Cells per 100 fibers in 7-week old and 18-month old TA and EOMs cross-sections demonstrated that EOM but not TA stem cell niche is retained throughout aging. PICs were determined as interstitial $PW1^{+}Pax7^{-}$ cells, satellite cells were determined as $Pax7^{+}$ cells underneath the basal lamina. (**D**) Cross-section of 7-week old EOMs as stained in (A) also revealed the presence of $Pax7^{+}$ cells totally or partially surrounded by basal lamina and often co-expressing PW1. Arrows indicate double-labelled $Pax7^{+}PW1^{+}$ interstitial cells. (**E**) Number of Pax7+ interstitial cells per 100 fibers in 7 w-old EOMs and TA cross-sections as stained in (A). For all graphs, values represent the mean number of cells ± s.e.m. Statistical significance was calculated from at least 3 animals of each condition. *p<0.05 **p<0.01 ***p<0.001.

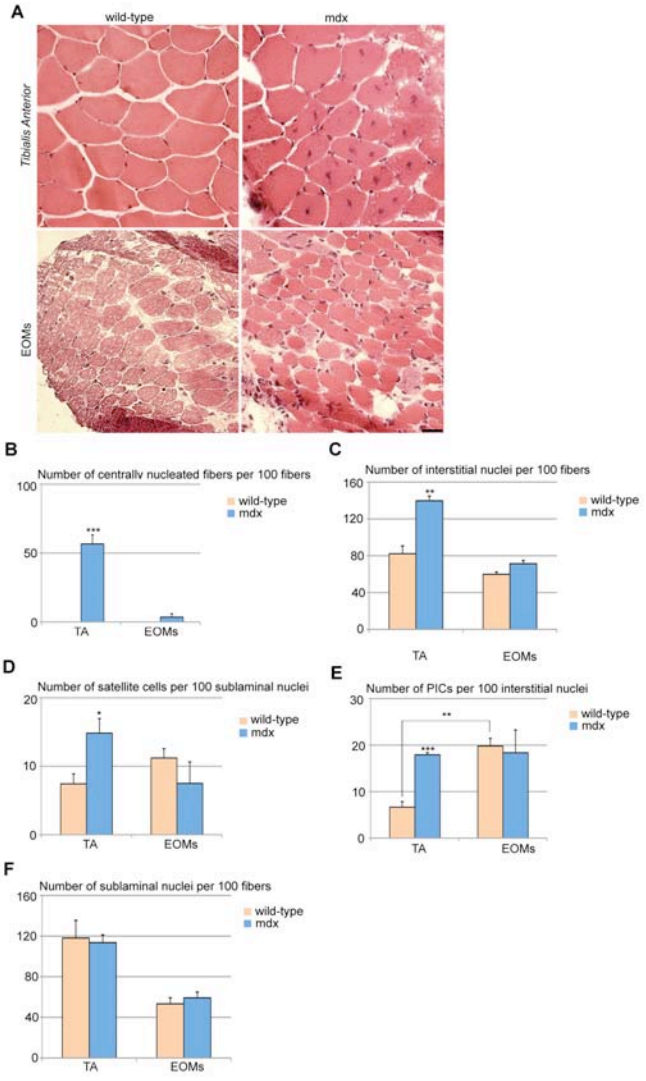

Figure 18. EOMs from *mdx* and wild-type mice exhibit a similar muscle stem cell niche. (**A**) Cross-sections of 7-week old TA (upper panels) and EOMs (lower panels) from *mdx* and age-matched wild-type mice stained with hematoxylin and eosin showed large regenerating areas in TA but not EOMs from *mdx* mice. (**B-C**) Number of centrally nucleated fibers (B) and interstitial nuclei (C) per 100 fibers indicated the presence of an ongoing regeneration process in *mdx* TA but not EOMs. (**D-E**) Number of satellite cells per 100 sublaminal nuclei (D) and PICs per 100 interstitial nuclei (E) revealed an activation of both progenitor cell types in TA but not EOMs from *mdx* mice, as compared to their wild-type counterparts. (**F**) Number of sublaminal nuclei per 100 fibers indicated no myonuclei addition in mdx EOMs as compared to wild-type. For all graphs, values represent the mean number ± s.e.m. Statistical significance was calculated from at least 3 animals of each condition. *p<0.05 **p<0.01 ***p<0.001.

DISCUSSION

We described previously a non-satellite cell progenitor population in the interstitium of postnatal muscle referred to as PW1-expressing interstitial cells (PICs) (Mitchell et al., 2010). Although both satellite cells and PICs express PW1/Peg3, satellite cells are strongly committed to the skeletal muscle lineage whereas a single PIC can generate both smooth and skeletal muscle *in vitro* (Mitchell et al., 2010). Genetic lineage-tracing studies demonstrated that PICs and satellite cells do not share a common progenitor despite their shared skeletal muscle potential (Mitchell et al., 2010). The different lineage origins of PICs and satellite cells are further underscored by results obtained here in which we show that PICs and satellite cells have distinct transcriptome signatures in both juvenile and adult stages. Even though our Affymetrix-based screen used juvenile (10 day old) satellite cells, we found that genes that have been ascribed to adult and therefore fully quiescent satellite cells are already clearly detected at high levels including Pax7, FGFR4, and c-met, however we also detected the expression of Myf5 and Ki67 consistent with a more activated state. During postnatal growth, PICs express many genes that play key roles during angiogenesis including the pericyte marker NG2 (Dellavalle et al., 2007). Pericytes also possess myogenic potential and are proposed to be the muscle resident postnatal equivalent of mesoangioblasts (Dellavalle et al., 2007; Sampaolesi et al., 2003). Similar to PICs, mesoangioblasts contribute to new myofibers following engraftment into damaged muscle (Sampaolesi et al., 2006; Sampaolesi et al., 2003) and show a mesenchymal and vascular-like profile (Brunelli et al., 2004). We note that mesoangioblasts express high levels of PW1 as well as PDGFRα (Pessina et al., 2012) suggesting a close relationship between these two skeletal muscle resident stem cells. Whereas embryonic mesoangioblasts derived from E10.5 dorsal aorta express Pax3 and require Pax3 for myogenic and adipogenic differentiation (Messina et al., 2009), we note that PICs are not

derived from a Pax3 expressing progenitor, however they initiate Pax3 and Pax7 expression upon myogenic differentiation (Mitchell et al., 2010). The precise relationship between PICs and mesoangioblasts remains to be fully elucidated.

In addition to non-satellite cell progenitors with myogenic potential, two recent reports have identified interstitial cells with adipogenic potential (Joe et al., 2010; Uezumi et al., 2010). It has been subsequently proposed that these two populations may be partially or completely overlapping (Natarajan et al., 2010). These cells, referred to here collectively as IAPs, are characterized by PDGFRα and high Sca1 expression (Joe et al., 2010; Uezumi et al., 2010). While these cells do not contribute directly to the generation of new myofibers in response to injury, they exert a pro-myogenic effect on satellite cells *in vitro* through paracrine interactions although the nature of the signals had not been elucidated (Joe et al., 2010). IAPs are also proposed to be the source of ectopic fat deposition in diseased muscle due to their ability to form fat *in vitro* and upon grafting either into diseased muscle or into pro-adipogenic sites *in vivo* (Joe et al., 2010; Uezumi et al., 2010). More recently, a study has described that white adipose tissue present in skeletal muscle contains a population of highly inducible brown fat ('beige') progenitors that express Sca1 and PDGFRα (Schulz et al., 2011). Since IAPs and PICs express high levels of Sca1 and PDGFRα in the adult, we wondered whether PICs and IAPs constituted a partially overlapping population of progenitors. This hypothesis seemed likely given our observation that PW1/Peg3 expression is found in all adult stem/progenitor cells examined to date including blood, brain, bone, skin and gut (Besson et al., 2011). If PW1/Peg3 serves as a pan-stem cell marker in adult tissues, we expect PW1/Peg3 expression to identify all progenitor cells types in a specific tissue containing a mixture of cell lineages such as skeletal muscle. In this study, we used the $PW1^{nlacZ}$ reporter mouse line (Besson et al., 2011) to purify PW1/Peg3 expressing cells from skeletal muscle during postnatal development and in the adult in order to determine

their cell fate potentials and specifically address the relationship of the various resident progenitor cells described to date. Our results demonstrate that IAPs constitute a sub-population of PICs that can be separated based upon PDGFRα expression. Specifically, PDGFRα$^+$ PICs are adipogenic progenitors whereas PDGFRα$^-$ PICs display myogenic potential. Sca1$^+$CD34$^+$PDGFRα$^+$ adipogenic progenitors have been shown to be present in abdominal murine white adipose tissue that are able to differentiate into both brown and white fat (Lee et al., 2012). Adipocyte progenitor cells isolated from skeletal muscle are highly committed to become brown fat, but can also give rise to white or 'beige' fat *in vitro* (Cannon and Nedergaard, 2012; Joe et al., 2010; Kajimura et al., 2008; Schulz et al., 2011; Seale et al., 2008; Seale et al., 2007) or *in vivo* (Joe et al., 2010). In this study, we report that PDGFRα$^+$ PICs express brown fat specific markers (Ucp1 and Prdm16) as well as markers for white/'beige' fat (i.e. Hoxc9) (Walden et al., 2012; Wu et al., 2012), suggesting that PDGFRα$^+$ PICs can generate 'beige' fat cells or a mixture of brown and white/'beige' adipocytes. We conclude that PW1/Peg3 expression identifies at least three progenitor populations in adult muscle: PW1$^+$Pax7$^+$ (satellite cells), PW1$^+$PDGFRα$^+$ (adipogenic progenitors), and myogenic interstitial cells that do not express Pax7 nor PDGFRα. Markers that are unique to the myogenic fraction of PICs remain to be elucidated and a search for such markers is presently underway. When cultured in adipogenic conditions, the myogenic PDGFRα$^-$ PICs express genes consistent with adipogenic activation although they fail to generate adipocytes. This raises the possibility that these cells possess the capacity to enter the adipogenic program but require additional signals. Sca1 is a marker widely used to enrich stem cells (Asakura et al., 2002; Benchaouir et al., 2004; Gumley et al., 1995; Tamaki et al., 2002), and is implicated in lineage commitment and stem cell self-renewal (Bonyadi et al., 2003; Ito et al., 2003). While all interstitial cells with myogenic or adipogenic potential express Sca1 and PW1/Peg3, we note that Sca1$^+$ cells that do not express

PW1/Peg3 are limited to a fibroblast-like phenotype in the conditions used in this study. In addition, it is noteworthy that Sca1 is restricted to few species and is not expressed in humans, consequently, our findings regarding PW1/Peg3 as a marker of stem cells may have additional impact as we have confirmed its expression in humans, pig and dog (Messina, *manuscript in preparation*).

Our analyses of early postnatal skeletal muscle progenitors revealed a transient population of PICs that expresses intermediate levels of Sca1 ($Sca1_{MED}$), which disappears between 3 and 5 weeks of age. A number of studies have suggested that addition of nuclei to myofibers is a primary mechanism of muscle growth up to 3 weeks of age whereas myofiber volume expansion underlies muscle growth at later stages (White et al., 2010). This switch in the cellular program underlying postnatal muscle growth is also concomitant with a change in the genetic requirement for *Pax7* and *Pax3*. Specifically, loss of *Pax7* and/or *Pax3* prior to 3 weeks of age leads to stunted postnatal growth and poor regeneration whereas loss of *Pax7/3* after 3 weeks of age has little effect (Lepper et al., 2009). Taken together, we propose that the transient juvenile population of PICs plays a role during early postnatal muscle growth, either through fusion with myofibers or by providing cues for myogenic progenitors. Interestingly, microarray analysis revealed specific expression of the GH receptor in $Sca1_{MED}$ juvenile PICs, suggesting a possible stimulation of the GH/IGF-1 axis in this cell type during postnatal muscle growth. Whether $Sca1_{MED}$ juvenile PICs fuse with myofibers or progressively up-regulate Sca1 expression by 3 weeks remains to be investigated.

In addition to a difference in levels of Sca1 expression, we note that adult PICs and juvenile $Sca1_{MED}$ and $Sca1_{HIGH}$ PICs express PDGFRα while only adult and juvenile $Sca1_{HIGH}$ PICs express Tie2 suggesting that the $Sca1_{HIGH}$ PICs in the juvenile and adult are the same cell population. In addition, we note that the $Sca1_{MED}$ PDGFRα^{+} juvenile population shows weak adipogenic

capacity when grown alone as compared to the unsorted population whereas the PDGFRα$^-$ population is the only fraction with myogenic potential. This suggests that the crosstalk between myogenic and adipogenic progenitors described in adult muscle by others (Joe et al., 2010; Uezumi et al., 2010) is present in juvenile in the PICs population.

Our data raise a more fundamental issue with regard to postnatal and adult stem cells. Satellite cells are quiescent and reside in a discreet anatomical location under the myofiber basal lamina whereas PICs reside in an interstitial location. Nonetheless, these cells are all progenitors that communicate with each other to support tissue integrity and regenerative responses (Pannerec et al., 2012). The observation that all these progenitors express PW1/Peg3 suggests a common regulatory program. A recent report has shown that *PW1/Peg3* is one member of a group of 10 parentally imprinted genes that are expressed in several somatic stem cell lineages in both mice and humans (Berg et al., 2011; Pannerec et al., 2012). We note that PW1/Peg3 participates in both intrinsic (p53) and extrinsic (inflammatory cytokine signaling) cell stress responses (Relaix et al., 2000; Relaix et al., 1998; Schwarzkopf et al., 2006), which may reflect a shared response mechanism to cell stress in stem cells. Future work will determine whether this common cell stress response mechanism in stem cells plays a role in pathological outcomes such as ectopic fat deposition and fibrosis that are commonly associated with late stage muscle diseases.

Ectopic fat and fibrosis constitute two features of degenerative diseases and are well described in muscular dystrophies (Glass, 2010; Serrano et al., 2011). Dystrophic muscle undergoes continuous cycles of degeneration and regeneration leading to chronic inflammation and an eventual depletion or exhaustion of the satellite cell pool (Tabebordbar et al., 2013). In addition, muscle fibers upregulate catabolic and autophagic pathways leading to a reduction of muscle mass and strength followed by their replacement with fibrosis and fat (Bonaldo and

Sandri, 2013). Coupled with these responses, satellite cells lose their regenerative capacity resulting in regenerative failure and the eventual loss of muscle tissue (Hikida, 2011; Jang et al., 2011). Several studies have reported that activation of the TGFβ/AcvR2B pathway stimulates fibrosis and that blocking this pathway *in vivo* can ameliorate the course of several muscle disorders, such as Duchenne muscular dystrophy (Bogdanovich et al., 2002; George Carlson et al., 2011; Pistilli et al., 2011), amyotrophic lateral sclerosis (Morrison et al., 2009), cancer-induced cachexia (Zhou et al., 2010a) and sarcopenia (Chiu et al., 2013). A promyogenic role has been proposed for interstitial progenitors (Joe et al., 2010; Murphy et al., 2011; Uezumi et al., 2010), however an abnormal or sustained activation of TGFβ pathway has been proposed to induce their overproliferation and deposition of fibrotic extracellular matrix (Uezumi et al., 2011).

PICs are highly responsive to perturbations to the muscle microenvironment including injury, age and changes in the expression of cell stress effectors including DNA damage repair mechanisms (Coletti et al., 2002; Didier et al., 2012; Nicolas et al., 2005; Schwarzkopf et al., 2006). In addition, *Pax7* mutant muscle exhibits a massive increase in PICs at birth prior to the loss of satellite cells suggesting an interaction between these cell populations (Mitchell et al., 2010). Moreover, PICs are present at high numbers during the marked increase of muscle mass that accompanies postnatal development (Mitchell et al., 2010). We report here that inhibition of the AcvR2B pathway leads to a marked increase in PICs. In addition, we show that PICs secrete FST and IGF-1 that act to block MST-mediated muscle atrophy (Amthor et al., 2004; Bodine et al., 2001; Lee et al., 2010; Rommel et al., 2001; Trendelenburg et al., 2009). The observation that satellite cells express MST and that PICs overcome the MST-mediated inhibition of satellite cell proliferation through secretion of FST and IGF-1 leads to a model in which satellite cell-mediated autocrine inhibition is neutralized by neighboring PICs. Given the

intimate anatomical relationship between PICs and satellite cells, we propose that PICs act primarily as niche support cells *in vivo*.

Satellite cell depletion provides an experimental platform for pathological conditions in which the satellite cell pool is reduced leading to ectopic fat and fibrosis following muscle injury (Sambasivan et al., 2011b). Inhibition of the AcvR2B pathway results in an increase in satellite cells and PICs in normal muscle, however we did not observe a significant rescue of the satellite cell population in satellite cell depleted muscle even though the PICs undergo a marked expansion. Nonetheless, we observe that regeneration is substantially rescued in RAP-031 treated satellite cell depleted muscle following injury suggesting that additional molecular signals, likely including cell stress mediated responses, are required. Our data confirm the requirement of satellite cells for regeneration (Lepper et al., 2011; Murphy et al., 2011; Sambasivan et al., 2011b) even though other non-satellite cells including PICs and pericytes have been identified with myogenic potential (Cappellari and Cossu, 2013; Pannerec et al., 2012). While lineage analyses reveal the majority of muscle fibers generated in the satellite cell depleted muscles come from a residual satellite cell population following inhibition of the AcvR2B pathway, we cannot exclude that PICs or other resident progenitor populations participate in muscle regeneration when the satellite cell compartment is intact. We note that a significant number of muscle fibers do not express the satellite cell lineage marker following regeneration in intact muscle ($mGFP^{-}mTomato^{+}$ labeled fibers) and that this number is increased following AcvR2B inhibition. Whether this is due to incomplete *Pax7*-mediated Cre activity or due to the participation of non-satellite cells will require the generation of additional lineage-specific markers for the myogenic PIC population.

While the inhibition of the AcvR2B pathway can restore muscle regeneration in satellite cell-depleted mice, we did not observe a significant rescue of the satellite cell pool suggesting that additional signals are required for satellite cell self-renewal.

Nonetheless, data provided in this study reveal that targeting the muscle stem cell niche should be considered in the design of therapeutic strategies aimed at restoring the regenerative potential of skeletal muscle in chronic muscle diseases.

Our data strongly support the hypothesis that interactions among muscle progenitor cells are important in regulating muscle homeostasis and regeneration and that alterations within the stem cell niche account for several muscle diseases. Nonetheless, some muscles, such as the EOMs, are resistant to several dystrophies as compared to other sets of skeletal muscles of the body (Porter, 2002; Porter et al., 1995), suggesting that muscle-type specific endogenous mechanisms operate in the stem cell niche leading to a more efficient regenerative response. We found that EOMs express a bigger number of PICs than satellite cells throughout postnatal life, in contrast to limb muscles where PICs and satellite cells are in equal amounts (1:1 ratio) during postnatal growth and adulthood. Nonetheless, old limb muscles exhibit an altered ratio between PICs and satellite cells, with a major loss within the PIC compartment rather than the satellite cell population, whereas the ratio between PICs and satellite cells is conserved in aged EOMs, although both cell types undergo a decline in number. As PICs secrete promyogenic factors, we suggest that EOM environment is more protected than limb muscle from damage or stress. Indeed, EOM stem cell niche from *mdx* mice do not display any particular difference as compared to wild type mice and *mdx* EOMs are not affected by the disease. It is interesting to note that the regeneration process undergoing in *mdx* limb muscles induces an increase of satellite cells and PICs up to a level comparable to the one observed in wild type EOMs. This suggests that mechanisms normally occurring during muscle regeneration to promote progenitor cell survival, activation and differentiation, are intrinsic to the EOM stem cell niche. Further studies of the EOMs promise to uncover the molecular cues ultimately leading to specific therapeutic approaches for congenital myopathies as well as muscle wasting.

MATERIALS AND METHODS

Mice. Animal models used were: C57Bl6J *PW1*^{IRESnLacZ} transgenic reporter mice (PW1^{nlacZ}), in which a nuclear operon lactose gene is expressed under the control of the Pw1 locus (Besson et al., 2011); C57Bl6J mice (Elevage Janvier); *GDF-8*/*myostatin-null* mice (Mst$^{-/-}$) (McPherron et al., 1997); knock-in heterozygous *Pax7*$^{DTR/+}$ mice, in which the diphteria toxin receptor (DTR) is expressed under the control of the *Pax7* promoter (Sambasivan et al., 2011b); *Tg:Pax7CreER*^{T2} mice, carrying a BAC where a tamoxifen-inducible Cre recombinase/estrogen receptor fusion protein, CreER^{T2} (Metzger and Chambon, 2001), is expressed under the control of *Pax7* (Mourikis et al., 2012); Rosa26^{mTomatoSTOPmGFP} mice (Jackson Laboratories). *Pax7*$^{DTR/+}$ mice were crossed with *Tg:Pax7CreER*^{T2} and Rosa26^{mTomatoSTOPmGFP} to obtain Pax7$^{DTR/+}$:Pax7CreER^{T2}:Rosa26^{mTomatoSTOPmGFP} animals. All work with mice was carried out in adherence to French government guidelines.

RAP-031 treatment. 5-weeks old C57Bl6 males, and 10-weeks old Pax7$^{DTR/+}$ or Pax7$^{DTR/+}$Pax7CreER^{T2}Rosa26^{mTomatoSTOPmGFP} mice were injected intraperitoneally with RAP-031 or vehicle (TBS) 10mg per kg^{-1}. Mice were weighed and dosed twice a week for 2 weeks and the day of sacrifice.

Tamoxifen treatment. 6 weeks-old Pax7$^{DTR/+}$:Pax7CreER^{T2}: Rosa26^{mTomatoSTOPmGFP} mice were injected intraperitoneally every day for 4 days with tamoxifen (250–300µl, 20 mg/ml; Sigma Aldrich) diluted in sunflower seed oil/5% ethanol.

Toxins injections. Mice were anaesthetized by intra-peritoneal injection of ketamine (100mg.kg^{-1}) and xylazine (10mg.kg^{-1}) in sterile saline solution. A total volume of 15-30µl was used for one single intramuscular injection of diphtheria toxin (DT) from *Corynebacterium diphtheria* (Sigma Aldrich) at 1ng.g^{-1} of body

weight or PBS into the TA muscle using 30G Hamilton syringe. Muscle injury was induced by intramuscular injection of 40µl of cardiotoxin from *Naja mossambica* (Latoxan) at a concentration of 10µM.

FACS analysis. For fluorescence-activated cell sorting, limb muscles from 1-7 week old $PW1^{nlacZ}$ or C57Bl6J mice were minced and digested in HBSS (Hank's Balanced Salt Solution, GIBCO) containing 2 $\mu g.ml^{-1}$ collagenase A (Roche), 2.4 $U.ml^{-1}$ dispase I (Roche), 10 $ng.ml^{-1}$ DNAse I (Roche), 0.4 mM $CaCl_2$ and 5 mM $MgCl_2$ as described previously (Besson et al., 2011; Mitchell et al., 2010). Primary antibodies at a concentration of 10 $ng.ml^{-1}$ were: rat anti-mouse CD45-APC (BD Biosciences), rat anti-mouse Ter119-APC (BD Biosciences), rat anti-mouse CD34-E450 (eBiosciences), rat anti-mouse Sca1-A700 (eBiosciences), and rat anti-mouse PDGFRα-PE (CD104a, eBiosciences). Cells were incubated for 30 minutes on ice. Cell pellets were washed twice before incubation with 5-Dodecanoylaminofluorescein Di-b-D-Galactopyranoside (C_{12}FDG, 60μM, Life Technologies) 1 hour at 37°C. Cells were washed once with ice-cold HBSS, filtered and re-suspended in HBSS containing 0.2% (w/v) BSA, 1% (v/v) penicillin-streptomycin and 10 $ng.ml^{-1}$ DNAse I. Flow cytometry analysis and cell sorting were performed on a FACSAria (Becton Dickinson) with appropriate isotype matching controls. $Ter119^+$ and $CD45^+$ cells were negatively selected and the remaining cells were gated based on their CD34 and Sca1 expression. PDGFRα positive or negative cells were sorted in the $Sca1_{HIGH}PW1^+$ and $Sca1_{HIGH}PW1^-$ fractions as well as the $Sca1_{MED}$ fraction. Purified cell populations were cultured as described below. For immunocytochemical analyses, freshly sorted cells (4,000 cells per well) were immediately centrifuged in 96-well plate (Becton Dickinson) coated with 0.1% porcine gelatin (Sigma) and subsequently reacted with X-Gal as described previously (Gross and Morgan, 1999). For immunofluorescence analyses, freshly sorted cells were immediately centrifuged onto 8-well chamber

glass slides (10,000 cells per well) (Thermo Scientific) for 5 minutes at 100g and immunostained for PW1 and Pax7 or PDGFRα, as described below. Quantitative analyses were performed by counting the number of positive cells out of a minimum of 300 cells in randomly chosen fields for each of three independent experiments.

Cell culture. Cells from limb muscles of 1-7 week old mice were obtained as described above. Immediately after sorting, cells were plated on gelatin-coated dishes at a density of 2,000 cells per cm^2 for myogenic differentiation and at a density of 6,000 cells per cm^2 for adipogenic differentiation. Cells were grown for one week in high-glucose Dulbecco's modified eagle medium (DMEM, Gibco) supplemented with 2.5 $ng.ml^{-1}$ bFGF (Invitrogen), 20% heat-inactivated FBS (Invitrogen), 10% heat-inactivated horse serum (Gibco), 1% (v/v) penicillin-streptomycin (Gibco), 1% (v/v) L-Glutamine (Gibco) and 1% (v/v) Na-pyruvate (Gibco). Medium was changed every 2 days. For myogenic differentiation, cells were transferred to differentiation medium (DM) for 2 days: DMEM containing 5% (v/v) horse serum and 1% (v/v) penicillin-streptomycin. For adipogenic differentiation, cells were transferred to adipogenic differentiation medium (ADM) for 5 days: DMEM containing 20% (v/v) FBS, 1% (v/v) penicillin-streptomycin, 0.25 μM dexamethasone (Sigma), 0.5 mM isobutylmethylxanthine (Sigma), 1 $\mu g.ml^{-1}$ insulin (Sigma) and 5 μM troglitazone (Sigma). Medium was changed every 2 days.

Transwell co-culture experiments: purified satellite cells were plated in the lower chamber at a density of 100 cells/cm^2. PICs were plated on the membrane of the insert well (1μm pore size, BD Biosciences) at 3,000 cells per cm^2. Cells were grown for 1 day in GM before adding the following factors: recombinant myostatin (R&D Systems) was added at 0, 20, 200 or 2000 $ng.mL^{-1}$: human follistatin blocking antibody (αFST) (R&D Systems), mouse IGF-1 blocking antibody (αIGF1) (R&D Systems) and isotype matched

IgG (R&D Systems) were used at 4µg.mL^{-1} (R&D Systems). After 2 days, cells were fixed with 4% (w/v) paraformaldehyde (Sigma Aldrich) and the number of cells per colony was counted. At least 3 independent experiments were performed for each condition.

Histological analyses. *Tibialis anterior* (TA), *soleus*, *plantaris* and *gastrocnemius* muscles were removed, weighed and snap frozen in liquid nitrogen-cooled isopentane (Sigma Aldrich) as previously described (Mitchell et al., 2010). In the case of Pax7$^{DTR/+}$:Pax7CreER^{T2}:Rosa26^{mTomatoSTOPmGFP} mice, TA muscles were fixed 2 hours in 4% (w/v) paraformaldehyde (Sigma Aldrich), incubated overnight in 20% (w/v) sucrose (Sigma Aldrich) and frozen in liquid nitrogen-cooled isopentane (Sigma Aldrich). Muscles were cryosectioned (7μm) before processing.

For immunofluorescence, TA cryosections were fixed in 4% (w/v) paraformaldehyde and processed for immunostaining as described previously (Mitchell et al., 2010). Primary antibodies used were: PW1 (Relaix et al., 1996) (rabbit, 1:3000), Pax7 (mouse, Developmental Studies Hybridoma Bank, 1:15), MyoD (mouse, BD Biosciences, 1:100), alpha-smooth muscle actin (rabbit, Sigma, 1:200), SM22-alpha (rabbit, Abcam, 1:200), MF20 (mouse, Developmental Studies Hybridoma Bank, 1:50), PDGFRα-biotin (mouse, R&D systems, 2.5ng.mL^{-1}), M-Cadherin (mouse, Nanotools, 1:100), Ki67 (mouse, BD Biosciences, 1:100), Ki67 (rabbit, Abcam, 1:100), GFP (chicken, Abcam, 1:500), laminin (rabbit, Sigma, 1:100). Antibody binding was revealed using species-specific secondary antibodies coupled to Alexa Fluor 488 (Molecular Probes), Cy3 or Cy5 (Jackson Immunoresearch). Nuclei were counterstained with DAPI (Sigma Aldrich).

To stain nuclei and muscle fibers, cryosections were stained with haematoxilin and eosin (H&E) (Sigma Aldrich).

To stain lipids, cells and cryosections were fixed in 10% formalin (Sigma Aldrich) for 5 minutes at 4°C, rinsed in water and then 100% propylene glycol (Sigma) for 10 minutes, stained with Oil red O (Sigma Aldrich) for 10 minutes at 60°C, placed in 85%

propylene glycol for 2 minutes and rinsed in water. Nuclei were counterstained with Mayer's Hematoxylin Solution (Sigma).

To detect collagen depositions, cryosections were stained with Mayer's haematoxylin (Sigma Aldrich) for 10 minutes, rinsed in running tap water for 20 minutes, then stained with 1.3% (w/v) Picro-sirius Red solution (Sigma Aldrich) for 45 minutes and washed twice in acidified water.

Fiber size distribution was measured from cryosections obtained from the mid-belly of TA stained with laminin, images were captured on a Zeiss AxioImagerZ1 microscope, and morphometric analysis was performed using MetaMorph7.5 (Molecular Devices).

Cells in culture were quantified by counting at least 300 cells from randomly chosen fields for each of 3 independent experiments. Fusion indexes were quantified by counting the number of nuclei in $MF20^+$ cells per total number of nuclei (Coletti et al., 2002; Mitchell et al., 2010; Schwarzkopf et al., 2006). Adipogenic potential was quantified by counting the number of nuclei in Oil red-O^+ cells per total number of nuclei. Images were acquired using a Leica DM-IL inverted fluorescence and light microscope, Leica DM fluorescence and light microscope or Leica SPE confocal microscope.

For quantitative analyses of immunostained tissues, positive cells were counted in at least 5 randomly chosen fields per muscle section of at least 3 animals for each condition.

Micro-array analysis. For micro-array analysis (GeneChip MOE 430 2.0, Affymetrix) RNA was extracted from freshly FACS sorted PICs and satellite cells from 1-week old C57Bl6 limb muscles, using RNeasy microkit (Qiagen) according to manufacturer's recommendations. Three independent samples for each experimental group were sent for analysis to PartnerChip (Génopole d'Evry, France). Statistical analysis was performed using a Fold Change threshold=1 and p-value=0,01. Subsequent analyses were performed using the Gene Ontology database. The

microarray analysis has been deposited in NCBI's Gene Expression Omnibus and is accessible through GEO Series accession number GSE40523 (http://www.ncbi.nlm.nih.gov/geo/query/acc.cgi?acc=GSE40523).

RNA extraction and RT-PCR. RNA extracts were prepared from a minimum of 2×10^4 freshly sorted cells using RNeasy Micro Kit (Qiagen) according to manufacturer's instructions, and reverse transcribed using the SuperScript First-Strand Synthesis System (Life Technologies). Semi-quantitative PCR was performed using ReddyMix Master Mix (Thermo Scientific) under the following cycling conditions: 94°C for 5 min followed by 30 cycles of amplification (94°C for 30 seconds, 60°C for 30 seconds and 72°C for 1 min) and a final incubation at 72°C for 10 minutes. Primers sequences used are listed in Table 3.

Statistical analysis. All statistics were performed using an unpaired Student's *t*-test in the StatView software. Values represent the mean ± s.e.m. *p<0.05, **p<0.01, ***p<0.001 and ****p<0.0001.

Gene	Forward primer	Reverse primer
18S	CGGCTACCACATCCAAGGAA	TATACGCTATTGGAGCTGGAA
CD68	AGGTCCAGGGAGGTTGTGA	CCGCCATGTAGTCCAGGTAG
FABP4/ Ap2	ACCCTCCTGTGCTGCAGCCTT	TGTGGCAAAGCCCACTCCCACT
FGFR4	ATCTTTCAGGGGACACCAGCTTTG	TGCCCTCTTTGTACCAGTGACGA
Hoxc9	GCAGCAAGCACAAAGAGGAGAAG	GCGTCTGGTACTTGGTGTAGGG
Ki67	GCATGTATCACCTGAGCCTGTGAA	TGACTTGGCCCCGAGATGTAGATT
Myf5	AGCTGGCTCTTCAGGAGACA	ACGTGATAGATAAGTCTGGAG
MyoD	ACATAGACTTGACAGGCCCCGA	AGACCTTCGATGTAGCGGATGG
Myogenin	CTAGAGGCCCTTGCTCAGGTC	GAAATGATCTCCTGGGTTGG
NG2	TCCAGATCACTGGGCCTTACTT	CTCTGAGGCATTAGCTAGCAGAAC
P2Y14	GAAGCCAGACGTGAAGGAGTTCAT	GCAAGCTTCGTCAACAGAATCCAG
Pax3	ACCAGGCATGGATTTTCAAGC	GAGGGGAGAGAGCATAGTC
Pax7	TCTTACTGCCCACCCACCTA	AGGAAGAAGTCCCAGCACAG
PDGFα	AGACCAGGACGGTCATTTACGAGA	CTTCCTGACATACTCCACTTTGGC
PDGFRα	GACGAGTGTCCTTCGCCAAAGTG	CAAAATCCGACCAAGCACGAGG
PDGFRβ	GCAGCGACACTCCAACAAGCA	TCACTCTCCCCAGTCAGGTTCAAG
Prdm16	CAGCACGGTGAAGCCATTC	GCGTGCATCCGCTTGTG
QPRT	GAACGGGTGGCTCTTAACAC	CAGGCTGCTACATTCCACCT
SM22	TAATGGCTTTGGGCAGTTTG	TGCAGTTGGCTGTCTGTGAA
Tie2	TGGACTCTTTAGCCGGCTTAGTTC	CAGTGGATCTTGGTGCTGGTTCAT
UCP1	ACTGCCACACCTCCAGTCATT	CTTTGCCTCACTCAGGATTGG
Vimentin	AGTCAAACGAGTACCGGAGACA	GTATTCACGAAGGTGACGAGCCAT
Myostatin	GGCTCAAACAGCCTGAATCCAA	CCAGTCCCATCCAAAGGCTTCAAA
Follistatin	CCCCAACTGCATCCCTTGTAAA	TCCAGGTGATGTTGGAACAGTC
ALK-2/ AcvR1	ATGACTACCTTCAGCTCACT	CTTCGCCAGAGAAGTTAATG
ALK-4/ AcvR1B	ACCGCTACACAGTGACCATT	TCTTCACATCTTCCTGCACG
ALK-5/ TGFβR1	ATCCATCACTAGATCGCCCT	CGATGGATCAGAAGGTACAAGA
AcvR2A	CTTAAGGCTAATGTGGTCTC	GACTAGATTCTTTGGGAGGA
AcvR2B	ATCGTCATCGGAAACCTCCC	CAGCCAGTGATCCTTAATC
TGFβR2	CGTGTGGAGGAAGAACAACA	TCTCAAACTGCTCTGAGGTG
Smad2	CGGAACCTGCATTCTGGTGTTCAA	CTCAGCAAACACTTCCCCACCTAT
Smad3	ATTTTCGTCCAGTCTCCCAACTGC	GCCTTTGACGAAGCTCATACGGAT
Smad4	AGGCAAAGGAGTGCAGTTGGAATG	TGACACTGCCGCAGATCAAAGA
BMP-2	TGCTCAGCATGTTTGGCCTGAA	AAACTCGTCACTGGGGACAGAACT
IGF-1 IEa (416 bp)	ATTTAAGATCTGCCTCTGTGACTTCTT	TCTTGTTTCCTGCACTTCCTCTACT
IGF-1 IEb (468 bp)	ATTTAAGATCTGCCTCTGTGACTTCTT	TCTTGTTTCCTGCACTTCCTCTACT
IGF-1R	GAGAAAAGGGAATTTCGTCCCAAATAAAAGG	CTATGGTGGAGAGGTAACAGAGGTC

Table 3. Primers used for semi-quantitative PCR.

REFERENCES:

Abu-Baker, A. and Rouleau, G. A. (2007). Oculopharyngeal muscular dystrophy: recent advances in the understanding of the molecular pathogenic mechanisms and treatment strategies. *Biochim Biophys Acta* **1772**, 173-85.

Adamo, M. L., Neuenschwander, S., LeRoith, D. and Roberts, C. T., Jr. (1993). Structure, expression, and regulation of the IGF-I gene. *Adv Exp Med Biol* **343**, 1-11.

Akpan, I., Goncalves, M. D., Dhir, R., Yin, X., Pistilli, E. E., Bogdanovich, S., Khurana, T. S., Ucran, J., Lachey, J. and Ahima, R. S. (2009). The effects of a soluble activin type IIB receptor on obesity and insulin sensitivity. *Int J Obes (Lond)* **33**, 1265-73.

Amthor, H., Nicholas, G., McKinnell, I., Kemp, C. F., Sharma, M., Kambadur, R. and Patel, K. (2004). Follistatin complexes Myostatin and antagonises Myostatin-mediated inhibition of myogenesis. *Dev Biol* **270**, 19-30.

Amthor, H., Otto, A., Vulin, A., Rochat, A., Dumonceaux, J., Garcia, L., Mouisel, E., Hourde, C., Macharia, R., Friedrichs, M. et al. (2009). Muscle hypertrophy driven by myostatin blockade does not require stem/precursor-cell activity. *Proc Natl Acad Sci U S A* **106**, 7479-84.

Anderson, B. C., Christiansen, S. P. and McLoon, L. K. (2008). Myogenic growth factors can decrease extraocular muscle force generation: a potential biological approach to the treatment of strabismus. *Invest Ophthalmol Vis Sci* **49**, 221-9.

Asakura, A., Seale, P., Girgis-Gabardo, A. and Rudnicki, M. A. (2002). Myogenic specification of side population cells in skeletal muscle. *J Cell Biol* **159**, 123-34.

Barbuti, A., Galvez, B. G., Crespi, A., Scavone, A., Baruscotti, M., Brioschi, C., Cossu, G. and DiFrancesco, D. (2010). Mesoangioblasts from ventricular vessels can differentiate in vitro into cardiac myocytes with sinoatrial-like properties. *J Mol Cell Cardiol* **48**, 415-23.

Beauchamp, J. R., Heslop, L., Yu, D. S., Tajbakhsh, S., Kelly, R. G., Wernig, A., Buckingham, M. E., Partridge, T. A. and Zammit, P. S. (2000). Expression of CD34 and Myf5 defines the majority of quiescent adult skeletal muscle satellite cells. *J Cell Biol* **151**, 1221-34.

Benchaouir, R., Rameau, P., Decraene, C., Dreyfus, P., Israeli, D., Pietu, G., Danos, O. and Garcia, L. (2004). Evidence for a resident subset of cells with SP phenotype in the C2C12 myogenic line: a tool to explore muscle stem cell biology. *Exp Cell Res* **294**, 254-68.

Berg, J. S., Lin, K. K., Sonnet, C., Boles, N. C., Weksberg, D. C., Nguyen, H., Holt, L. J., Rickwood, D., Daly, R. J. and Goodell, M. A. (2011). Imprinted genes that regulate early mammalian growth are coexpressed in somatic stem cells. *PLoS One* **6**, e26410.

Bernasconi, P., Di Blasi, C., Mora, M., Morandi, L., Galbiati, S., Confalonieri, P., Cornelio, F. and Mantegazza, R. (1999). Transforming growth factor-beta1 and fibrosis in congenital muscular dystrophies. *Neuromuscul Disord* **9**, 28-33.

Bernasconi, P., Torchiana, E., Confalonieri, P., Brugnoni, R., Barresi, R., Mora, M., Cornelio, F., Morandi, L. and Mantegazza, R. (1995). Expression of transforming growth factor-beta 1 in dystrophic patient muscles correlates with fibrosis. Pathogenetic role of a fibrogenic cytokine. *J Clin Invest* **96**, 1137-44.

Besson, V., Smeriglio, P., Wegener, A., Relaix, F., Nait Oumesmar, B., Sassoon, D. A. and Marazzi, G. (2011). PW1 gene/paternally expressed gene 3 (PW1/Peg3) identifies multiple adult stem and progenitor cell populations. *Proc Natl Acad Sci U S A* **108**, 11470-5.

Birbrair, A., Zhang, T., Wang, Z. M., Messi, M. L., Enikolopov, G. N., Mintz, A. and Delbono, O. (2013). Role of pericytes in skeletal muscle regeneration and fat accumulation. *Stem Cells Dev* **22**, 2298-314.

Bismuth, K. and Relaix, F. (2010). Genetic regulation of skeletal muscle development. *Exp Cell Res* **316**, 3081-6.

Bodine, S. C., Stitt, T. N., Gonzalez, M., Kline, W. O., Stover, G. L., Bauerlein, R., Zlotchenko, E., Scrimgeour, A., Lawrence, J. C., Glass, D. J. et al. (2001). Akt/mTOR pathway is a crucial regulator of skeletal muscle hypertrophy and can prevent muscle atrophy in vivo. *Nat Cell Biol* **3**, 1014-9.

Bogdanovich, S., Krag, T. O., Barton, E. R., Morris, L. D., Whittemore, L. A., Ahima, R. S. and Khurana, T. S. (2002). Functional improvement of dystrophic muscle by myostatin blockade. *Nature* **420**, 418-21.

Bohnsack, B. L., Gallina, D., Thompson, H., Kasprick, D. S., Lucarelli, M. J., Dootz, G., Nelson, C., McGonnell, I. M. and Kahana, A. (2011). Development of extraocular muscles requires early signals from periocular neural crest and the developing eye. *Arch Ophthalmol* **129**, 1030-41.

Bonaldo, P. and Sandri, M. (2013). Cellular and molecular mechanisms of muscle atrophy. *Dis Model Mech* **6**, 25-39.

Bonyadi, M., Waldman, S. D., Liu, D., Aubin, J. E., Grynpas, M. D. and Stanford, W. L. (2003). Mesenchymal progenitor self-renewal deficiency leads to age-dependent osteoporosis in Sca-1/Ly-6A null mice. *Proc Natl Acad Sci U S A* **100**, 5840-5.

Brack, A. S., Conboy, M. J., Roy, S., Lee, M., Kuo, C. J., Keller, C. and Rando, T. A. (2007). Increased Wnt signaling during aging alters muscle stem cell fate and increases fibrosis. *Science* **317**, 807-10.

Brueckner, J. K., Itkis, O. and Porter, J. D. (1996). Spatial and temporal patterns of myosin heavy chain expression in developing rat extraocular muscle. *J Muscle Res Cell Motil* **17**, 297-312.

Brunelli, S., Tagliafico, E., De Angelis, F. G., Tonlorenzi, R., Baesso, S., Ferrari, S., Niinobe, M., Yoshikawa, K., Schwartz, R. J., Bozzoni, I. et al.

(2004). Msx2 and necdin combined activities are required for smooth muscle differentiation in mesoangioblast stem cells. *Circ Res* **94**, 1571-8.
Buckingham, M. and Montarras, D. (2008). Skeletal muscle stem cells. *Curr Opin Genet Dev* **18**, 330-6.
Bunting, K. D. (2002). ABC transporters as phenotypic markers and functional regulators of stem cells. *Stem Cells* **20**, 11-20.
Burghes, A. H., Logan, C., Hu, X., Belfall, B., Worton, R. G. and Ray, P. N. (1987). A cDNA clone from the Duchenne/Becker muscular dystrophy gene. *Nature* **328**, 434-7.
Burkin, D. J. and Kaufman, S. J. (1999). The alpha7beta1 integrin in muscle development and disease. *Cell Tissue Res* **296**, 183-90.
Cannon, B. and Nedergaard, J. (2012). Cell biology: Neither brown nor white. *Nature* **488**, 286-7.
Cappellari, O. and Cossu, G. (2013). Pericytes in development and pathology of skeletal muscle. *Circ Res* **113**, 341-7.
Carmeli, E., Moas, M., Reznick, A. Z. and Coleman, R. (2004). Matrix metalloproteinases and skeletal muscle: a brief review. *Muscle Nerve* **29**, 191-7.
Chazaud, B., Sonnet, C., Lafuste, P., Bassez, G., Rimaniol, A. C., Poron, F., Authier, F. J., Dreyfus, P. A. and Gherardi, R. K. (2003). Satellite cells attract monocytes and use macrophages as a support to escape apoptosis and enhance muscle growth. *J Cell Biol* **163**, 1133-43.
Chen, J. and von Bartheld, C. S. (2004). Role of exogenous and endogenous trophic factors in the regulation of extraocular muscle strength during development. *Invest Ophthalmol Vis Sci* **45**, 3538-45.
Chiu, C. S., Peekhaus, N., Weber, H., Adamski, S., Murray, E. M., Zhang, H. Z., Zhao, J. Z., Ernst, R., Lineberger, J., Huang, L. et al. (2013). Increased Muscle Force Production and Bone Mineral Density in ActRIIB-Fc-Treated Mature Rodents. *J Gerontol A Biol Sci Med Sci* **68**, 1181-92.
Clop, A., Marcq, F., Takeda, H., Pirottin, D., Tordoir, X., Bibe, B., Bouix, J., Caiment, F., Elsen, J. M., Eychenne, F. et al. (2006). A mutation creating a potential illegitimate microRNA target site in the myostatin gene affects muscularity in sheep. *Nat Genet* **38**, 813-8.
Coletti, D., Yang, E., Marazzi, G. and Sassoon, D. (2002). TNFalpha inhibits skeletal myogenesis through a PW1-dependent pathway by recruitment of caspase pathways. *EMBO J* **21**, 631-42.
Conboy, I. M., Conboy, M. J., Wagers, A. J., Girma, E. R., Weissman, I. L. and Rando, T. A. (2005). Rejuvenation of aged progenitor cells by exposure to a young systemic environment. *Nature* **433**, 760-4.
Davies, J. E., Berger, Z. and Rubinsztein, D. C. (2006). Oculopharyngeal muscular dystrophy: potential therapies for an aggregate-associated disorder. *Int J Biochem Cell Biol* **38**, 1457-62.

Day, K., Shefer, G., Shearer, A. and Yablonka-Reuveni, Z. (2010). The depletion of skeletal muscle satellite cells with age is concomitant with reduced capacity of single progenitors to produce reserve progeny. *Dev Biol* **340**, 330-43.
De Angelis, L., Berghella, L., Coletta, M., Lattanzi, L., Zanchi, M., Cusella-De Angelis, M. G., Ponzetto, C. and Cossu, G. (1999). Skeletal myogenic progenitors originating from embryonic dorsal aorta coexpress endothelial and myogenic markers and contribute to postnatal muscle growth and regeneration. *J Cell Biol* **147**, 869-78.
Dellavalle, A., Maroli, G., Covarello, D., Azzoni, E., Innocenzi, A., Perani, L., Antonini, S., Sambasivan, R., Brunelli, S., Tajbakhsh, S. et al. (2011). Pericytes resident in postnatal skeletal muscle differentiate into muscle fibres and generate satellite cells. *Nat Commun* **2**, 499.
Dellavalle, A., Sampaolesi, M., Tonlorenzi, R., Tagliafico, E., Sacchetti, B., Perani, L., Innocenzi, A., Galvez, B. G., Messina, G., Morosetti, R. et al. (2007). Pericytes of human skeletal muscle are myogenic precursors distinct from satellite cells. *Nat Cell Biol* **9**, 255-67.
Didier, N., Hourde, C., Amthor, H., Marazzi, G. and Sassoon, D. (2012). Loss of a single allele for Ku80 leads to progenitor dysfunction and accelerated aging in skeletal muscle. *EMBO Mol Med* **4**, 910-23.
Dobrowolny, G., Aucello, M., Molinaro, M. and Musaro, A. (2008). Local expression of mIgf-1 modulates ubiquitin, caspase and CDK5 expression in skeletal muscle of an ALS mouse model. *Neurol Res* **30**, 131-6.
Dobrowolny, G., Giacinti, C., Pelosi, L., Nicoletti, C., Winn, N., Barberi, L., Molinaro, M., Rosenthal, N. and Musaro, A. (2005). Muscle expression of a local Igf-1 isoform protects motor neurons in an ALS mouse model. *J Cell Biol* **168**, 193-9.
Doherty, M. J., Ashton, B. A., Walsh, S., Beresford, J. N., Grant, M. E. and Canfield, A. E. (1998). Vascular pericytes express osteogenic potential in vitro and in vivo. *J Bone Miner Res* **13**, 828-38.
Doyle, M. J., Zhou, S., Tanaka, K. K., Pisconti, A., Farina, N. H., Sorrentino, B. P. and Olwin, B. B. (2011). Abcg2 labels multiple cell types in skeletal muscle and participates in muscle regeneration. *J Cell Biol* **195**, 147-63.
Evans, D. J. and Noden, D. M. (2006). Spatial relations between avian craniofacial neural crest and paraxial mesoderm cells. *Dev Dyn* **235**, 1310-25.
Farrington-Rock, C., Crofts, N. J., Doherty, M. J., Ashton, B. A., Griffin-Jones, C. and Canfield, A. E. (2004). Chondrogenic and adipogenic potential of microvascular pericytes. *Circulation* **110**, 2226-32.
Feng, C. and Von Bartheld, C. S. (2010). Schwann cells as a source of insulin-like growth factor-1 for extraocular muscles. *Muscle Nerve* **41**, 478-86.
Fukada, S., Higuchi, S., Segawa, M., Koda, K., Yamamoto, Y., Tsujikawa, K., Kohama, Y., Uezumi, A., Imamura, M., Miyagoe-Suzuki, Y. et al. (2004). Purification and cell-surface marker characterization of quiescent

satellite cells from murine skeletal muscle by a novel monoclonal antibody. *Exp Cell Res* **296**, 245-55.

Fukada, S., Uezumi, A., Ikemoto, M., Masuda, S., Segawa, M., Tanimura, N., Yamamoto, H., Miyagoe-Suzuki, Y. and Takeda, S. (2007). Molecular signature of quiescent satellite cells in adult skeletal muscle. *Stem Cells* **25**, 2448-59.

Gentile, M. A., Nantermet, P. V., Vogel, R. L., Phillips, R., Holder, D., Hodor, P., Cheng, C., Dai, H., Freedman, L. P. and Ray, W. J. (2010). Androgen-mediated improvement of body composition and muscle function involves a novel early transcriptional program including IGF1, mechano growth factor, and induction of {beta}-catenin. *J Mol Endocrinol* **44**, 55-73.

George Carlson, C., Bruemmer, K., Sesti, J., Stefanski, C., Curtis, H., Ucran, J., Lachey, J. and Seehra, J. S. (2011). Soluble activin receptor type IIB increases forward pulling tension in the mdx mouse. *Muscle Nerve* **43**, 694-9.

Gilmour, R. S. (1994). The implications of insulin-like growth factor mRNA heterogeneity. *J Endocrinol* **140**, 1-3.

Glass, D. J. (2010). Signaling pathways perturbing muscle mass. *Curr Opin Clin Nutr Metab Care* **13**, 225-9.

Grobet, L., Martin, L. J., Poncelet, D., Pirottin, D., Brouwers, B., Riquet, J., Schoeberlein, A., Dunner, S., Menissier, F., Massabanda, J. et al. (1997). A deletion in the bovine myostatin gene causes the double-muscled phenotype in cattle. *Nat Genet* **17**, 71-4.

Gros, J., Manceau, M., Thome, V. and Marcelle, C. (2005). A common somitic origin for embryonic muscle progenitors and satellite cells. *Nature* **435**, 954-8.

Gross, J. G. and Morgan, J. E. (1999). Muscle precursor cells injected into irradiated mdx mouse muscle persist after serial injury. *Muscle Nerve* **22**, 174-85.

Gumley, T. P., McKenzie, I. F. and Sandrin, M. S. (1995). Tissue expression, structure and function of the murine Ly-6 family of molecules. *Immunol Cell Biol* **73**, 277-96.

Harel, I., Nathan, E., Tirosh-Finkel, L., Zigdon, H., Guimaraes-Camboa, N., Evans, S. M. and Tzahor, E. (2009). Distinct origins and genetic programs of head muscle satellite cells. *Dev Cell* **16**, 822-32.

Hewitt, S. C., Li, Y., Li, L. and Korach, K. S. (2010). Estrogen-mediated regulation of Igf1 transcription and uterine growth involves direct binding of estrogen receptor alpha to estrogen-responsive elements. *J Biol Chem* **285**, 2676-85.

Hikida, R. S. (2011). Aging changes in satellite cells and their functions. *Curr Aging Sci* **4**, 279-97.

Hill, J. J., Davies, M. V., Pearson, A. A., Wang, J. H., Hewick, R. M., Wolfman, N. M. and Qiu, Y. (2002). The myostatin propeptide and the

follistatin-related gene are inhibitory binding proteins of myostatin in normal serum. *J Biol Chem* **277**, 40735-41.
Irintchev, A., Zeschnigk, M., Starzinski-Powitz, A. and Wernig, A. (1994). Expression pattern of M-cadherin in normal, denervated, and regenerating mouse muscles. *Dev Dyn* **199**, 326-37.
Ito, C. Y., Li, C. Y., Bernstein, A., Dick, J. E. and Stanford, W. L. (2003). Hematopoietic stem cell and progenitor defects in Sca-1/Ly-6A-null mice. *Blood* **101**, 517-23.
Jacoby, J., Ko, K., Weiss, C. and Rushbrook, J. I. (1990). Systematic variation in myosin expression along extraocular muscle fibres of the adult rat. *J Muscle Res Cell Motil* **11**, 25-40.
Jang, Y. C., Sinha, M., Cerletti, M., Dall'Osso, C. and Wagers, A. J. (2011). Skeletal muscle stem cells: effects of aging and metabolism on muscle regenerative function. *Cold Spring Harb Symp Quant Biol* **76**, 101-11.
Joe, A. W., Yi, L., Natarajan, A., Le Grand, F., So, L., Wang, J., Rudnicki, M. A. and Rossi, F. M. (2010). Muscle injury activates resident fibro/adipogenic progenitors that facilitate myogenesis. *Nat Cell Biol* **12**, 153-63.
Johns, N., Stephens, N. A. and Fearon, K. C. (2013). Muscle wasting in cancer. *Int J Biochem Cell Biol*.
Joulia, D., Bernardi, H., Garandel, V., Rabenoelina, F., Vernus, B. and Cabello, G. (2003). Mechanisms involved in the inhibition of myoblast proliferation and differentiation by myostatin. *Exp Cell Res* **286**, 263-75.
Kajimura, S., Seale, P., Tomaru, T., Erdjument-Bromage, H., Cooper, M. P., Ruas, J. L., Chin, S., Tempst, P., Lazar, M. A. and Spiegelman, B. M. (2008). Regulation of the brown and white fat gene programs through a PRDM16/CtBP transcriptional complex. *Genes Dev* **22**, 1397-409.
Kallestad, K. M., Hebert, S. L., McDonald, A. A., Daniel, M. L., Cu, S. R. and McLoon, L. K. (2011). Sparing of extraocular muscle in aging and muscular dystrophies: a myogenic precursor cell hypothesis. *Exp Cell Res* **317**, 873-85.
Kambadur, R., Sharma, M., Smith, T. P. and Bass, J. J. (1997). Mutations in myostatin (GDF8) in double-muscled Belgian Blue and Piedmontese cattle. *Genome Res* **7**, 910-6.
Kanisicak, O., Mendez, J. J., Yamamoto, S., Yamamoto, M. and Goldhamer, D. J. (2009). Progenitors of skeletal muscle satellite cells express the muscle determination gene, MyoD. *Dev Biol* **332**, 131-41.
Karow, M., Sanchez, R., Schichor, C., Masserdotti, G., Ortega, F., Heinrich, C., Gascon, S., Khan, M. A., Lie, D. C., Dellavalle, A. et al. (2012). Reprogramming of pericyte-derived cells of the adult human brain into induced neuronal cells. *Cell Stem Cell* **11**, 471-6.

Keire, P., Shearer, A., Shefer, G. and Yablonka-Reuveni, Z. (2013). Isolation and culture of skeletal muscle myofibers as a means to analyze satellite cells. *Methods Mol Biol* **946**, 431-68.
Kelly, R. G., Jerome-Majewska, L. A. and Papaioannou, V. E. (2004). The del22q11.2 candidate gene Tbx1 regulates branchiomeric myogenesis. *Hum Mol Genet* **13**, 2829-40.
Kemaladewi, D. U., de Gorter, D. J., Aartsma-Rus, A., van Ommen, G. J., ten Dijke, P., t Hoen, P. A. and Hoogaars, W. M. (2012). Cell-type specific regulation of myostatin signaling. *FASEB J* **26**, 1462-72.
Khanna, S., Cheng, G., Gong, B., Mustari, M. J. and Porter, J. D. (2004). Genome-wide transcriptional profiles are consistent with functional specialization of the extraocular muscle layers. *Invest Ophthalmol Vis Sci* **45**, 3055-66.
Khanna, S., Merriam, A. P., Gong, B., Leahy, P. and Porter, J. D. (2003). Comprehensive expression profiling by muscle tissue class and identification of the molecular niche of extraocular muscle. *FASEB J* **17**, 1370-2.
Khurana, T. S., Prendergast, R. A., Alameddine, H. S., Tome, F. M., Fardeau, M., Arahata, K., Sugita, H. and Kunkel, L. M. (1995). Absence of extraocular muscle pathology in Duchenne's muscular dystrophy: role for calcium homeostasis in extraocular muscle sparing. *J Exp Med* **182**, 467-75.
Kitamura, K., Miura, H., Miyagawa-Tomita, S., Yanazawa, M., Katoh-Fukui, Y., Suzuki, R., Ohuchi, H., Suehiro, A., Motegi, Y., Nakahara, Y. et al. (1999). Mouse Pitx2 deficiency leads to anomalies of the ventral body wall, heart, extra- and periocular mesoderm and right pulmonary isomerism. *Development* **126**, 5749-58.
Koncarevic, A., Cornwall-Brady, M., Pullen, A., Davies, M., Sako, D., Liu, J., Kumar, R., Tomkinson, K., Baker, T., Umiker, B. et al. (2010). A soluble activin receptor type IIb prevents the effects of androgen deprivation on body composition and bone health. *Endocrinology* **151**, 4289-300.
Langley, B., Thomas, M., Bishop, A., Sharma, M., Gilmour, S. and Kambadur, R. (2002). Myostatin inhibits myoblast differentiation by down-regulating MyoD expression. *J Biol Chem* **277**, 49831-40.
Latres, E., Amini, A. R., Amini, A. A., Griffiths, J., Martin, F. J., Wei, Y., Lin, H. C., Yancopoulos, G. D. and Glass, D. J. (2005). Insulin-like growth factor-1 (IGF-1) inversely regulates atrophy-induced genes via the phosphatidylinositol 3-kinase/Akt/mammalian target of rapamycin (PI3K/Akt/mTOR) pathway. *J Biol Chem* **280**, 2737-44.
Lawlor, M. W., Read, B. P., Edelstein, R., Yang, N., Pierson, C. R., Stein, M. J., Wermer-Colan, A., Buj-Bello, A., Lachey, J. L., Seehra, J. S. et al. (2011). Inhibition of activin receptor type IIB increases strength and lifespan in myotubularin-deficient mice. *Am J Pathol* **178**, 784-93.

Lee, S. J., Lee, Y. S., Zimmers, T. A., Soleimani, A., Matzuk, M. M., Tsuchida, K., Cohn, R. D. and Barton, E. R. (2010). Regulation of muscle mass by follistatin and activins. *Mol Endocrinol* **24**, 1998-2008.
Lee, S. J. and McPherron, A. C. (2001). Regulation of myostatin activity and muscle growth. *Proc Natl Acad Sci U S A* **98**, 9306-11.
Lee, Y. H., Petkova, A. P., Mottillo, E. P. and Granneman, J. G. (2012). In vivo identification of bipotential adipocyte progenitors recruited by beta3-adrenoceptor activation and high-fat feeding. *Cell Metab* **15**, 480-91.
Lepper, C., Conway, S. J. and Fan, C. M. (2009). Adult satellite cells and embryonic muscle progenitors have distinct genetic requirements. *Nature* **460**, 627-31.
Lepper, C., Partridge, T. A. and Fan, C. M. (2011). An absolute requirement for Pax7-positive satellite cells in acute injury-induced skeletal muscle regeneration. *Development* **138**, 3639-46.
Lescaudron, L., Peltekian, E., Fontaine-Perus, J., Paulin, D., Zampieri, M., Garcia, L. and Parrish, E. (1999). Blood borne macrophages are essential for the triggering of muscle regeneration following muscle transplant. *Neuromuscul Disord* **9**, 72-80.
Liadaki, K., Casar, J. C., Wessen, M., Luth, E. S., Jun, S., Gussoni, E. and Kunkel, L. M. (2012). beta4 integrin marks interstitial myogenic progenitor cells in adult murine skeletal muscle. *J Histochem Cytochem* **60**, 31-44.
Mann, C. J., Perdiguero, E., Kharraz, Y., Aguilar, S., Pessina, P., Serrano, A. L. and Munoz-Canoves, P. (2011). Aberrant repair and fibrosis development in skeletal muscle. *Skelet Muscle* **1**, 21.
Mauro, A. (1961). Satellite cell of skeletal muscle fibers. *J Biophys Biochem Cytol* **9**, 493-5.
McCarthy, J. J., Mula, J., Miyazaki, M., Erfani, R., Garrison, K., Farooqui, A. B., Srikuea, R., Lawson, B. A., Grimes, B., Keller, C. et al. (2011). Effective fiber hypertrophy in satellite cell-depleted skeletal muscle. *Development* **138**, 3657-66.
McCroskery, S., Thomas, M., Maxwell, L., Sharma, M. and Kambadur, R. (2003). Myostatin negatively regulates satellite cell activation and self-renewal. *J Cell Biol* **162**, 1135-47.
McCroskery, S., Thomas, M., Platt, L., Hennebry, A., Nishimura, T., McLeay, L., Sharma, M. and Kambadur, R. (2005). Improved muscle healing through enhanced regeneration and reduced fibrosis in myostatin-null mice. *J Cell Sci* **118**, 3531-41.
McLellan, A. S., Kealey, T. and Langlands, K. (2006). An E box in the exon 1 promoter regulates insulin-like growth factor-I expression in differentiating muscle cells. *Am J Physiol Cell Physiol* **291**, C300-7.
McLoon, L. K., Rowe, J., Wirtschafter, J. and McCormick, K. M. (2004). Continuous myofiber remodeling in uninjured extraocular myofibers: myonuclear turnover and evidence for apoptosis. *Muscle Nerve* **29**, 707-15.

McLoon, L. K., Thorstenson, K. M., Solomon, A. and Lewis, M. P. (2007). Myogenic precursor cells in craniofacial muscles. *Oral Dis* **13**, 134-40.
McLoon, L. K. and Wirtschafter, J. (2002a). Activated satellite cells are present in uninjured extraocular muscles of mature mice. *Trans Am Ophthalmol Soc* **100**, 119-23; discussion 123-4.
McLoon, L. K. and Wirtschafter, J. (2003). Activated satellite cells in extraocular muscles of normal adult monkeys and humans. *Invest Ophthalmol Vis Sci* **44**, 1927-32.
McLoon, L. K. and Wirtschafter, J. D. (2002b). Continuous myonuclear addition to single extraocular myofibers in uninjured adult rabbits. *Muscle Nerve* **25**, 348-58.
McPherron, A. C., Huynh, T. V. and Lee, S. J. (2009). Redundancy of myostatin and growth/differentiation factor 11 function. *BMC Dev Biol* **9**, 24.
McPherron, A. C., Lawler, A. M. and Lee, S. J. (1997). Regulation of skeletal muscle mass in mice by a new TGF-beta superfamily member. *Nature* **387**, 83-90.
McPherron, A. C. and Lee, S. J. (2002). Suppression of body fat accumulation in myostatin-deficient mice. *J Clin Invest* **109**, 595-601.
Meeson, A. P., Hawke, T. J., Graham, S., Jiang, N., Elterman, J., Hutcheson, K., Dimaio, J. M., Gallardo, T. D. and Garry, D. J. (2004). Cellular and molecular regulation of skeletal muscle side population cells. *Stem Cells* **22**, 1305-20.
Messina, G., Sirabella, D., Monteverde, S., Galvez, B. G., Tonlorenzi, R., Schnapp, E., De Angelis, L., Brunelli, S., Relaix, F., Buckingham, M. et al. (2009). Skeletal muscle differentiation of embryonic mesoangioblasts requires pax3 activity. *Stem Cells* **27**, 157-64.
Metzger, D. and Chambon, P. (2001). Site- and time-specific gene targeting in the mouse. *Methods* **24**, 71-80.
Mitchell, K. J., Pannerec, A., Cadot, B., Parlakian, A., Besson, V., Gomes, E. R., Marazzi, G. and Sassoon, D. A. (2010). Identification and characterization of a non-satellite cell muscle resident progenitor during postnatal development. *Nat Cell Biol* **12**, 257-66.
Morrison, B. M., Lachey, J. L., Warsing, L. C., Ting, B. L., Pullen, A. E., Underwood, K. W., Kumar, R., Sako, D., Grinberg, A., Wong, V. et al. (2009). A soluble activin type IIB receptor improves function in a mouse model of amyotrophic lateral sclerosis. *Exp Neurol* **217**, 258-68.
Mosher, D. S., Quignon, P., Bustamante, C. D., Sutter, N. B., Mellersh, C. S., Parker, H. G. and Ostrander, E. A. (2007). A mutation in the myostatin gene increases muscle mass and enhances racing performance in heterozygote dogs. *PLoS Genet* **3**, e79.
Mourikis, P., Sambasivan, R., Castel, D., Rocheteau, P., Bizzarro, V. and Tajbakhsh, S. (2012). A critical requirement for notch signaling in maintenance of the quiescent skeletal muscle stem cell state. *Stem Cells* **30**, 243-52.

Murphy, M. M., Lawson, J. A., Mathew, S. J., Hutcheson, D. A. and Kardon, G. (2011). Satellite cells, connective tissue fibroblasts and their interactions are crucial for muscle regeneration. *Development* **138**, 3625-37.
Musaro, A. and Barberi, L. (2010). Isolation and culture of mouse satellite cells. *Methods Mol Biol* **633**, 101-11.
Musaro, A., Dobrowolny, G. and Rosenthal, N. (2007). The neuroprotective effects of a locally acting IGF-1 isoform. *Exp Gerontol* **42**, 76-80.
Musaro, A., McCullagh, K., Paul, A., Houghton, L., Dobrowolny, G., Molinaro, M., Barton, E. R., Sweeney, H. L. and Rosenthal, N. (2001). Localized Igf-1 transgene expression sustains hypertrophy and regeneration in senescent skeletal muscle. *Nat Genet* **27**, 195-200.
Natarajan, A., Lemos, D. R. and Rossi, F. M. (2010). Fibro/adipogenic progenitors: a double-edged sword in skeletal muscle regeneration. *Cell Cycle* **9**, 2045-6.
Nicolas, N., Marazzi, G., Kelley, K. and Sassoon, D. (2005). Embryonic deregulation of muscle stress signaling pathways leads to altered postnatal stem cell behavior and a failure in postnatal muscle growth. *Dev Biol* **281**, 171-83.
Noden, D. M. and Francis-West, P. (2006). The differentiation and morphogenesis of craniofacial muscles. *Dev Dyn* **235**, 1194-218.
Noden, D. M. and Schneider, R. A. (2006). Neural crest cells and the community of plan for craniofacial development: historical debates and current perspectives. *Adv Exp Med Biol* **589**, 1-23.
O'Sullivan, D. C., Szestak, T. A. and Pell, J. M. (2002a). Regulation of hepatic insulin-like growth factor I leader exonusage in lambs: effect of immunization against growth hormone-releasing factor and subsequent growth hormone treatment. *J Anim Sci* **80**, 1074-82.
O'Sullivan, D. C., Szestak, T. A. and Pell, J. M. (2002b). Regulation of IGF-I mRNA by GH: putative functions for class 1 and 2 message. *Am J Physiol Endocrinol Metab* **283**, E251-8.
Oberbauer, A. M. (2013). The Regulation of IGF-1 Gene Transcription and Splicing during Development and Aging. *Front Endocrinol (Lausanne)* **4**, 39.
Ohtsuki, T., Otsuki, M., Murakami, Y., Hirata, K., Takeuchi, S. and Takahashi, S. (2007). Alternative leader-exon usage in mouse IGF-I mRNA variants: class 1 and class 2 IGF-I mRNAs. *Zoolog Sci* **24**, 241-7.
Okada, M., Payne, T. R., Zheng, B., Oshima, H., Momoi, N., Tobita, K., Keller, B. B., Phillippi, J. A., Peault, B. and Huard, J. (2008). Myogenic endothelial cells purified from human skeletal muscle improve cardiac function after transplantation into infarcted myocardium. *J Am Coll Cardiol* **52**, 1869-80.
Oldham, J. M., Martyn, J. A., Sharma, M., Jeanplong, F., Kambadur, R. and Bass, J. J. (2001). Molecular expression of myostatin and MyoD is greater in double-muscled than normal-muscled cattle fetuses. *Am J Physiol Regul Integr Comp Physiol* **280**, R1488-93.

Olson, L. E. and Soriano, P. (2009). Increased PDGFRalpha activation disrupts connective tissue development and drives systemic fibrosis. *Dev Cell* **16**, 303-13.

Pacheco-Pinedo, E. C., Budak, M. T., Zeiger, U., Jorgensen, L. H., Bogdanovich, S., Schroder, H. D., Rubinstein, N. A. and Khurana, T. S. (2009). Transcriptional and functional differences in stem cell populations isolated from extraocular and limb muscles. *Physiol Genomics* **37**, 35-42.

Pallafacchina, G., Francois, S., Regnault, B., Czarny, B., Dive, V., Cumano, A., Montarras, D. and Buckingham, M. (2010). An adult tissue-specific stem cell in its niche: a gene profiling analysis of in vivo quiescent and activated muscle satellite cells. *Stem Cell Res* **4**, 77-91.

Pannerec, A., Marazzi, G. and Sassoon, D. (2012). Stem cells in the hood: the skeletal muscle niche. *Trends Mol Med* **18**, 599-606.

Partridge, T. A. (2013). The mdx mouse model as a surrogate for Duchenne muscular dystrophy. *FEBS J* **280**, 4177-86.

Pertille, A., de Carvalho, C. L., Matsumura, C. Y., Neto, H. S. and Marques, M. J. (2010). Calcium-binding proteins in skeletal muscles of the mdx mice: potential role in the pathogenesis of Duchenne muscular dystrophy. *Int J Exp Pathol* **91**, 63-71.

Pessina, P., Conti, V., Tonlorenzi, R., Touvier, T., Meneveri, R., Cossu, G. and Brunelli, S. (2012). Necdin enhances muscle reconstitution of dystrophic muscle by vessel-associated progenitors, by promoting cell survival and myogenic differentiation. *Cell Death Differ* **19**, 827-38.

Philippou, A., Maridaki, M., Halapas, A. and Koutsilieris, M. (2007). The role of the insulin-like growth factor 1 (IGF-1) in skeletal muscle physiology. *In Vivo* **21**, 45-54.

Pistilli, E. E., Bogdanovich, S., Goncalves, M. D., Ahima, R. S., Lachey, J., Seehra, J. and Khurana, T. (2011). Targeting the activin type IIB receptor to improve muscle mass and function in the mdx mouse model of Duchenne muscular dystrophy. *Am J Pathol* **178**, 1287-97.

Pistilli, E. E., Bogdanovich, S., Mosqueira, M., Lachey, J., Seehra, J. and Khurana, T. S. (2010). Pretreatment with a soluble activin type IIB receptor/Fc fusion protein improves hypoxia-induced muscle dysfunction. *Am J Physiol Regul Integr Comp Physiol* **298**, R96-R103.

Porter, J. D. (2002). Extraocular muscle: cellular adaptations for a diverse functional repertoire. *Ann N Y Acad Sci* **956**, 7-16.

Porter, J. D., Baker, R. S., Ragusa, R. J. and Brueckner, J. K. (1995). Extraocular muscles: basic and clinical aspects of structure and function. *Surv Ophthalmol* **39**, 451-84.

Porter, J. D., Israel, S., Gong, B., Merriam, A. P., Feuerman, J., Khanna, S. and Kaminski, H. J. (2006). Distinctive morphological and gene/protein expression signatures during myogenesis in novel cell lines from extraocular and hindlimb muscle. *Physiol Genomics* **24**, 264-75.

Porter, J. D., Khanna, S., Kaminski, H. J., Rao, J. S., Merriam, A. P., Richmonds, C. R., Leahy, P., Li, J. and Andrade, F. H. (2001). Extraocular muscle is defined by a fundamentally distinct gene expression profile. *Proc Natl Acad Sci U S A* **98**, 12062-7.

Porter, J. D., Merriam, A. P., Khanna, S., Andrade, F. H., Richmonds, C. R., Leahy, P., Cheng, G., Karathanasis, P., Zhou, X., Kusner, L. L. et al. (2003). Constitutive properties, not molecular adaptations, mediate extraocular muscle sparing in dystrophic mdx mice. *FASEB J* **17**, 893-5.

Rebbapragada, A., Benchabane, H., Wrana, J. L., Celeste, A. J. and Attisano, L. (2003). Myostatin signals through a transforming growth factor beta-like signaling pathway to block adipogenesis. *Mol Cell Biol* **23**, 7230-42.

Relaix, F., Montarras, D., Zaffran, S., Gayraud-Morel, B., Rocancourt, D., Tajbakhsh, S., Mansouri, A., Cumano, A. and Buckingham, M. (2006). Pax3 and Pax7 have distinct and overlapping functions in adult muscle progenitor cells. *J Cell Biol* **172**, 91-102.

Relaix, F., Rocancourt, D., Mansouri, A. and Buckingham, M. (2005). A Pax3/Pax7-dependent population of skeletal muscle progenitor cells. *Nature* **435**, 948-53.

Relaix, F., Wei, X., Li, W., Pan, J., Lin, Y., Bowtell, D. D., Sassoon, D. A. and Wu, X. (2000). Pw1/Peg3 is a potential cell death mediator and cooperates with Siah1a in p53-mediated apoptosis. *Proc Natl Acad Sci U S A* **97**, 2105-10.

Relaix, F., Wei, X. J., Wu, X. and Sassoon, D. A. (1998). Peg3/Pw1 is an imprinted gene involved in the TNF-NFkappaB signal transduction pathway. *Nat Genet* **18**, 287-91.

Relaix, F., Weng, X., Marazzi, G., Yang, E., Copeland, N., Jenkins, N., Spence, S. E. and Sassoon, D. (1996). Pw1, a novel zinc finger gene implicated in the myogenic and neuronal lineages. *Dev Biol* **177**, 383-96.

Relaix, F. and Zammit, P. S. (2012). Satellite cells are essential for skeletal muscle regeneration: the cell on the edge returns centre stage. *Development* **139**, 2845-56.

Rios, R., Carneiro, I., Arce, V. M. and Devesa, J. (2002). Myostatin is an inhibitor of myogenic differentiation. *Am J Physiol Cell Physiol* **282**, C993-9.

Rodeheffer, M. S. (2010). Tipping the scale: muscle versus fat. *Nat Cell Biol* **12**, 102-4.

Rommel, C., Bodine, S. C., Clarke, B. A., Rossman, R., Nunez, L., Stitt, T. N., Yancopoulos, G. D. and Glass, D. J. (2001). Mediation of IGF-1-induced skeletal myotube hypertrophy by PI(3)K/Akt/mTOR and PI(3)K/Akt/GSK3 pathways. *Nat Cell Biol* **3**, 1009-13.

Rushbrook, J. I., Weiss, C., Ko, K., Feuerman, M. H., Carleton, S., Ing, A. and Jacoby, J. (1994). Identification of alpha-cardiac myosin heavy chain mRNA and protein in extraocular muscle of the adult rabbit. *J Muscle Res Cell Motil* **15**, 505-15.

Sacco, A., Doyonnas, R., Kraft, P., Vitorovic, S. and Blau, H. M. (2008). Self-renewal and expansion of single transplanted muscle stem cells. *Nature* **456**, 502-6.
Sakuma, K. and Yamaguchi, A. (2013). Sarcopenic obesity and endocrinal adaptation with age. *Int J Endocrinol* **2013**, 204164.
Sambasivan, R., Gayraud-Morel, B., Dumas, G., Cimper, C., Paisant, S., Kelly, R. G. and Tajbakhsh, S. (2009). Distinct regulatory cascades govern extraocular and pharyngeal arch muscle progenitor cell fates. *Dev Cell* **16**, 810-21.
Sambasivan, R., Kuratani, S. and Tajbakhsh, S. (2011a). An eye on the head: the development and evolution of craniofacial muscles. *Development* **138**, 2401-15.
Sambasivan, R. and Tajbakhsh, S. (2007). Skeletal muscle stem cell birth and properties. *Semin Cell Dev Biol* **18**, 870-82.
Sambasivan, R., Yao, R., Kissenpfennig, A., Van Wittenberghe, L., Paldi, A., Gayraud-Morel, B., Guenou, H., Malissen, B., Tajbakhsh, S. and Galy, A. (2011b). Pax7-expressing satellite cells are indispensable for adult skeletal muscle regeneration. *Development* **138**, 3647-56.
Sampaolesi, M., Blot, S., D'Antona, G., Granger, N., Tonlorenzi, R., Innocenzi, A., Mognol, P., Thibaud, J. L., Galvez, B. G., Barthelemy, I. et al. (2006). Mesoangioblast stem cells ameliorate muscle function in dystrophic dogs. *Nature* **444**, 574-9.
Sampaolesi, M., Torrente, Y., Innocenzi, A., Tonlorenzi, R., D'Antona, G., Pellegrino, M. A., Barresi, R., Bresolin, N., De Angelis, M. G., Campbell, K. P. et al. (2003). Cell therapy of alpha-sarcoglycan null dystrophic mice through intra-arterial delivery of mesoangioblasts. *Science* **301**, 487-92.
Sassoon, D., Lyons, G., Wright, W. E., Lin, V., Lassar, A., Weintraub, H. and Buckingham, M. (1989). Expression of two myogenic regulatory factors myogenin and MyoD1 during mouse embryogenesis. *Nature* **341**, 303-7.
Schienda, J., Engleka, K. A., Jun, S., Hansen, M. S., Epstein, J. A., Tabin, C. J., Kunkel, L. M. and Kardon, G. (2006). Somitic origin of limb muscle satellite and side population cells. *Proc Natl Acad Sci U S A* **103**, 945-50.
Schuelke, M., Wagner, K. R., Stolz, L. E., Hubner, C., Riebel, T., Komen, W., Braun, T., Tobin, J. F. and Lee, S. J. (2004). Myostatin mutation associated with gross muscle hypertrophy in a child. *N Engl J Med* **350**, 2682-8.
Schulz, T. J., Huang, T. L., Tran, T. T., Zhang, H., Townsend, K. L., Shadrach, J. L., Cerletti, M., McDougall, L. E., Giorgadze, N., Tchkonia, T. et al. (2011). Identification of inducible brown adipocyte progenitors residing in skeletal muscle and white fat. *Proc Natl Acad Sci U S A* **108**, 143-8.
Schulze, P. C., Fang, J., Kassik, K. A., Gannon, J., Cupesi, M., MacGillivray, C., Lee, R. T. and Rosenthal, N. (2005). Transgenic overexpression of locally acting insulin-like growth factor-1 inhibits ubiquitin-

mediated muscle atrophy in chronic left-ventricular dysfunction. *Circ Res* **97**, 418-26.
Schwarzkopf, M., Coletti, D., Sassoon, D. and Marazzi, G. (2006). Muscle cachexia is regulated by a p53-PW1/Peg3-dependent pathway. *Genes Dev* **20**, 3440-52.
Scicchitano, B. M., Rizzuto, E. and Musaro, A. (2009). Counteracting muscle wasting in aging and neuromuscular diseases: the critical role of IGF-1. *Aging (Albany NY)* **1**, 451-7.
Seale, P., Bjork, B., Yang, W., Kajimura, S., Chin, S., Kuang, S., Scime, A., Devarakonda, S., Conroe, H. M., Erdjument-Bromage, H. et al. (2008). PRDM16 controls a brown fat/skeletal muscle switch. *Nature* **454**, 961-7.
Seale, P., Kajimura, S., Yang, W., Chin, S., Rohas, L. M., Uldry, M., Tavernier, G., Langin, D. and Spiegelman, B. M. (2007). Transcriptional control of brown fat determination by PRDM16. *Cell Metab* **6**, 38-54.
Seale, P., Sabourin, L. A., Girgis-Gabardo, A., Mansouri, A., Gruss, P. and Rudnicki, M. A. (2000). Pax7 is required for the specification of myogenic satellite cells. *Cell* **102**, 777-86.
Serrano, A. L., Mann, C. J., Vidal, B., Ardite, E., Perdiguero, E. and Munoz-Canoves, P. (2011). Cellular and molecular mechanisms regulating fibrosis in skeletal muscle repair and disease. *Curr Top Dev Biol* **96**, 167-201.
Shavlakadze, T., Winn, N., Rosenthal, N. and Grounds, M. D. (2005). Reconciling data from transgenic mice that overexpress IGF-I specifically in skeletal muscle. *Growth Horm IGF Res* **15**, 4-18.
Shelton, G. D. and Engvall, E. (2007). Gross muscle hypertrophy in whippet dogs is caused by a mutation in the myostatin gene. *Neuromuscul Disord* **17**, 721-2.
Shih, H. P., Gross, M. K. and Kioussi, C. (2008). Muscle development: forming the head and trunk muscles. *Acta Histochem* **110**, 97-108.
Siriett, V., Platt, L., Salerno, M. S., Ling, N., Kambadur, R. and Sharma, M. (2006). Prolonged absence of myostatin reduces sarcopenia. *J Cell Physiol* **209**, 866-73.
Smythe, G. M., Shavlakadze, T., Roberts, P., Davies, M. J., McGeachie, J. K. and Grounds, M. D. (2008). Age influences the early events of skeletal muscle regeneration: studies of whole muscle grafts transplanted between young (8 weeks) and old (13-21 months) mice. *Exp Gerontol* **43**, 550-62.
Soltys, J., Gong, B., Kaminski, H. J., Zhou, Y. and Kusner, L. L. (2008). Extraocular muscle susceptibility to myasthenia gravis: unique immunological environment? *Ann N Y Acad Sci* **1132**, 220-4.
Spencer, R. F. and Porter, J. D. (1988). Structural organization of the extraocular muscles. *Rev Oculomot Res* **2**, 33-79.
Sussenbach, J. S., Steenbergh, P. H. and Holthuizen, P. (1992). Structure and expression of the human insulin-like growth factor genes. *Growth Regul* **2**, 1-9.

Tabebordbar, M., Wang, E. T. and Wagers, A. J. (2013). Skeletal muscle degenerative diseases and strategies for therapeutic muscle repair. *Annu Rev Pathol* **8**, 441-75.

Tamaki, T., Akatsuka, A., Ando, K., Nakamura, Y., Matsuzawa, H., Hotta, T., Roy, R. R. and Edgerton, V. R. (2002). Identification of myogenic-endothelial progenitor cells in the interstitial spaces of skeletal muscle. *J Cell Biol* **157**, 571-7.

Tanaka, K. K., Hall, J. K., Troy, A. A., Cornelison, D. D., Majka, S. M. and Olwin, B. B. (2009). Syndecan-4-expressing muscle progenitor cells in the SP engraft as satellite cells during muscle regeneration. *Cell Stem Cell* **4**, 217-25.

Ten Broek, R. W., Grefte, S. and Von den Hoff, J. W. (2010). Regulatory factors and cell populations involved in skeletal muscle regeneration. *J Cell Physiol* **224**, 7-16.

Thies, R. S., Chen, T., Davies, M. V., Tomkinson, K. N., Pearson, A. A., Shakey, Q. A. and Wolfman, N. M. (2001). GDF-8 propeptide binds to GDF-8 and antagonizes biological activity by inhibiting GDF-8 receptor binding. *Growth Factors* **18**, 251-9.

Thomas, M., Langley, B., Berry, C., Sharma, M., Kirk, S., Bass, J. and Kambadur, R. (2000). Myostatin, a negative regulator of muscle growth, functions by inhibiting myoblast proliferation. *J Biol Chem* **275**, 40235-43.

Tonlorenzi, R., Dellavalle, A., Schnapp, E., Cossu, G. and Sampaolesi, M. (2007). Isolation and characterization of mesoangioblasts from mouse, dog, and human tissues. *Curr Protoc Stem Cell Biol* **Chapter 2**, Unit 2B 1.

Trendelenburg, A. U., Meyer, A., Rohner, D., Boyle, J., Hatakeyama, S. and Glass, D. J. (2009). Myostatin reduces Akt/TORC1/p70S6K signaling, inhibiting myoblast differentiation and myotube size. *Am J Physiol Cell Physiol* **296**, C1258-70.

Uezumi, A., Fukada, S., Yamamoto, N., Takeda, S. and Tsuchida, K. (2010). Mesenchymal progenitors distinct from satellite cells contribute to ectopic fat cell formation in skeletal muscle. *Nat Cell Biol* **12**, 143-52.

Uezumi, A., Ito, T., Morikawa, D., Shimizu, N., Yoneda, T., Segawa, M., Yamaguchi, M., Ogawa, R., Matev, M. M., Miyagoe-Suzuki, Y. et al. (2011). Fibrosis and adipogenesis originate from a common mesenchymal progenitor in skeletal muscle. *J Cell Sci* **124**, 3654-64.

Wagner, K. R., McPherron, A. C., Winik, N. and Lee, S. J. (2002). Loss of myostatin attenuates severity of muscular dystrophy in mdx mice. *Ann Neurol* **52**, 832-6.

Walden, T. B., Hansen, I. R., Timmons, J. A., Cannon, B. and Nedergaard, J. (2012). Recruited vs. nonrecruited molecular signatures of brown, "brite," and white adipose tissues. *Am J Physiol Endocrinol Metab* **302**, E19-31.

Wallace, G. Q. and McNally, E. M. (2009). Mechanisms of muscle degeneration, regeneration, and repair in the muscular dystrophies. *Annu Rev Physiol* **71**, 37-57.

Wang, Y. X. and Rudnicki, M. A. (2012). Satellite cells, the engines of muscle repair. *Nat Rev Mol Cell Biol* **13**, 127-33.
White, R. B., Bierinx, A. S., Gnocchi, V. F. and Zammit, P. S. (2010). Dynamics of muscle fibre growth during postnatal mouse development. *BMC Dev Biol* **10**, 21.
Wieczorek, D. F., Periasamy, M., Butler-Browne, G. S., Whalen, R. G. and Nadal-Ginard, B. (1985). Co-expression of multiple myosin heavy chain genes, in addition to a tissue-specific one, in extraocular musculature. *J Cell Biol* **101**, 618-29.
Wright, W. E., Sassoon, D. A. and Lin, V. K. (1989). Myogenin, a factor regulating myogenesis, has a domain homologous to MyoD. *Cell* **56**, 607-17.
Wu, J., Bostrom, P., Sparks, L. M., Ye, L., Choi, J. H., Giang, A. H., Khandekar, M., Virtanen, K. A., Nuutila, P., Schaart, G. et al. (2012). Beige adipocytes are a distinct type of thermogenic fat cell in mouse and human. *Cell* **150**, 366-76.
Yablonka-Reuveni, Z. (2011). The skeletal muscle satellite cell: still young and fascinating at 50. *J Histochem Cytochem* **59**, 1041-59.
Yin, H., Price, F. and Rudnicki, M. A. (2013). Satellite cells and the muscle stem cell niche. *Physiol Rev* **93**, 23-67.
Zacharias, A. L., Lewandoski, M., Rudnicki, M. A. and Gage, P. J. (2011). Pitx2 is an upstream activator of extraocular myogenesis and survival. *Dev Biol* **349**, 395-405.
Zammit, P. S. (2008). All muscle satellite cells are equal, but are some more equal than others? *J Cell Sci* **121**, 2975-82.
Zammit, P. S., Partridge, T. A. and Yablonka-Reuveni, Z. (2006a). The skeletal muscle satellite cell: the stem cell that came in from the cold. *J Histochem Cytochem* **54**, 1177-91.
Zammit, P. S., Relaix, F., Nagata, Y., Ruiz, A. P., Collins, C. A., Partridge, T. A. and Beauchamp, J. R. (2006b). Pax7 and myogenic progression in skeletal muscle satellite cells. *J Cell Sci* **119**, 1824-32.
Zeiger, U., Mitchell, C. H. and Khurana, T. S. (2010). Superior calcium homeostasis of extraocular muscles. *Exp Eye Res* **91**, 613-22.
Zhao, Y., Haginoya, K., Sun, G., Dai, H., Onuma, A. and Iinuma, K. (2003). Platelet-derived growth factor and its receptors are related to the progression of human muscular dystrophy: an immunohistochemical study. *J Pathol* **201**, 149-59.
Zheng, B., Cao, B., Crisan, M., Sun, B., Li, G., Logar, A., Yap, S., Pollett, J. B., Drowley, L., Cassino, T. et al. (2007). Prospective identification of myogenic endothelial cells in human skeletal muscle. *Nat Biotechnol* **25**, 1025-34.
Zheng, B., Li, G., Chen, W. C., Deasy, B. M., Pollett, J. B., Sun, B., Drowley, L., Gharaibeh, B., Usas, A., Peault, B. et al. (2013). Human myogenic

endothelial cells exhibit chondrogenic and osteogenic potentials at the clonal level. *J Orthop Res* **31**, 1089-95.

Zhou, L., Porter, J. D., Cheng, G., Gong, B., Hatala, D. A., Merriam, A. P., Zhou, X., Rafael, J. A. and Kaminski, H. J. (2006). Temporal and spatial mRNA expression patterns of TGF-beta1, 2, 3 and TbetaRI, II, III in skeletal muscles of mdx mice. *Neuromuscul Disord* **16**, 32-8.

Zhou, S., Schuetz, J. D., Bunting, K. D., Colapietro, A. M., Sampath, J., Morris, J. J., Lagutina, I., Grosveld, G. C., Osawa, M., Nakauchi, H. et al. (2001). The ABC transporter Bcrp1/ABCG2 is expressed in a wide variety of stem cells and is a molecular determinant of the side-population phenotype. *Nat Med* **7**, 1028-34.

Zhou, X., Wang, J. L., Lu, J., Song, Y., Kwak, K. S., Jiao, Q., Rosenfeld, R., Chen, Q., Boone, T., Simonet, W. S. et al. (2010a). Reversal of cancer cachexia and muscle wasting by ActRIIB antagonism leads to prolonged survival. *Cell* **142**, 531-43.

Zhou, Y., Liu, D. and Kaminski, H. J. (2010b). Myosin heavy chain expression in mouse extraocular muscle: more complex than expected. *Invest Ophthalmol Vis Sci* **51**, 6355-63.

Zhou, Y., Liu, D. and Kaminski, H. J. (2011). Pitx2 regulates myosin heavy chain isoform expression and multi-innervation in extraocular muscle. *J Physiol* **589**, 4601-14.

Zhu, X., Topouzis, S., Liang, L. F. and Stotish, R. L. (2004). Myostatin signaling through Smad2, Smad3 and Smad4 is regulated by the inhibitory Smad7 by a negative feedback mechanism. *Cytokine* **26**, 262-72.

LIST OF PUBLICATIONS

Journal articles

Pannérec, A.[†], **Formicola, L.**[†], Besson, V., Marazzi, G. and Sassoon, D.A. (2013). "Defining skeletal muscle resident progenitors and their cell fate potentials". *Development* 140*,* 2879-2891.
[†] Equal contribution.

Conference abstracts and presentations

- **Formicola, L**., Pannérec, A., Besson, V., Gayraud-Morel, B., Tajbakhsh, S., Lachey, J., Sehra, J.S., Marazzi, G. and Sassoon, D.A. "Targeting stem cell niche interactions to improve muscle regeneration". *ICAN (Institute of Cardiometabolism and Nutrition) Scientific Day*, September 20th 2013, Paris (France). Oral communication.

- Pannérec, A., **Formicola, L.**, Besson, V., Gayraud-Morel, B., Tajbakhsh, S., Lachey, J., Sehra, J.S., Marazzi, G. and Sassoon, D.A. "Defining skeletal muscle stem cell niche: resident progenitor cell fate potentials and reciprocal interactions". *2nd Annual Meeting REVIVE consortium*, February 19th-20th 2013, Belle-Eglise (France). Oral communication.

- **Formicola, L.**, Pannérec, A., Besson, V., Marazzi, G. and Sassoon D.A. "The muscle stem cell niche". *Optistem/Endostem annual meeting 2012*, April 2nd-5th 2012, Barcelona (Spain). Oral communication.

- **Formicola, L.**, Pannérec, A., Besson, V., Marazzi, G. and Sassoon D.A. "The muscle stem cell niche". *IFR14 annual scientific day 2012,* March 15th 2012, Paris (France). Oral communication.